Holistic sizing and operational optimisation of domestic micro-CHP and hybrid energy storage system

Yu, Dongmin

Award date:
2016

Awarding institution:
University of Bath

Holistic sizing and operational optimisation of domestic micro-CHP and hybrid energy storage system

Dongmin Yu

A thesis submitted for the degree of Doctor of Philosophy

University of Bath

Department of Electronic and Electrical Engineering

May 2016

Abstract

With the growth of the distributed power generation market and the increasing integration of energy systems, more and more low carbon technologies are being installed at the domestic building level to optimise daily energy cost and reduce carbon emissions.

The objective of this thesis is to optimise domestic building daily energy cost, and to identify ways of reducing the installation and maintenance costs of all domestic energy infrastructures. In this thesis, general energy conversion, storage and transmission in domestic buildings are considered. The first key part of this thesis is to size a combined heat and power (CHP) unit based on the Maximum Rectangle (MR) method and use the Genetic Algorithm (GA) method to optimize daily energy cost for a building without an energy storage system. The second key part of the thesis is to size a hybrid energy storage system (HESS) and develop a new rule-based energy control rule to optimise energy cost for a building with an energy storage system.

The results show that after sizing the HESS, the daily benefit-cost ratio of the HESS is increased by approximately a factor of two over previous work. Additionally, the proposed rule based energy control model can yield up to 19.8% energy cost saving compared to a system dependent solely on electricity from the grid and using a boiler to generate heat. This ratio is almost equal to the previous work, but the present work increases customers' comfort level by treating all load as critical. In addition, the optimization approach in this thesis is more real-world feasible, because it is not possible for exact loads to be known in advance.

The results also show that daily energy cost saving for a building with HESSs and the appropriate control rule is approximately 47% higher than a building with a well-sized CHP but no HESS; and the capacity of CHP can also be reduced when the HESS is installed. Thus, the installation and maintenance costs of HESSs can be offset by reducing the capacity of CHP to some extent. In addition, the proposed control algorithm and HESSs have outstanding performance in improving the effective CHP output efficiency and average CHP input to output ratio. This proves the combination of HESS and the proposed rule-base control algorithm can reduce carbon emissions and make full use of CHP capacity.

However at present, the benefit to cost ratios of case studies of such domestic energy systems are always lower than 11% giving a negative return on investment. This figure is mainly limited by the high manufacturing price of HESSs and CHP. In the medium to long term future, the downward trend in battery and CHP manufacturing costs, coupled with changing energy tariffs are likely to lead to overwhelmingly positive cost benefit for this technology.

Acknowledgements

This thesis shows the result of my three-year research activity at the centre for the sustainable power distribution of the University of Bath. Many people have supported me during this time. In particular, I would like to express my thanks to:

- Dr Simon Le Blond for his supervision and support, and particularly for taking a risk to agree to supervise a Chinese student whose English is not good enough.
- Professor Raj Aggarwal, for his patience and advice during this period. Also, he gave many opportunities to me to improve my personal skills and abilities.
- Dr Roderick Dunn, for his open-minded discussions and warm heart.
- Dr Francis Robinson and Professor Furong Li, who have always been happy to review my paper and to offer some really useful advice.
- Professor Zhengming Zhao, Dr Ting Lu and Mr Xudong Wang, who offered me a lot of technical help in Tsinghua. They co-operated with me during the research that will be shown in Chapter 4.
- All my colleagues and friends at the University of Bath and Tsinghua University for having a good time.
- China Scholarship Council for offering a scholarship to pursue my studies in the United Kingdom as a PhD student.

Finally, I would like to thank my parents Xiaoshu Sun and Jing Yu, for their great support and encouragement.

Dongmin Yu

Bath, March 2016

Contents

List of figures

Chapter 2

Chapter 3

Chapter 4

Chapter 5

Appendix

List of symbols

a, b, c and d	Coefficients
$a_{1m}, \ldots, a_{mm}$	Coefficients
$B_{CHP}\ (t)$	Benefit, in monetary terms that CHP can generate at the t^{th} minute
$\boldsymbol{C}$	Coupling matrix
$c_1, \ldots, c_m$	Coefficients
$C_{\alpha\alpha}$, $C_{\beta\alpha}$,..,.$C_{\omega\omega}$	Elements in coupling matrix
C_b	Average daily cost of battery storage system
C_{bi}	The unit price of the battery
C_{bm}	The annual maintenance cost of battery
C_{boiler}	Boiler operation cost
C_{chp}	CHP operation cost
$C_{CHP}\ (t)$	The cost of implementing CHP in the t^{th} minute
$C_e(t)$	Electricity price in t^{th} minute
$C_g(t)$	Gas price in t^{th} minute
C_{grid}	Electricity costs bought from grid
C_{si}	Unit installation cost of the supercapacitor
C_{sm}	Annual maintenance cost of the supercapacitor
C_{Theo}	Theoretical minimum operation cost
$\boldsymbol{D}$	Backwards coupling matrix
dt	Discharge time
dV	The difference between maximum supercapacitor operation voltage and minimum supercapacitor operation voltage
$\dot{\boldsymbol{E}}$	Storage energy derivatives vector
E_α	Total energy stored in the device
e_α	Energy exchange efficiency
$E_a(T)$	Total energy stored in the energy storage equipment after a certain period T

$E_{CHP}\ (t)$	Effective value of electrical power contribution due to CHP in the t^{th} minute
E_{fp}	The amount of energy shortage for the first peak demand
E_s	Total daily energy cost saving in pence
E_{sn}	EES for n^{th} high/intermediate price time
E_{sp}	The amount of energy shortage for the second peak demand
$E_{Theo}{}^{i}$	The amount of theoretical surplus electrical energy generated in each minute before the first peak
E_{Total}	Total surplus electrical energy
$F(t)$	Daily energy cost
$F(x)$	Scalar-valued objective functions
$g(x)$	The conservation of power
h_{CHP}	Average CHP input power to rated power ratio
$H_{CHP}\ (t)$	Effective value of heat power contribution due to CHP in the t^{th} minute
$h(x)$	Limits
i	The average current
I_{max}	Maximum discharge current of the battery
i_{maxs}	Maximum output current of the supercapacitor
i_{mins}	Minimum output current of the supercapacitor
$K(t)$	The state of the CHP
L'	Number of samples
$\boldsymbol{L}$	Output energy vector
$L_{\alpha}, L_{\beta}, \ldots, L_{\omega}$	Elements in output vectors
$\boldsymbol{L_{out}^{b}}$	Output of the system
$\boldsymbol{M}$	Energy storage vector at the output side of an energy hub
$\boldsymbol{M_E}$	Equivalent energy storage vector
Min C	Minimum average daily system cost

N	The number of discharge cycles
N'	Total days in the sampling data
N_{on}^{t}	The number of days that CHP is switched on
n	The number of full discharge cycles in a day
$\boldsymbol{P}$	Input energy vector
$P_{\alpha}, P_{\beta}, \ldots, P_{\omega}$	Elements in input vectors
$P_{CHPin}(t)$	Imported gas to supply the CHP in tth minute
$P_{E}(t)$	Electricity energy demand in t^{th} minute
$P_{Ein}(t)$	Imported average electrical energy from the grid in tth minute
$P_{Gin}(t)$	Imported gas to supply the boiler in tth minute
$P_{H}(t)$	Heat energy demand in t^{th} minute
P_{on}^{t}	Probability of CHP switch on' in the t^{th} minute
$P_{pE}(t+1)$	Predicted electricity demand in $(t+1)^{th}$ minute
$P_{pH}(t+1)$	Predicted heat demand in $(t+1)^{th}$ minute
$\boldsymbol{P_{in}^{a}}$	Input of the system
P_{max}	Maximum output power of the battery
P_{R}	Rated/optimal power/capacity of CHP
P_{sto}^{i}	Energy flow entering or leaving a storage
$\boldsymbol{Q}$	Energy storage vector at the input side of an energy hub
Q_{α}	Power exchange
q_{a}	The accumulative capacity of batteries
q_{b}	The battery capacity
q_{d}	The daily effective battery capacity consumption
q_{eb}	Effective battery capacity
Q_{s}	Supercapacitor installation capacity
q_{s}	Capacitance of the supercapacitor
$q(SOC)$	A function of the effective weighting factor of the battery at different SOC
$\tilde{Q}_{\alpha}$	Internal power

$\boldsymbol{S}$	The storage coupling matrix
t_{fs}	The first peak demand start time
T_L	The life span of the HESS in days
V_b	Battery output voltage
V_{max}	Maximum output voltage of the supercapacitor
V_{min}	Minimum output voltage of the supercapacitor
V_o	HESS operation voltage
x	The electricity demand in Watts
$x_1, \ldots, x_m$	The variables that need to be determined
y	The duration in hours
Y	The life span of the HESS in years
ΔE_α	The change in energy
Δt	The time period of energy change
α	Scaling factor of effective battery discharge capacity and battery rated capacity
β	Scaling factor of battery accumulative capacity and battery rated capacity
μ	Time scaling factor
τ	Time constant for the supercapacitor
η_B	The boiler's gas to heat conversion efficiency
$\widetilde{\eta_{CHP}}$	Effective CHP energy efficiency
η_{CHPE}	CHP output electricity efficiency
$\eta_{CHPE(t)}$	CHP output electricity efficiency in t^{th} minute
η_{CHPH}	CHP output heat efficiency
$\eta_{CHPH(t)}$	CHP output heat efficiency in t^{th} minute
η_{Ki}	The conversion efficiency of the generic converter i
ξ_E	The CHP electricity output efficiency coefficient
ξ_H	The CHP heat output efficiency coefficient
ε_{ki}^{a}	The portion between the load a covered by the converter Ki and the load a
ζ	A scaling factor

List of tables

Chapter 2

Chapter 3

Chapter 4

Chapter 5

Chapter 6

Chapter 1. Introduction

1.1 Background and motivation

After the industrial revolution broke out in the middle of the 18th century, energy consumption increased rapidly. The reason for this is citizens had higher requirements of living quality. Also it is widely accepted that living standards are in proportion to energy consumption [1]. However, this has the potential to cause an energy crisis and climate change.

After that, centralized power generation concept was proposed in the middle of 20th century to improve power generation efficiency [2]. However, the transmission and distribution (T&D) losses can be very high if power stations are built far away from a city.

Nowadays, distributed generation (DG) concept has been proposed to reduce T&D losses, improve energy generation efficiency, and improve energy system flexibility and stability. Also, many nations have introduced legally binding targets to reduce carbon emissions, for example, the UK government aims to reduce carbon emissions by 80 percent by 2050 compared with 1990 levels [3].

Recently, large industrial and commercial customers have begun to participate in Smart Grid (SG) programs, for example, demand side management (DSM) and demand response (DR), to save energy costs and reduce CO_2 emissions. However, the domestic sector has shown less interest in SG technologies, because of their individually smaller impact on the grid and the technical difficulties in aggregating large numbers of customers [4, 5].

At present, energy consumption in buildings (41%) represents the majority of global energy consumption, compared with industry (30%) and transportation (29%) [6]. Moreover, a significant form of energy consumption at building level is electricity, which in some countries accounts for as much as 70%. As a result, nearly half (47%) of energy use in residential buildings is lost in electricity transmission and distribution [6]. It is therefore urgent to develop cost-effective and practical methods to control energy consumption in residential dwellings.

As a key component of future smart buildings, battery energy storage systems (BESSs) are well suited to domestic buildings due to their relatively safe, silent, scalable, low maintenance, and efficient characteristics [7]. BESSs are widely used in domestic buildings to reduce electricity grid imports, supply backup electric power in the form of uninterruptible power supplies and store redundant energy generated by any co-located distributed energy generation system [8]. However, the relatively high manufacturing price and short life time of BESSs significantly increase the cost of 'smart house' systems.

The number of CHP units installed in domestic buildings has rapidly increased in recent years, due to the fact that CHP has the potential to increase energy efficiency, to improve energy controllability and to reduce energy cost and carbon emission. The CHP systems can utilize up to 90 percent of a fossil fuel's energy and can generate heat and power at the same time [9]. Considering the fact that the input energy sources of CHP are normally very cheap and installation cost of CHP is relatively low, more CHP systems are installed in domestic buildings. However, CHP output efficiencies can be influenced by CHP input power, especially its electricity output efficiency. Therefore, to increase CHP output efficiencies, the CHP should work in rated power. But by doing this, CHP may generate redundant energy at some time in a day.

From aforementioned background, two conclusions can be summarised:

1. CHP systems are high energy efficiency systems and they can simultaneously generate heat and power. The installation and operation cost of CHP system are relatively low which makes it become popular in domestic house. To make full use of CHP and improve energy efficiencies, CHP should always work close to rated power. Therefore, sizing the capacity of CHP properly has great benefits in improving energy efficiency and reducing energy cost.
2. Even though the manufacturing price of BESSs is relatively high and the lifetime of BESSs is relatively short, combining BESSs with CHP system has potential benefits to improve energy system overall efficiency, reduce energy cost and increase system stability by adding BESSs as backup power system.

Therefore, if the CHP and BESSs can be sized in advance and they can be operated in a smart way, domestic energy cost savings and energy efficiencies can be further increased without significantly increasing investment costs.

1.2 Thesis outline

The rest of this thesis is organized as follows:

Chapter 2: Energy Hub models (EH) and system definition describes mathematical multi-energy system models which are called EH models. After introducing the EH models, terraced houses, which are a typical building, are introduced and their daily heat and electricity demands are simulated by the Strathclyde University and CREST models. In this chapter, all parameters that may need to be used in later chapters are listed.

Chapter 3: Sizing CHP and domestic building energy cost optimization deals with CHP installation capacity and domestic building energy cost optimization problems. In this chapter, the Maximum Rectangle (MR) and Genetic Algorithm (GA) methods are used to size the CHP and then, the GA method is used to calculate domestic energy costs for different sizing results. No energy storage system is considered in this chapter.

Chapter 4: Sizing hybrid energy storage systems (HESSs, which contain battery energy storage systems (BESSs) and supercapacitor storage systems) analyses the factors that can potentially affect the life time and the investment cost of the BESSs. After that, the HESS model is proposed to extend the life time and reduce the investment cost of BESSs. Then, the daily investment cost function is established which is solely related to battery capacity. The theoretical best size of the HESS can be calculated in this chapter by solving the daily investment cost function of the HESS.

Chapter 5: Rule-based control algorithm operational cost optimization of domestic buildings presents a novel control algorithm for optimising operational costs of a combined domestic micro-CHP, boiler, battery and heat storage system. This chapter illustrates the importance of the control algorithm. Also, this chapter shows that with the combination of HESSs and CHP systems, the installation cost of the EH system has not been significantly increased, however the daily energy cost savings have been greatly improved. In other words, system daily return on investment has been improved.

Chapter 6: Results and analysis compares the daily investment cost, daily benefit cost ratio, effective energy efficiency of CHP and average CHP input power to rated power ratio between the houses only installed CHP and the houses installed CHP and HESS. This chapter shows the importance of the HESSs and gives suggestions to households on selecting CHP and HESSs.

Chapter 7: Conclusions and further work summarizes the main achievements of this thesis and analyses the limitations of this work. By analysing the limitation of this work, further work is proposed.

1.3 Executive summary of key contributions in each chapter

Chapter 3: Sizing CHP and domestic building energy cost optimization

1. The MR method and the GA method were used to find the best CHP size and the optimal operational cost of the Energy Hub. By using the MR to size the CHP, the variables in GA were reduced. This reduced the computation time.

2. The CHP output efficiencies (both heat and electricity) were formulated to functions which were related to the input power.

3. Heat demand dependent and electrical demand dependent CHP sizing were both considered, and at the same time, two types of CHP were also considered in this chapter.

Chapter 4: Sizing hybrid energy storage systems

4. Three key factors (State of Charge (SOC), charge/discharge current and control strategy) were comprehensively considered for the optimization of sizing the HESS.

5. In order to reduce variables, the optimization problem was formulated to a function related solely to battery capacity for simplification.

6. Defining the operation area of HESSs graphically was very useful in avoiding battery capacity saturation, battery discharge current saturation and battery SOC saturation.

Chapter 5: Rule-based control algorithm operational cost optimization of domestic buildings

7. This work proposed a rule based Energy Hub optimization method, which was computationally efficient and easy to implement.

8. The simulation time step of the proposed method was 1 min, which reflected the variation of the loads in domestic buildings.

9. The work proposed a simple load prediction rule and binary CHP switch control. By doing that, the error rate of CHP control caused by load prediction were very low (less than 3%). Meanwhile, due to CHP always working at rated power, the whole system energy efficiency was greatly improved.

10. A dual battery system was proposed to support the micro-CHP as system electricity suppliers. By doing this, the overall battery system lifetime was improved.

11. This work considered the re-start time of the CHP system; and by using the ‘removing glitch’ and the ‘filling gap’ method, the CHP worked in a more constraint aware way.

Chapter 2. The Energy Hub models and system definition

In order to reduce energy cost and acquire reliable and sustainable energy resources, many optimization rules, including demand side management, dynamic programming, the genetic algorithm, priority list and so on, are proposed for solving energy generation, transmission, conversion, protection and storage problems [10-14]. Nowadays, many engineers are continuing work on finding better optimization models and laws, although existing methods are adequate for solving energy system problems. The Energy Hub model, which was introduced into detail by Martin Geidl in 2007, is a powerful example of a new optimization model for multi-energy system problems [15].

2.1 The Energy Hub model

2.1.1 Energy Hub concepts and functions

The Energy Hub model can be used to model multi-energy carriers in a single energy system or energy flow between different energy systems. Figure 2.1 shows an example of an Energy Hub, which contains a gas tank, a gas turbine, heat storage and a heat exchanger.

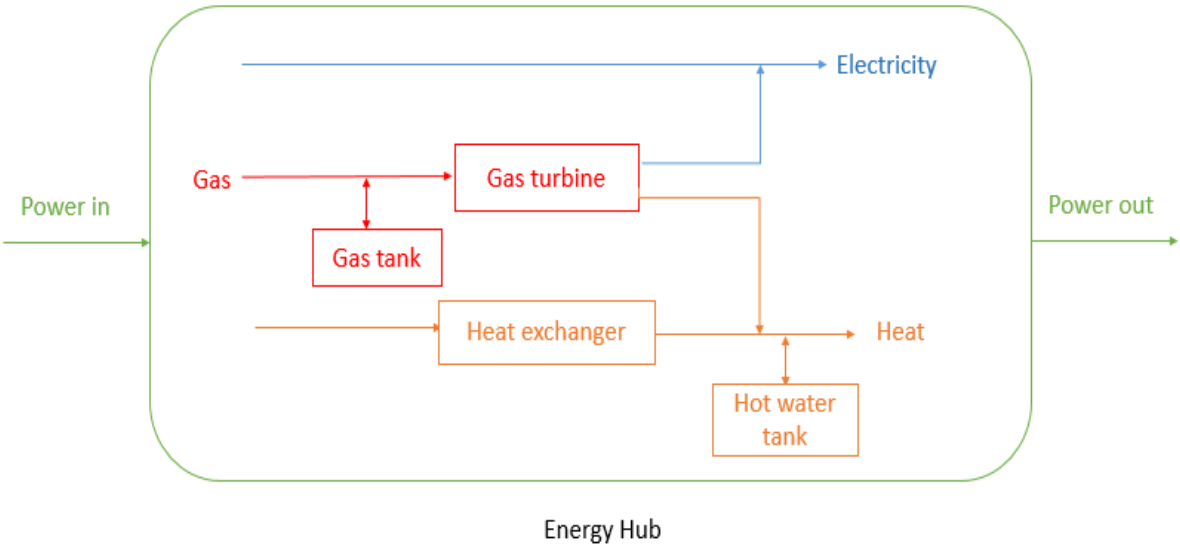

Figure 2.1 An example of an Energy Hub (which contains gas tank, gas turbine, heat storage and heat exchanger).

Transmission (direct connection), conversion and storage are three basic functions of an Energy Hub. In an Energy Hub, energy resources (e.g., electricity) can be transmitted from an input to the output without changing form or significantly changing quality, and this is called a direct connection. Besides that, energy resources can be converted from one form to another. For example, CHP can convert gas to heat and power. This is its second function: conversion. Finally, some Energy Hubs contain storage infrastructures, which are used to store energy that can be used later.

2.1.2 Applications and benefits

Energy Hub models, which were first proposed to deal with Greenfield Design studies [16], can be applied to many facilities; for example, power plants, island power systems and domestic buildings.

Compared with other models, Energy Hub models have clear benefits. First, Energy Hub models have two functions: they can be applied to a single energy system (for example, a house, a hospital and so on), and they can be used to analyse the power flow between each single energy system. Then, from energy diversity aspect, Energy Hubs perform better due to their multiple energy sources. Multiple energy sources improve the availability of energy for the load, because the load is no longer dependent on a single supplier. Moreover, system flexibility is increased by offering more pathways to supply the load. These multiple pathways also increase the optimization potential. Another advantage of Energy Hub models is that the implementation and energy cost, related emission, and other criteria can be optimized by choosing different combinations of input energy vectors. Finally, electrical energy system loss is reduced due to electrical energy storage systems being installed locally, which significantly improves electrical energy efficiency [17].

2.1.3 Energy Hub modelling

Before modelling the Energy Hub, three assumptions will be made. Firstly, within Energy Hubs there are no other form of losses besides conversion losses and storage losses. Secondly, the system being modelled has already reached a steady-state. The third assumption is that energy always flows from inputs to outputs.

The Martin Geidl model

Generally speaking, in Energy Hub modelling, the power flow within an Energy Hub is usually represented by different kinds of matrices and vectors. The Geidl model is used to analyze how does output vector change with different coupling matrices at given inputs.

In order to derive the relationship between input vectors and output vectors of an Energy Hub, energy conversions must be introduced. There are four kinds of convertors: single input and single output, single input and multiple outputs, multiple inputs and single output and multiple inputs and multiple outputs. For all kinds of conversions, coupling factors are less or equal to 1. Figure 2.2 shows the energy conversion system in an Energy Hub.

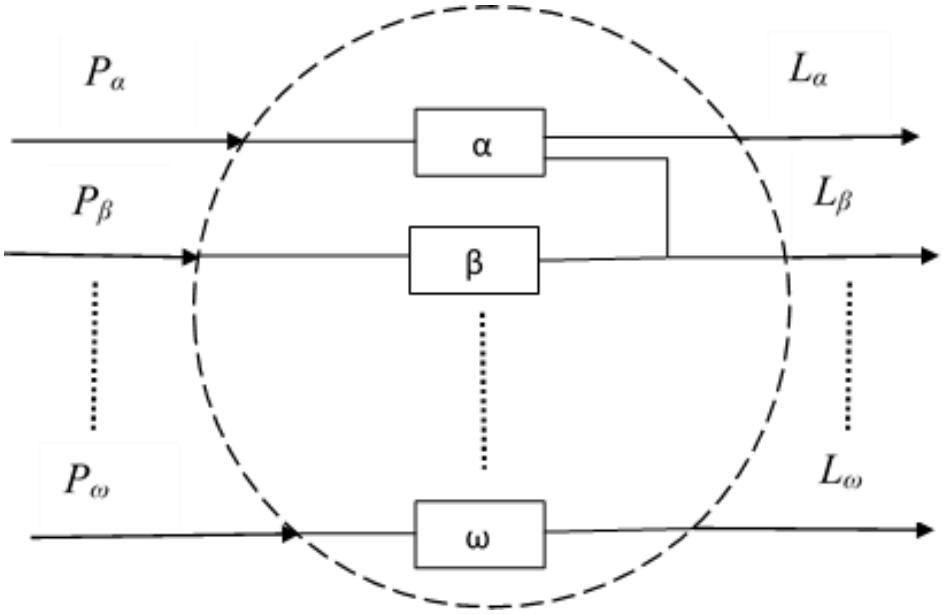

Figure 2.2 The energy conversion system in an Energy Hub.

The formulation of energy conversion in an Energy Hub can be represented as:

$$\begin{bmatrix} L_\alpha \\ L_\beta \\ \vdots \\ L_\omega \end{bmatrix} = \begin{bmatrix} c_{\alpha\alpha} & c_{\beta\alpha} & \cdots & c_{\omega\alpha} \\ c_{\alpha\beta} & c_{\beta\beta} & & c_{\omega\beta} \\ \vdots & \vdots & \ddots & \vdots \\ c_{\alpha\omega} & c_{\beta\omega} & \cdots & c_{\omega\omega} \end{bmatrix} \begin{bmatrix} P_\alpha \\ P_\beta \\ \vdots \\ P_\omega \end{bmatrix} \quad (2.1)$$

Where $P_\alpha, P_\beta, \ldots, P_\omega$ are elements in input vectors, are $L_\alpha, L_\beta, \ldots, L_\omega$ elements in output vectors and $C_{\alpha\alpha}, C_{\beta\alpha}, \ldots, C_{\omega\omega}$ are elements in coupling matrix. Note that the conversion

efficiency will be equal to the coupling factor only when the convertor has single input and single output.

The mathematical formulation is simple when an Energy Hub only contains the energy conversion system; however, for most Energy Hubs, the energy storage system is a crucial part. System complexity will be greatly increased if energy storage elements are added in the Energy Hub system [18, 19]. In addition, the Energy Hub model will no longer be a linear one (considering the facts that storage elements have standby loss and storage systems charge/ discharge efficiencies might not be constant). Figure 2.3 shows a simplified model of an Energy Hub which contains storage elements.

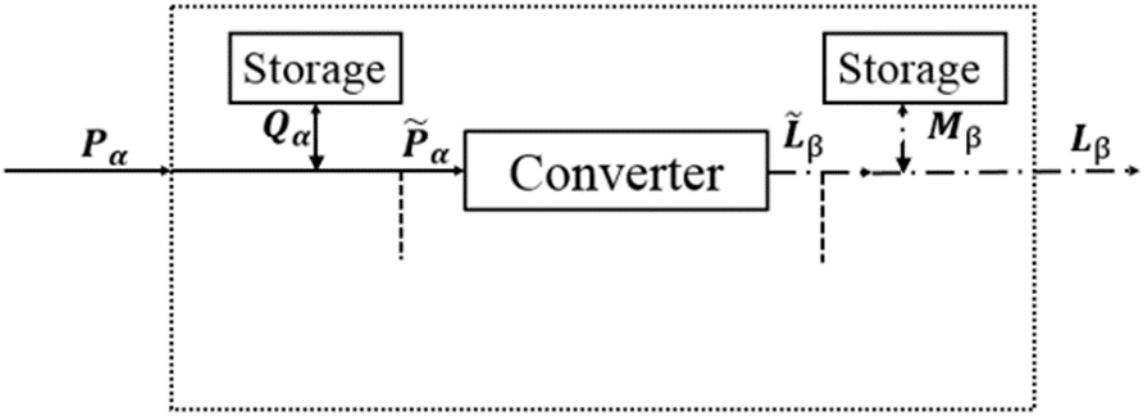

Figure 2.3 A simplified version of an Energy Hub which contains storage elements.

As Figure 2.3 shows, in general, energy flows in an Energy Hub can be written as:

$$\boldsymbol{L} + \boldsymbol{M} = \boldsymbol{C}[\,\boldsymbol{P} - \boldsymbol{Q}] \tag{2.2}$$

where $\boldsymbol{C}$ represents the coupling matrix and normally does not equal to the energy conversion efficiency. $\boldsymbol{L}$ and $\boldsymbol{P}$ are the output energy vector and the input energy vector of hub respectively. $\boldsymbol{M}$ and $\boldsymbol{Q}$ are the energy storage vector at the output and the input side of an Energy Hub, respectively. If a new vector $\boldsymbol{M_E}$, the equivalent energy storage vector, is defined as:

$$\boldsymbol{M_E} = \boldsymbol{CQ} + \boldsymbol{M} \tag{2.3}$$

Then, energy flows within an Energy Hub can be expressed as:

$$\boldsymbol{L} = \boldsymbol{CP} - \boldsymbol{M_E} \tag{2.4}$$

In order to get $\boldsymbol{M_E}$, more research should be done to analyse storage devices. Figure 2.4 shows a model of an energy storage device. Total energy stored in the device is E_α, internal power is $\tilde{Q}_\alpha$, and power exchange is Q_α.

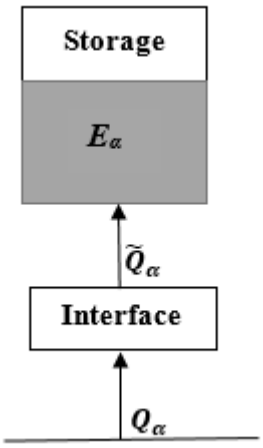

Figure 2.4 A model of energy storage device.

Now, internal power and power exchange can be related as:

$$\tilde{Q}_{\boldsymbol{\alpha}} = e_\alpha Q_\alpha \tag{2.5}$$

where e_α is energy exchange efficiency. To be specific, this factor is not constant and can be influenced by the direction of energy flow.

$$e_\alpha = \begin{cases} e_\alpha^+ & if\ Q_\alpha \geq 0 \quad (charging/standby) \\ \frac{1}{e_\alpha^-} & else \qquad\qquad\qquad (discharging) \end{cases} \tag{2.6}$$

Thus, the total energy stored in the energy storage equipment after a certain period T, ($E_\alpha(T)$), is:

$$E_\alpha(T) = E_\alpha(0) + \int_0^T \tilde{Q}_\alpha(t)dt \tag{2.7}$$

For steady-state consideration, power flows in the energy storage equipment ($\tilde{Q}_\alpha$) can be approximated by:

$$\tilde{Q}_\alpha = \frac{dE_\alpha}{dt} \approx \frac{\Delta E_\alpha}{\Delta t} \triangleq \dot{E}_\alpha \tag{2.8}$$

$\Delta E_\alpha$is the change in energy and Δt is the time period of energy change. For a steady-state case, the slope $\frac{dE_\alpha}{dt}$ is almost a constant. So combine equations (2.3), (2.5), (2.8) and Figure 2.3, the general expression for $\boldsymbol{M_E}$ is:

$$M_\beta^{eq} = c_{\alpha\beta} Q_\alpha + M_\beta = \frac{\boldsymbol{c_{\alpha\beta}}}{\boldsymbol{e_\alpha}} \dot{\mathrm{E}}_{\boldsymbol{\alpha}} + \frac{\mathbf{1}}{\boldsymbol{e_\beta}} \dot{\mathrm{E}}_{\boldsymbol{\beta}} \tag{2.9}$$

The matrices expression for energy storage systems in an Energy Hub can be written as:

$$\underbrace{\begin{bmatrix} M_\alpha^{eq} \\ M_\beta^{eq} \\ \vdots \\ M_\omega^{eq} \end{bmatrix}}_{\boldsymbol{M}} = \underbrace{\begin{bmatrix} s_{\alpha\alpha} & s_{\beta\alpha} & \cdots & s_{\omega\alpha} \\ s_{\alpha\beta} & s_{\beta\beta} & & s_{\omega\beta} \\ \vdots & \vdots & \ddots & \vdots \\ s_{\alpha\omega} & s_{\beta\omega} & \cdots & s_{\omega\omega} \end{bmatrix}}_{\boldsymbol{S}} \underbrace{\begin{bmatrix} \dot{\mathrm{E}}_\alpha \\ \dot{\mathrm{E}}_\beta \\ \vdots \\ \dot{\mathrm{E}}_\omega \end{bmatrix}}_{\boldsymbol{\dot{E}}} \tag{2.10}$$

$\boldsymbol{S}$ and $\boldsymbol{\dot{E}}$ represent the storage coupling matrix and the storage energy derivatives vector respectively.

Overall, the basic relationship between the inputs and the outputs of an Energy Hub is:

$$\boldsymbol{L} = \boldsymbol{CP} - \boldsymbol{S}\dot{\mathrm{E}} = [\boldsymbol{C} \quad -\boldsymbol{S}] \begin{bmatrix} \boldsymbol{P} \\ \boldsymbol{\dot{E}} \end{bmatrix} \tag{2.11}$$

The Fabrizio Model

Fabrizio used a similar method to model an Energy Hub. The only difference is that Fabrizio focused on analyzing how to achieve minimum cost at a given demand [20].

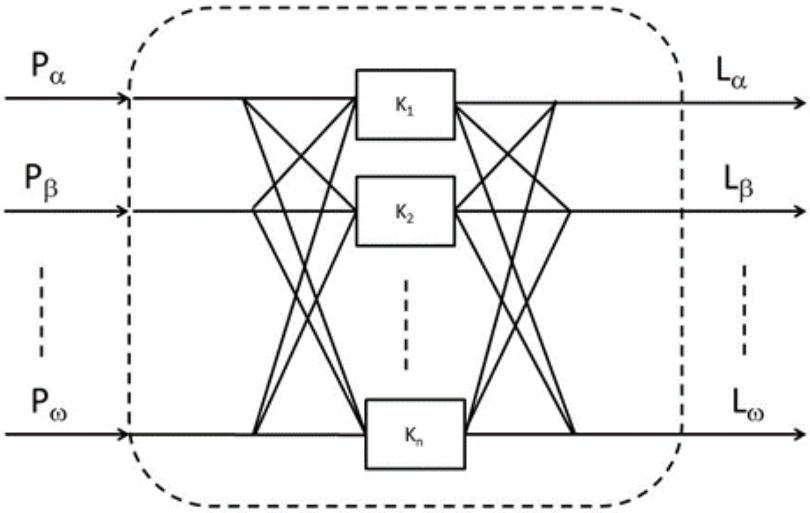

Figure 2.5 A generic Energy Hub model without energy storage equipment [3].

In this model, input power is expressed as the sum of output power plus stored energy. Without energy storage, input power (for a multi-energy carriers system, shown in Figure 2.5) can be written as:

$$\boldsymbol{P_{in}^{\alpha}} = \frac{\varepsilon_{k1}^{a}}{\eta_{K1}} \boldsymbol{L_{out}^{a}} + \frac{\varepsilon_{k2}^{b}}{\eta_{K2}} \boldsymbol{L_{out}^{b}} + \cdots \tag{2.12}$$

η_{Ki} is the conversion efficiency of the generic converter i, and $\eta_{Ki}$is greater than zero and less than one. ε_{ki}^{a} is the portion between the load a covered by the converter K_i and the load a. $\boldsymbol{P_{in}^{i}}$ and $\boldsymbol{L_{out}^{b}}$ are the inputs and outputs of the system, respectively.

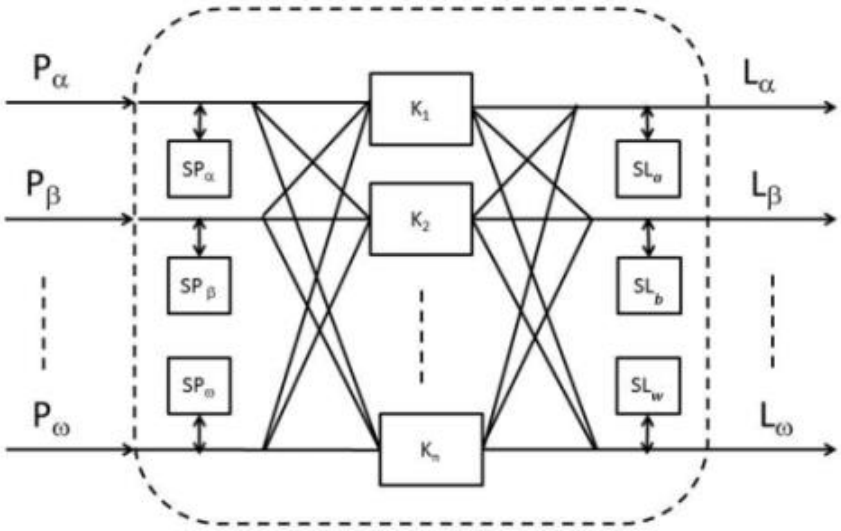

Figure 2.6 A complete version of Fabrizio Energy Hub Model [3].

There will be small modifications to the formula, when energy storage systems are added in. Figure 2.6 is a complete version of the Fabrizio Energy Hub Model. The mathematical expression for $\boldsymbol{P_{in}^{\alpha}}$ will be:

$$\boldsymbol{P_{in}^{\alpha}} = \frac{\boldsymbol{\varepsilon_{k1}^{a}(1+\Omega^{a})}}{\boldsymbol{\eta_{K1}(1-\Omega^{\alpha})}} \boldsymbol{L_{out}^{a}} + \frac{\boldsymbol{\varepsilon_{k2}^{b}(1+\Omega^{b})}}{\boldsymbol{\eta_{K2}(1-\Omega^{\beta})}} \boldsymbol{L_{out}^{b}} + \cdots \tag{2.13a}$$

$$\Omega^{i} = \frac{\boldsymbol{P_{sto}^{i}}}{\boldsymbol{P_{out/in}^{i}}} \tag{2.13b}$$

A new parameter Ω^{i} is defined as the storage factor of energy i. Ω^{i} relates the energy flow –entering or leaving the storage- to the energy flow at the input or at the output of the hub. P_{sto}^{i} is energy flow entering or leaving a storage. For $\Omega > 0$, the store is charging and vice versa. Now, the matrix representation of the Fabrizio Energy Hub model can be summarised as:

$$\begin{bmatrix} P_{\alpha} \\ P_{\beta} \\ \vdots \\ P_{\omega} \end{bmatrix} = \begin{bmatrix} D_{\alpha\alpha} & D_{\beta\alpha} & \cdots & D_{\omega\alpha} \\ D_{\alpha\beta} & D_{\beta\beta} & \cdots & D_{\omega\beta} \\ \vdots & \vdots & \ddots & \vdots \\ D_{\alpha\omega} & D_{\beta\omega} & \vdots & D_{\omega\omega} \end{bmatrix} \begin{bmatrix} L_{\alpha} \\ L_{\beta} \\ \vdots \\ L_{\omega} \end{bmatrix} \tag{2.14}$$

Also, it can be expressed in a simple way; equation (2.15) is the model's mathematical representation.

$$\boldsymbol{P_{in}} = \boldsymbol{D} * \boldsymbol{L_{out}} \tag{2.15}$$

In equation (2.15), $\boldsymbol{D}$ is called backwards coupling matrix. The backward coupling matrix can clearly show energy conversion, transmission and storage in an Energy Hub.

2.1.4 Energy Hub optimization

At the moment there are two existing Energy Hub models, it is likely that there will be more in the future. When using these models to deal with energy-system optimization requires formulating all problems into mathematical functions. Normally, energy cost and green-house gas emission are the key factors that need to be considered. In order to get a reasonable answer, engineers need to find the maximum or the minimum value of the objective functions.

The mathematical formulations (nonlinear) of the general optimization question are the followings:

$$Minimize \qquad F(x) \tag{2.16}$$

$$Subject\ to \qquad g(x) = 0 \tag{2.17}$$

$$h(x) \leq 0 \tag{2.18}$$

where $F(x)$ are scalar-valued objective functions, $g(x)$ normally comes from the conservation of power and $h(x)$ normally comes from limits, e.g. maximum output power, or number of converters.

Energy Hub models can be used to link different energy carriers in a multi-energy carrier system together. This will offer a more comprehensive guide to deal with energy cost, energy generation, carbon emission and low energy efficiency problems within a domestic building. Therefore, more and more researchers use Energy Hub models to optimize power flow and carbon emission in domestic buildings.

On the other hand, Energy Hub models translate entire engineering problems to mathematical problems. By solving equality and inequality constrains, a theoretical optima result can be acquired. However, this might not yield the best result in the optimization criteria. This is because for a non-convex function, there are many local minimums. Due to this reason, it will be helpful to apply this model to different control algorithms and compare the different results.

Even though Energy Hub models have slight limitations, for instance, the system always assumed to reach a steady state, they are still a very useful tool to analyze power flow within a domestic building. In this thesis, Energy Hub models will first be used, together with the genetic algorithm and the maximum rectangle algorithm, to size the capacity of a CHP and optimize daily energy cost for a domestic building without an energy storage system. Then Energy Hub models will be used, together with the proposed rule-based energy control algorithm to optimize daily energy cost for a domestic building with a energy storage system. With Energy Hub models, heat and electricity energy within a domestic building can be coherently considered, which will give a better energy cost optimization result.

2.2 System definition

There are many physical and behavioral factors that can significantly influence the energy demand in domestic buildings. For example, dwelling size, building shape and climate are physical factors, and these factors are highly related to climate and building design. On the other hand, the way people use heaters, washing machines and so on are behavioral factors, which may be slightly influenced by season, but strongly related to households' habits. Thus, even for the same type of domestic building, energy consumption pattern is different for different households [21].

Many existing works [21-26], describe how to model energy consumption in domestic buildings. This thesis will use the CREST electricity model, which was demonstrated in [23], to generate daily electricity load and use Strathclyde University heat model, which was demonstrated in [21], to generate daily heat load. This is because both of these models are based on analyzing UK domestic building energy consumption and therefore the load generated by these models are more accurate to reflect energy consumption at domestic building level in the UK.

As mentioned before, energy demand can be significantly influenced by physical and behavioral factors. Therefore this thesis will use, a terraced houses built in the UK between 1984 and 1997, which were all occupied by four people, as an example to test the proposed optimization rules.

The gas price is based on the current UK domestic gas price which is around 5 pence/ kWh, and the electricity tariff is obtained in [27], which proposes a dynamic system of tariffs which vary on a half hourly timescale. The daily electricity price in each minute for different seasons is shown in Figure 2.7.

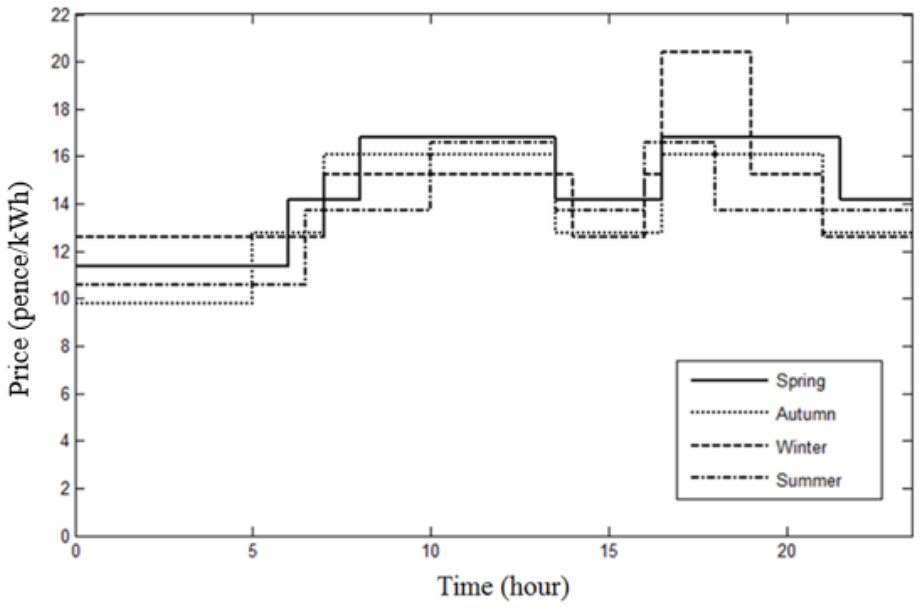

Figure 2.7 Daily electricity price in different seasons.

For a conventional building, electricity can only be obtained directly via the grid and heat can be acquired from the gas grid via a boiler. The overall heat efficiency of a boiler in this thesis is assumed to be 88% [28]. The daily energy cost of the conventional building will be used as the base case in this thesis. In next chapters, by adding a high cost, high efficiency micro CHP unit in the building is the main distinction compared with the conventional building. Even though it needs to consume energy, the high output efficiency from co-generation makes it still one of the most promising technologies to resolve energy–related problems [29]. Compared to renewable energy, CHP is more stable and controllable, and moreover it can generate heat and electricity at the same time. In this thesis, there are two types of micro CHP which will be introduced- gas engine CHP and fuel cell. The rated heat efficiencies of gas engine CHP and fuel cell CHP are 66% and 50 %, and rated electricity efficiencies of gas engine CHP and fuel cell CHP are 22% and 37% [30].

The energy storage system installed in this building is comprised by two parts. The hybrid energy storage system (HESS) is used to store electrical energy and hot water tank is used to store heat. In the thesis, the overall efficiency of battery, supercapacitor and water tank are 80%, 98% and 70% respectively [31, 32]. The standby loss of the battery is set as 2% per month [33]. The standby loss of the hot water tank strongly depends on ambient temperature and the design of the hot water tank [32], therefore, the standby loss of the hot water tank storage is set as 25% a day. Figure 2.8 are used

to show the energy carriers and the layout of energy infrastructures in the building and Table 2.1 is a summary of key system parameters.

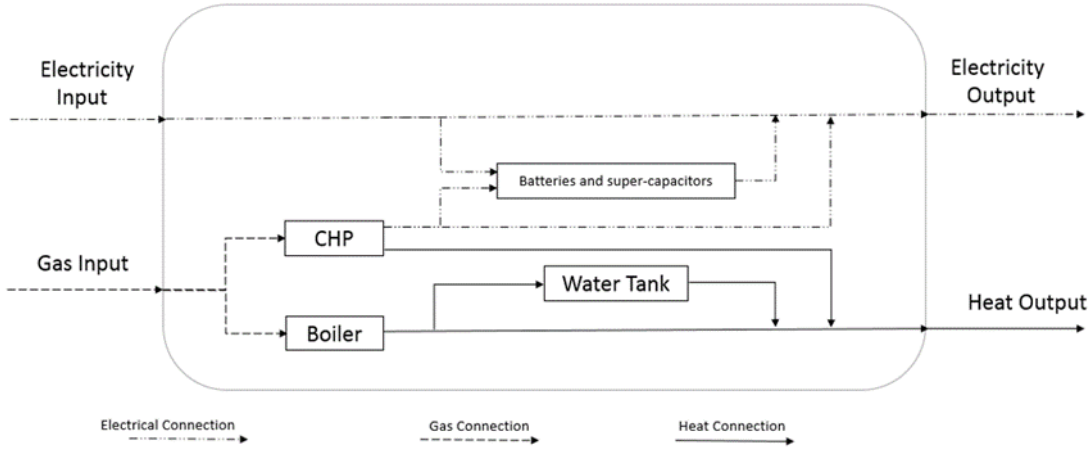

Figure 2.8 Energy flow in the smart building.

Table 2.1 Key system parameters used in the thesis.

Parameters	Value	References
Boiler gas to heat conversion efficiency	88%	[28]
Gas engine CHP rated electricity conversion efficiency	22%	[30]
Gas engine CHP rated heat conversion efficiency	66%	[30]
Fuel cell CHP rated electricity conversion efficiency	37%	[30]
Fuel cell CHP rated heat conversion efficiency	50%	[30]
Battery system overall efficiency	80%	[31]
Supercapacitor system overall efficiency	98%	[31]
Hot water tank energy storage efficiency	70%	[32]
Battery storage system monthly standby loss	2%	[33]
Hot water tank storage system daily standby loss	25%	[32]

Chapter 3. Sizing CHP and domestic building energy cost optimization

The number of CHP units installed in domestic buildings is increasing rapidly in recent years, due to the fact that CHP has the potential to increase energy efficiency, to improve energy controllability and to reduce energy costs and carbon emissions [29]. However, installing CHP with inappropriate capacity may increase energy costs and reduce energy efficiency. In addition, the high manufacturing cost of battery storage systems makes batteries less affordable in domestic buildings. Therefore, this chapter will attempt to size the capacity of CHP and optimize daily energy costs for a domestic building with only CHP installed.

At the beginning of this chapter, electricity and heat loads are used as sizing criteria in finding the best capacities of gas engine and fuel cell CHP with the help of the maximum rectangle method (MR). Subsequently, the genetic algorithm optimisation technique (GA) will be used to optimise the daily energy costs of the different cases. Then, heat and electricity loads are jointly considered for sizing different types of CHP and for optimizing the daily energy costs through the GA method. Finally, it will be suggested that optimization results show that the GA sizing method gives a higher average daily energy cost saving, which is 13% reduction compared to the base case defined in chapter 2. However to get this result, there will be about 3% energy efficiency reduction and 7% input power to rated power ratio reduction compared to using the MR method and heat demand in sizing CHP.

3.1 Introduction

Combined heat and power units are regarded as one of the most promising low carbon technologies in solving energy-related problems, because they have many advantages when compared with other energy generation technologies [29]. First, compared to conventional energy generation systems, CHP systems have much higher overall output efficiencies and because of that CHP units are installed to reduce carbon emission [34]. Secondly, in the case of renewable energy generation systems, climate change has less influence on CHP system control [35]. Moreover, the installation cost

of a CHP unit is gradually decreasing. In [36], it is predicted that by the end of 2015 the capital cost of a CHP system will be around €374/ kW. Similar to the prediction results shown in [36], the micro-CHP installation costs in 2016 is £300 /kW [37]. Therefore more micro-CHP units, whose output power are ‘kW levels’, are being installed in domestic buildings.

Batteries are still one of mature technologies to store electricity, and they can be used to improve energy system efficiency and to reduce carbon emission; however, the installation cost and maintenance cost of a battery storage system are very high. Therefore it is worth considering whether it is economical to install a battery storage system in a domestic building whose electricity load is supplied by a CHP unit and the grid and the heat load is supplied by a CHP unit and gas boiler.

Without an energy storage system, the key factors that can influence the daily energy costs and energy efficiency of aforementioned buildings are the capacity of the CHP and the type of CHP [30]. Previous literature has already shown that the electricity output efficiency of micro-CHP is a quarter of its rated value when the CHP is operated at 10% of its rated power. Meanwhile, the heat output efficiency can also be reduced, if the CHP is working at low input power [29]. To increase energy efficiency and reduce emission, it is always preferable to have small capacity CHP in buildings. However, small scale CHP cannot meet the load at the peak demand time, even though it works at rated power. This will significantly increase the system’s daily energy costs. To reduce this cost, it is preferable to have large size capacity CHP. Thus, to improve both energy efficiency and system daily benefits it is important to size CHP in domestic buildings.

To get an appropriate capacity of CHP, selecting sizing criteria is crucial, because optimization results will differ depending upon the optimization criteria used. Types of CHP and particular demand are two popular criteria that are used to size the CHP.

This research considers two common types of CHP: gas engine and fuel cell. The main difference between these two CHP units is in output efficiency. Fuel cell CHP normally has a higher electricity to heat output efficiency ratio compared to gas engine CHP [38]. In [39], the rated electricity to heat output efficiency ratios for the fuel cell and gas engine CHP are about 33% and 74% respectively.

In domestic buildings, there are normally two types of demands: heat and electricity. They can be used as another criteria to size CHP. This is because the heat and electricity consumption patterns in a domestic house are quite different from each other. In [36, 40], using the heat demand curve to size and control the CHP is preferable, because CHP thermal output efficiency is normally greater than electricity, and in [36], it is assumed that the redundant electricity can be sold back to the grid. However, there are increasingly higher requirements to sell electricity back to the grid in Europe. For example the European standard EN50160 states that the 10-min average root mean square voltage deviation should not exceed ± 10% of the nominal voltage [41]. Considering this and the fact that many electricity meters do not have ability to record electricity sent back to the grid, this chapter assumes that there is no financial benefit from export, thus export is avoided.

When dealing with energy system problems, many optimization algorithms can be used, for example the genetic algorithm (GA) [42, 43], maximum rectangle method (MR) [44], linear programming (LP) [45, 46], and non-linear programming (NLP) [47-49].

In this chapter, the MR will be used to optimize the size of gas engine and fuel cell CHP for a domestic house, based firstly on the daily heat load and secondly on the electricity load curves. This is because the MR can cover an ‘average’ heat and electricity demand instead of covering the maximal heat or electricity demand, and thus make full use of CHP capacity and improve CHP output efficiencies [36]. After that, because the GA is a powerful tool to deal with multivariable non-linear problems, the GA will be used to calculate the optimal daily operational cost. To test the optimization results generated by the MR and GA methods, the GA method will be used individually to find the best size of gas engine and fuel cell CHP, and to calculate the theoretical minimum daily energy cost. At this time, heat and electricity demand will be considered together.

To reduce variables in the optimization algorithms, [50] assumes that the CHP output efficiencies are constants for different operational conditions. However, this assumption gives a higher energy efficiency and a lower daily energy cost in optimization results. In order to eliminate the impacts of this assumption, this chapter uses the experimental results in [29] to formulate the CHP output efficiencies as

functions that are only related to CHP input power. This will improve the accuracy of optimization results and the output efficiencies of CHP.

The major contributions of this chapter are: 1) Two different sizing CHP methods (the MR and the GA) are used to find the optimal size of CHP. The computation time is significantly reduced by using the MR method and the optimal costs are lower when using the GA method. 2) The CHP output efficiencies are formulated to functions which are only related to input power and this gives a more accurate optimization result compared to using constant CHP output efficiencies as optimization criteria. 3) Different types of CHP and loads are considered as sizing criteria, and the optimization results will give suggestions for engineers on how to choose and size CHP.

3.2 Optimization methodology

3.2.1 The genetic algorithm method

The genetic algorithm method is popular in solving optimization problems, and previous literature has proven that it is especially successful in solving single objective optimization problems. Moreover, for multi-objective optimization problems, the genetic algorithm is intelligent enough to balance the trade-offs between each conflicting objective [43].

Compared with other optimization algorithms, the genetic algorithm method shows its strong ability of dealing with non-linear and non-continuous optimization problems [51]. The genetic algorithm can give highly accurate results, however it normally needs a relatively long computation time.

There are four key factors of the genetic algorithm: chromosomes (individuals), selection, crossover and mutation. By analogy to natural evolution, individuals are the solution candidates and each individual contains some variables. The set of individuals is called the population and the number of individuals in each population is population size. The selection process selects high-quality individuals and removes low-quality individuals. In this process, the genetic algorithm defines a scale value called fitness, and this value can be used to show the performance of the optimization results. Finally,

crossover and mutation are the most important part of the GA. The crossover and mutation are used to generate new solutions within the search space. The offspring produced after the crossover and mutation will perform better in their environment due to higher fitness. The algorithm is terminated successfully when an individual emerges with an acceptably high fitness. In the following work, the chromosome, selection, crossover and mutation values used in this thesis are the default values of the GA in MATLAB optimization toolbox.

As mentioned before, to get accurate results, the GA needs to take a longer computation time. However, this time is dependent on the generation and population size. Large and small generation and population size will reduce calculation efficiency.

3.2.2 The maximum rectangle method

The maximum rectangle method is normally used to size the energy generation equipment in a power system [36, 44]. Compared with other optimization algorithms, the maximum rectangle method focuses on finding the best capacity of an energy generator which can cover majority of energy consumption instead of covering the maximal demand.

To implement this method, loads (electricity or heat) distribution curves normally need to be acquired in advance. Figure 3.1 is an example of the maximum rectangle design method. By inserting the rectangles, the MR method tries to find the rectangle which has the maximum area. The width of the selected rectangle is the theoretical best capacity of generator.

As long as the load distribution curve can be formulated, this method can find the optimal generator capacity very quickly. Using the MR method to size generators always gives a higher benefit cost ratio to energy systems, because the MR method tries to find the energy generator’s capacity which can cover majority of energy consumption.

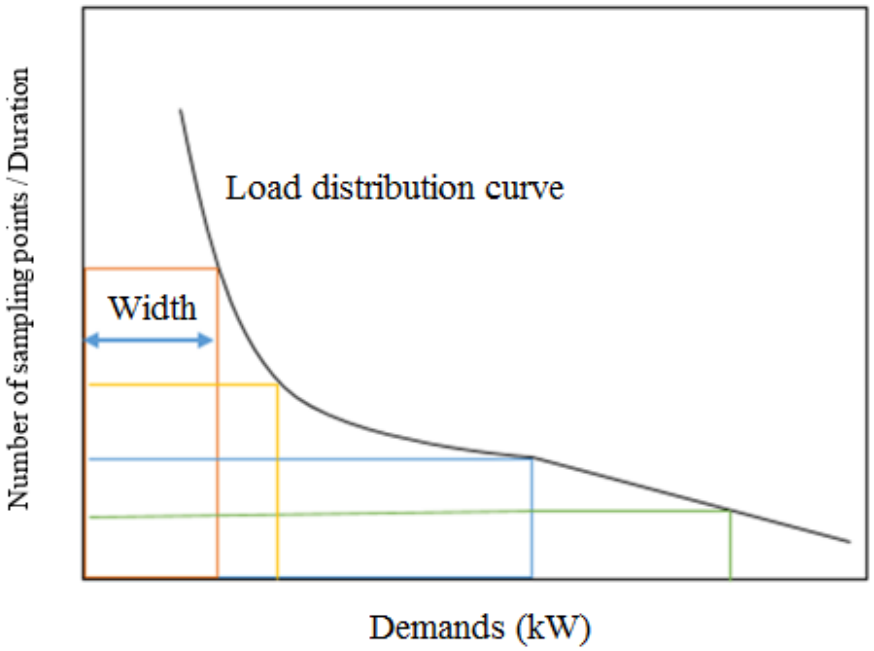

Figure 3.1 An example of the maximum rectangle design method.

3.2.3 The linear programming method

In power systems, the linear programming method is normally used to solve the optimal power flow and energy cost reduction problems [46, 52-54]. Use of the linear programming method is proposed to acquire the best outcome of a mathematical model whose constraints and objective functions can normally be expressed by linear relationships. The mathematical descriptions of the linear programming method can be outlined as:

$$\text{Maximize} \quad F(x) = c_1x_1 + c_2x_2 + \cdots + c_mx_m \tag{3.1a}$$

$$\text{Subject to} \quad a_{11}x_1 + \cdots + a_{1m}x_m \leq b_1$$

$$\cdots$$

$$a_{m1}x_1 + \cdots + a_{mm}x_m \leq b_m \tag{3.1b}$$

$$\text{and} \quad x_1, \ldots, x_m \geq 0 \tag{3.1c}$$

In equation (3.1a), (3.1b) and (3.1c), $a_{1m}, \ldots, a_{mm}$ and $c_1, \ldots, c_m$ are coefficients and $x_1, \ldots, x_m$ are the variables that need to be determined. Three steps need to be taken to solve

the linear programming problems. First, constraints and the objective function need to be listed. After that, it will be possible to find the feasible optimization area based on constraints. The final step will be finding the global minimum or maximum value of the function which is located in the feasible region.

The linear programming method is very adept at handling inequality constrains. However, all constrains are linearized when applying the linear programming method, and this can lead to loss of accuracy in the optimization results.

3.2.4 The nonlinear programming method

Similarly to the linear programming method, the nonlinear programming method can be used to solve the optimal power flow and energy cost reduction problems [55, 56]. The mathematical expression of the nonlinear programming method is similar to the linear one, and the only difference is that constraints and the objective function do not necessarily need to be linear functions. The nonlinear programming has outstanding performance in solving the convex optimization problem. However, for a non-convex function, this method has trouble in distinguishing the local minimums and the global minimum. Therefore, for a non-convex optimization problem, the nonlinear programming method is not the best choice.

3.3 CHP sizing and system optimization

In the following parts, 3.3.1 demonstrates how to size CHP by the MR method according to different sizing criteria. After obtaining the best CHP capacities for different sizing criteria, 3.3.2 shows how to use the GA method to optimise the daily energy cost. Similar to 3.3.2, 3.3.3 uses the same methodology (GA) to optimize the daily energy cost for different types of CHP and find the theoretical best CHP capacities for different CHP. In 3.3.4, effective CHP energy efficiency and average CHP input power to rated power ratio will be defined to test CHP efficacy performance.

3.3.1. Sizing CHP by the MR method

To use the MR method to size CHP based on electricity loads, five steps need to be taken.

Firstly, recording every minute's electricity demand in a year as sampling points is necessary. Secondly, the minimum and the maximum electricity demands in a year need to be found, and then equally divided into 10-20 intervals between maximum and minimum electricity demands. Because too many intervals (greater than 20) will cause the load distribution curve fluctuates, and this will give trouble to formulate load distribution curve. On the other hand, few intervals (less than 10) will reduce the accuracy of curve fitting result. Therefore, 10-20 intervals between maximum and minimum electricity demands are needed. Thirdly, all sampling points need to be placed into related intervals and the number of sampling points in each interval must be calculated. The fourth step is to plot the load distribution curve as shown in Figure 3.1. Finally, based on the load distribution curve, sufficient rectangles need to be drawn as shown in Figure 3.1, and a rectangle which has the maximum area can be found. The demand (width) of this rectangle should be the capacity of CHP rated electricity output. At this step, the more rectangles that are plotted, the more accurate a result will be acquired.

3.3.2 Daily energy costs optimization by the GA method

By applying the Energy Hub model and the Genetic Algorithm to the domestic building that was proposed in Chapter 2, the objective function can be written as:

$$F(t) = \sum_{t=1}^{t=1440} P_{Ein}(t) \times C_e(t) + P_{Gin}(t) \times C_g(t) + P_{CHPin}(t) \times C_g(t) \quad (3.2)$$

In equation (3.2), $F(t)$ is the daily energy cost, $C_e(t)$ and $C_g(t)$ are the electricity price and gas price in each minute in a day respectively, and $P_{Ein}(t)$, $P_{Gin}(t)$ and $P_{CHPin}(t)$ are the imported average electrical energy from the grid, imported gas to supply the boiler and imported gas to supply the CHP in each minute respectively. To meet the electricity demand and heat demand in the building, the equality constraints can be generated as:

$$P_E(t) = P_{Ein}(t) + \eta_{CHPE} \times P_{CHPin}(t) \quad (3.3)$$

$$P_H(t) = P_{Gin}(t) * \eta_B + \eta_{CHPH} \times P_{CHPin}(t) \quad (3.4)$$

In equation (3.3) and (3.4), $P_E(t)$ and $P_H(t)$ are the electrical energy demand and heat demand of the domestic building respectively in each minute. η_{CHPE} and η_{CHPH} are the

CHP output electricity and heat efficiency respectively. η_B is the boiler's gas to heat conversion efficiency. In addition, system limitations give extra inequality constraints which can be listed as follows:

$$\eta_{CHPEmin} \leq \eta_{CHPE} \leq \eta_{CHPEmax} \tag{3.5}$$

$$\eta_{CHPHmin} \leq \eta_{CHPH} \leq \eta_{CHPHmax} \tag{3.6}$$

$$P_{CHPin}(t) = 0 \text{ or } \zeta \times P_R \leq P_{CHPin}(t) \leq P_R \tag{3.7}$$

$$P_{Ein}(t) \geq 0 \tag{3.8}$$

$$P_{Gin}(t) \geq 0 \tag{3.9}$$

Equation (3.5) and (3.6) describe the CHP electricity and heat output efficiency limitation. Equation (3.7) shows that a CHP unit can either be switched off or work at its feasible operational conditions. In equation (3.7), P_R is rated/optimal power/capacity of CHP and ζ is a scaling factor. In [29], CHP input power can vary from 10% to 100% to its rated power. In this work, ζ is set as 10% and the optimal capacities acquired by the MR method will be used to find the daily optimal energy cost for each scenario. Equation (3.8) and (3.9) demonstrate that the electricity and heat can only be imported, not exported. In other words, they describe the direction of power flow.

As mentioned in the Introduction to this chapter, both CHP heat and electricity output efficiencies decrease if CHP is working at low input power situations. In this work, CHP output efficiencies are formulated to functions which relate to CHP input power. Table 3.1 shows the efficiencies of the CHP for different CHP inputs, obtained from [27].

Table 3.1 Output efficiencies of the CHP for different input power [29].

Input power/ Rated power (%)	Electricity efficiency (%)	Heat efficiency (%)
10	7.8	38.4
25	16.3	34.5
50	24.2	36.4
75	27.3	41.1
100	28.1	41.0

Based on Table 3.1, the electricity and heat output efficiencies of a general CHP unit can be formulated with the MATLAB curve fitting toolbox as follows:

$$\eta_{CHPE} = \xi_E \times \left(11.67 \times \log\left(\left(\frac{P_{CHPin}(t)}{P_R}\right) \times 100\right) - 0.06459 \times \left(\left(\frac{P_{CHPin}(t)}{P_R}\right) \times 100\right) - 18.76\right) \quad (3.10)$$

$$\eta_{CHPH} = \xi_H \times \left(0.1256 \times \left(\left(\frac{P_{CHPin}(t)}{P_R}\right) \times 100\right) + 82.32 \times \left(\left(\frac{P_R}{P_{CHPin}(t)}\right) \times 100\right) + 28.73\right) \quad (3.11)$$

In (3.10) and (3.11), ξ_E and ξ_H are the CHP electricity and heat output efficiency coefficients, and these values only relate to the type of CHP, or in other words, the design of CHP. Table 3.2 summarizes the electricity and heat output efficiency coefficients of the gas engine and the fuel cell CHP used in this chapter.

Table 3.2 Summary of gas engine and fuel cell CHP electricity and heat output efficiency coefficients.

Type of CHP	Electricity output efficiency coefficients (ξ_E)	Heat output efficiency coefficients (ξ_H)
Gas Engine	0.783	1.610
Fuel Cell	1.298	1.187

3.3.3 Theoretical best capacity of CHP by the GA method

In this section, the GA method is used to optimise the daily energy costs for a system with different CHP installation capacities. Then, by comparing the daily energy costs for different CHP installation capacities, the theoretical best CHP capacity can be acquired. However, considering the fact that the GA method normally takes a long computation time to get the optimization results and that the output of commercial CHP are normally quantised to 100 watt, this work will calculate the best capacity of each type of CHP in hundred watt discrete increments.

The objective functions, constraints and equations of this work are similar to 3.3.2. However, compared to 3.3.2, P_R will be treated as another new variable. This work will first find the feasible CHP capacity region and then find the best capacity of both type of CHP. The CHP output power will first be assumed to be 1000 W, and there will be 500 W increase every time until the output power of CHP reaches a point after which the daily energy cost will always increase with the increase of CHP capacity. At this stage, the GA method will be used to calculate the average daily energy cost for each CHP capacity. By plotting the rated capacity and average yearly energy costs graph, a feasible CHP capacity region can be acquired. Then the maximum and minimum capacity of this region is divided into 5 equal intervals, which means that 4 more samples need to be tested. By using the GA method to optimise daily energy costs of these four points, the theoretical best CHP can be acquired. Figure 3.2 is a diagram to show this method.

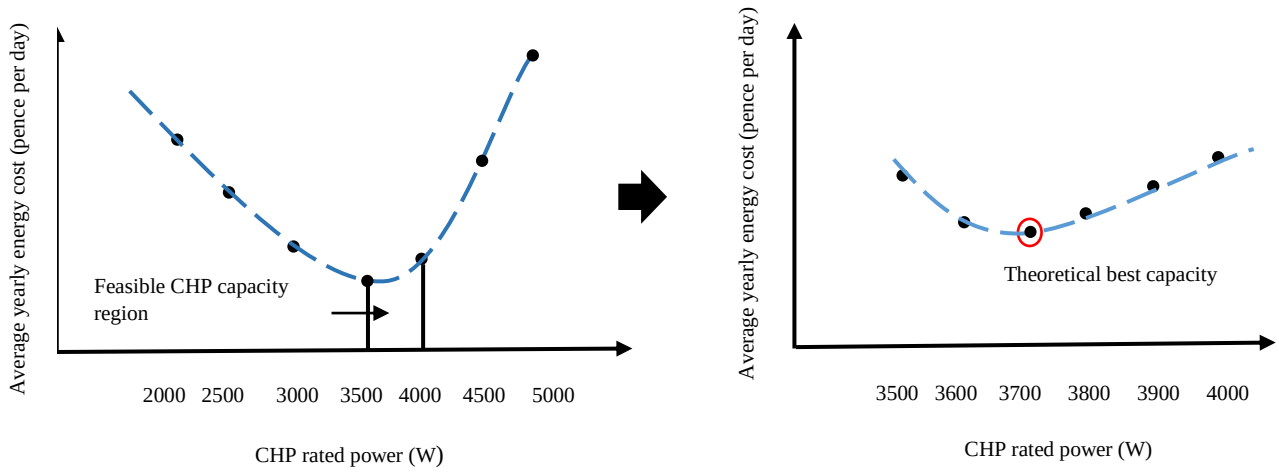

Figure 3.2 Using the GA method to find the theoretical best CHP capacity.

3.3.4 Effective CHP energy efficiency and average CHP input power to rated power ratio

As mentioned in the chapter introduction, CHP is a high output efficiency energy generator. However, system energy efficiency can be significantly reduced if an inappropriate capacity CHP unit is installed. Here, two parameters are defined to test the performance of CHP sizing results. First, the effective CHP energy efficiency is defined to calculate the average whole year CHP energy efficiency with different CHP capacities. Another parameter, average CHP input power to rated power ratio, is defined to illustrate whether the CHP is fully utilised. Equation (3.12) and (3.13) are the functions to show effective CHP energy efficiency and average CHP input power to rated power ratio.

$$\widetilde{\eta_{CHP}} = \frac{\sum_{t=1}^{t=L}(\eta_{CHPE}(t)+\eta_{CHPH}(t))}{L'}, \qquad (\eta_{CHPE}(t) + \eta_{CHPH}(t)) > 0 \tag{3.12}$$

$$h_{CHP} = \sum_{t=1}^{t=L}(P_{CHPin}(t)/P_R)\,/L' \tag{3.13}$$

In (3.12), $\widetilde{\eta_{CHP}}$ is effective CHP energy efficiency, $\eta_{CHPE}(t)$ and $\eta_{CHPH}(t)$ are the CHP electricity and heat output efficiency in t^{th} minute respectively and L' is the number of samples. In (3.12), both $\eta_{CHPE}(t)$ and $\eta_{CHPH}(t)$ should be greater than zero, because to calculate the effective CHP energy efficiency, the CHP switch off state should not be considered. In (3.13), h_{CHP} is the average CHP input power to rated power ratio.

3.4 Optimization results

3.4.1 CHP sizing results

The electricity demand distribution curve for the terraced house which was built between 1984 and 1997 is shown in Figure 3.3. Figure 3.3 indicates that the electricity loads are less than 1 kW most of the time of during the year for this household.

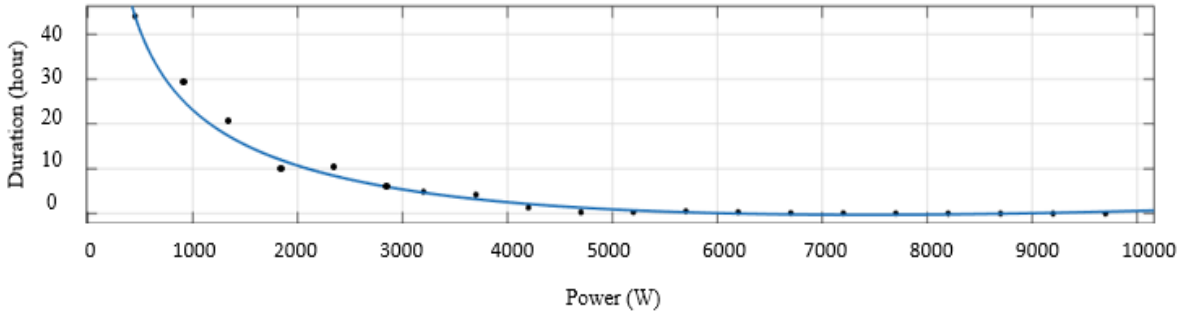

Figure 3.3 The electricity demand distribution curve for the terraced house which was built between 1984 and 1997.

By using the curve fitting tool in MATLAB, it is straightforward to formulate the relationship between electricity demands and the number of sampling points (duration) as:

$$y = a \times \frac{1}{x} + b \times x + c + d \times \log(x) \tag{3.14}$$

where a, b, c and d are coefficients and x is the electricity demand in Watts and y is the duration in hours. In this case, curve fitting results show that: a=8217; b=0.002193; c=117.3; d=-15.14. After obtaining the electricity demand distribution curve, the rectangles can be drawn in the diagram. In this work, the width of rectangles increase 1 W per increment and the width of rectangles start at 300 W, and end at 3000 W. This is because from Figure 3.3, domestic CHP electricity demand is normally greater than 300 W and less than 3 kW. Figure 3.4 shows the area of the rectangles against different CHP electrical output power.

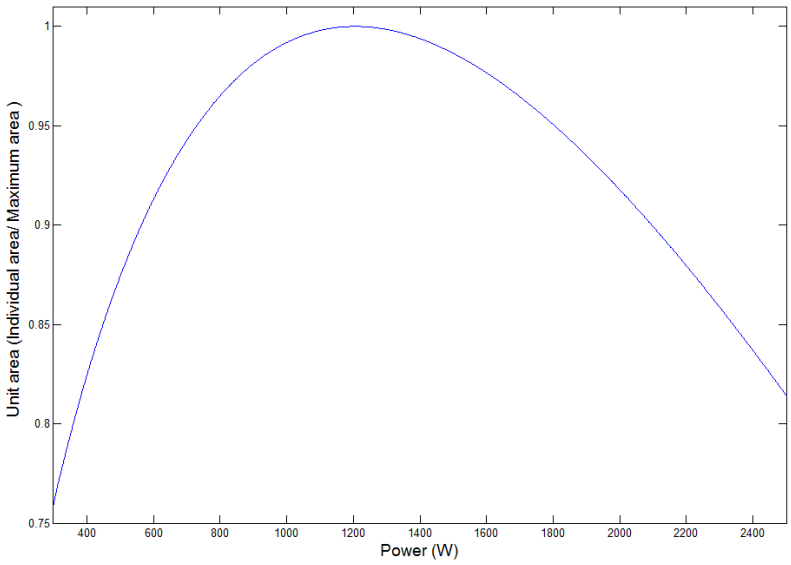

Figure 3.4 The area of rectangles for different CHP electrical output power.

Figure 3.4 shows that when the electrical output of CHP is 1206 W, the rectangle will obtain the maximum area. Based on previous gas engine and fuel cell CHP heat and electricity efficiencies assumptions (shown in page 17), the heat output of gas engine and fuel cell CHP should be 3618 W and 1630 W, respectively. In other words, if the electricity load is used as a criterion to size CHP, the optimal rated capacity of gas engine and fuel cell CHP should be 5482 W and 3259 W respectively.

The optimization process is the same when the heat demand is used as a criterion to size the capacity of CHP. Figure 3.5 shows the heat demand distribution curve for the terraced house which was built between 1984 and 1997. From Figure 3.5, the domestic heat demand for a terraced house are less than 3 kW in most cases.

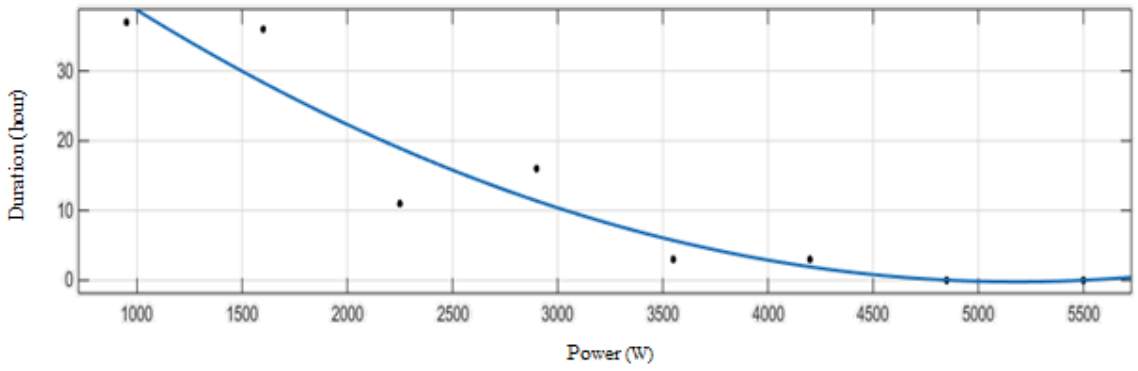

Figure 3.5 The heat demand distribution curve for the terraced house which was built between 1984 and 1997.

By using MATLAB curve fitting tool, the mathematic formulation of heat demands and the number of sampling points (duration) can be represented as:

$$y = a + b \times x + c \times x^2 \tag{3.15}$$

where a, b, and c are coefficients and x is the heat demand in Watts and y is the duration in hours. In this case, curve fitting results show that: a=59.58; b=-0.02308; c=2.226×10^{-6}. By applying the maximum rectangle method to the heat demand distribution curve, the area of rectangles for different CHP output power is plotted in Figure 3.6.

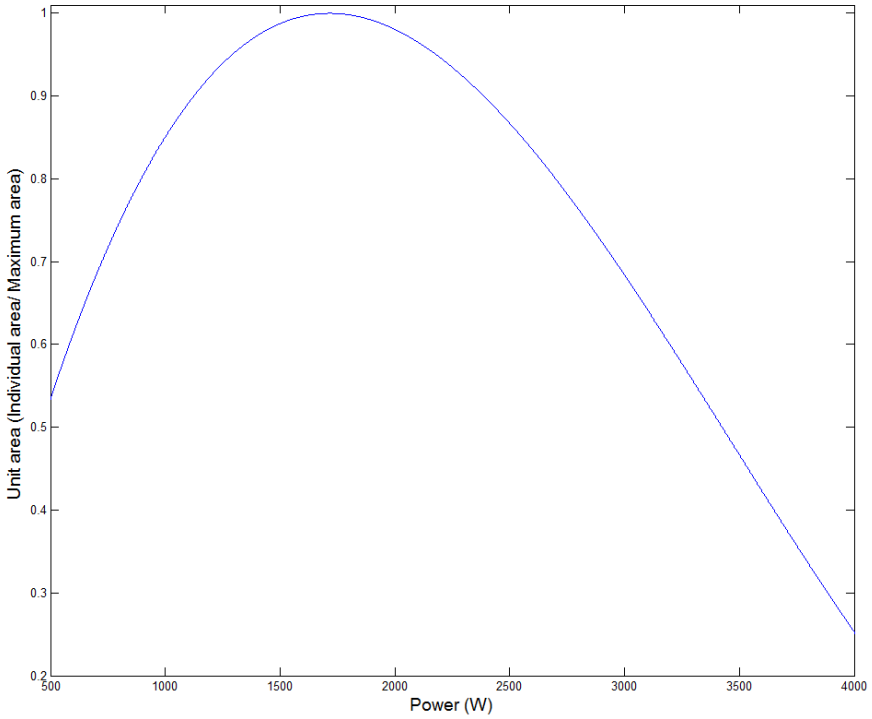

Figure 3.6 The area of rectangles for different CHP heat output power.

Figure 3.6 indicates that by setting the rated heat output power of CHP as 1717 W, most of the heat demands can be supplied by the CHP during the year. Based on previous gas engine and fuel cell CHP heat and electricity efficiencies assumptions (shown in page 17), the capacity of electricity power for fuel cell CHP and gas engine CHP should be set as 1271 W and 571 W, respectively. Thus, if the heat demand is used as the criterion to size CHP, the optimal capacity of fuel cell CHP and gas engine CHP should be 3434 W and 2602 W. Table 3.3 is a summary of optimal capacities of different types of CHP based on different optimizing criteria.

Table 3.3 Optimal capacities of different types of CHP based on different types of loads.

Types of loads	Types of CHP	Optimal electrical output of CHP (W)	Optimal heat output of CHP (W)	Optimal rated power of CHP (P_R) (W)
Electricity	Gas	1206	3618	5482
	Cell		1630	3259
Heat	Gas	572	1717	2602
	Cell	1271		3434

Table 3.3 shows that the optimal capacities of fuel cell CHP are nearly the same for this building, when either electricity loads or heat loads are chosen as optimizing criteria. However the optimal capacities of gas engine CHP can be significantly different when the heat load and the electricity load are used as optimizing criteria. The result from Table 3.3 shows that the optimal capacity of electricity dependant sizing gas engine CHP is twice the capacity of heat dependant sizing gas engine CHP.

As indicated in Chapter 2, physical factors, for example the age of buildings and type of buildings, have significant influence on the heat consumption pattern. Therefore, these factors need to be considered for different houses as futher optimization criteria. On the other hand, behavioral factors, due to a households' energy consumption patterns are different from each other and difficult to predict, so here these factors are not considered. Table 3.4 shows the general optimal capacities of CHP by choosing type of loads, type of CHP, the age of buildings and the type of buildings as optimizing criteria. In Table 3.4, all the heat loads are generated by the Strathclyde University heat model [21], and this model considers the types of buildings and the age of buildings.

Table 3.4 Optimal capacities of CHP based on different optimizing criteria.

Types of loads	Types of buildings	The age of buildings	Types of CHP	Optimal electrical output of CHP (W)	Optimal heat output of CHP (W)	Optimal rated power of CHP (W)
Electricity	Does not matter	Does not matter	Gas	1206	3618	5482
			Cell		1630	3259
Heat	D	1945-1983	Gas	1005	3014	4567
			Cell	2230		6028
		1984-1997	Gas	749	2246	3403
			Cell	1662		4492
		1998-2002	Gas	521	1563	2368
			Cell	1157		3126
	SD	1945-1983	Gas	932	2796	4236
			Cell	2069		5592
		1984-1997	Gas	588	1763	2671
			Cell	1035		3526
		1998-2002	Gas	508	1523	2308
			Cell	1066		3046
	T	1945-1983	Gas	767	2301	3486
			Cell	1702		4602
		1984-1997	Gas	572	1717	2602
			Cell	1271		3434
		1998-2002	Gas	504	1511	2289
			Cell	1118		3022

Considering that the physical factors have less influence on the electricity demands in a domestic building compared to heat demands, so in the CREST model, the electricity consumption pattern is more significantly affected by households' behaviours, rather than physical factors. This is the reason why electricity load based CHP sizing has the same optimal capacity for all domestic buildings in Table 3.4.

Another three conclusions can be acquired from Table 3.4. First, the capacity of CHP always increases as the age of buildings increases. Then, detached houses (shown as 'D' in Table 3.4.) consume more heat compared with semi-detached houses and terraced houses (shown as 'SD' and 'T', respectively in Table 3.4). Last, the optimal rated capacity for fuel cell CHP is always higher than gas engine CHP when the heat load is used as sizing criteria.

After obtaining the optimal size of CHP in all cases, the GA method was be used to optimise daily energy costs, and this process coherently considers the energy demands and energy tariff. In the following part, a terraced house, which was built between 1984 and 1997, will be used as an example to calculate daily energy costs for four different cases which were shown in Table 3.3. Similar work can be done to calculate other types of building's daily energy costs by using the MATLAB codes which are shown in Appendix 1.

3.4.2 Daily energy costs optimization results

By using the proposed methods in 3.3.1 and 3.3.2, the optimization results (CHP output efficiencies and the average daily energy costs) of different seasons are shown in this section. Figure 3.7 a) ,b) ,c) and d) show the CHP output efficiencies (including heat, electricity and overall efficiencies) in each minute of a typical spring working day based on different optimizing criteria.

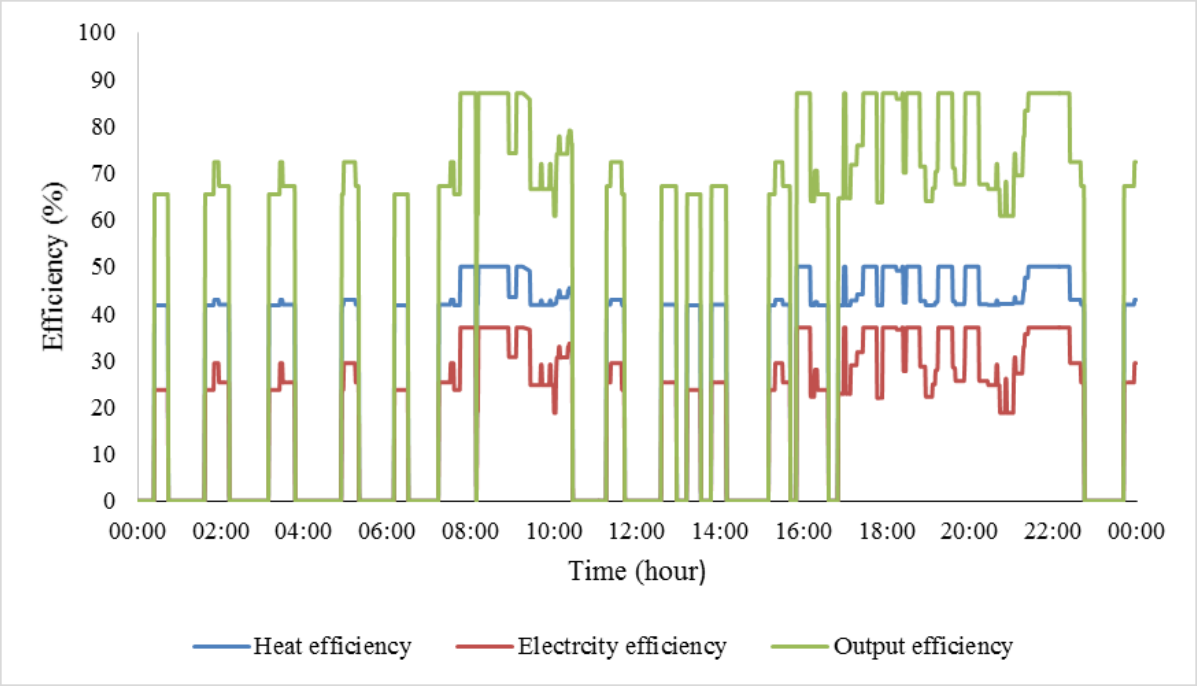

a) Spring, fuel cell CHP, heat dependant sizing CHP

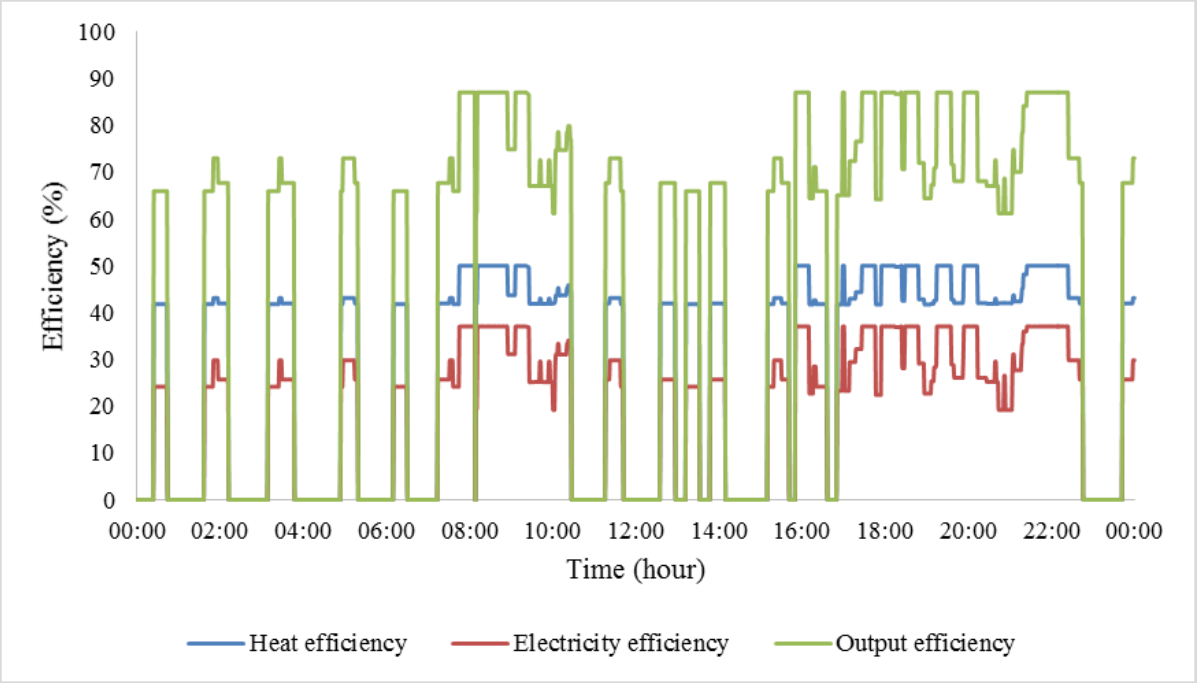

b) Spring, fuel cell CHP, electricity dependant sizing CHP

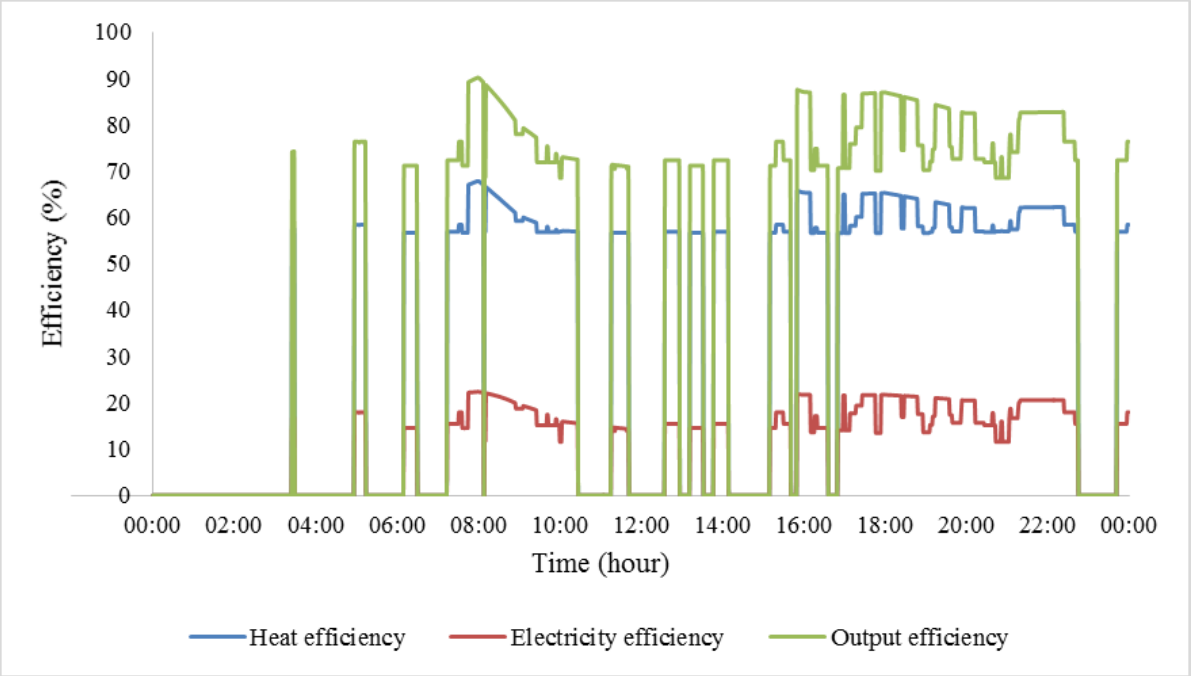

c) Spring, gas engine CHP, heat dependant sizing CHP

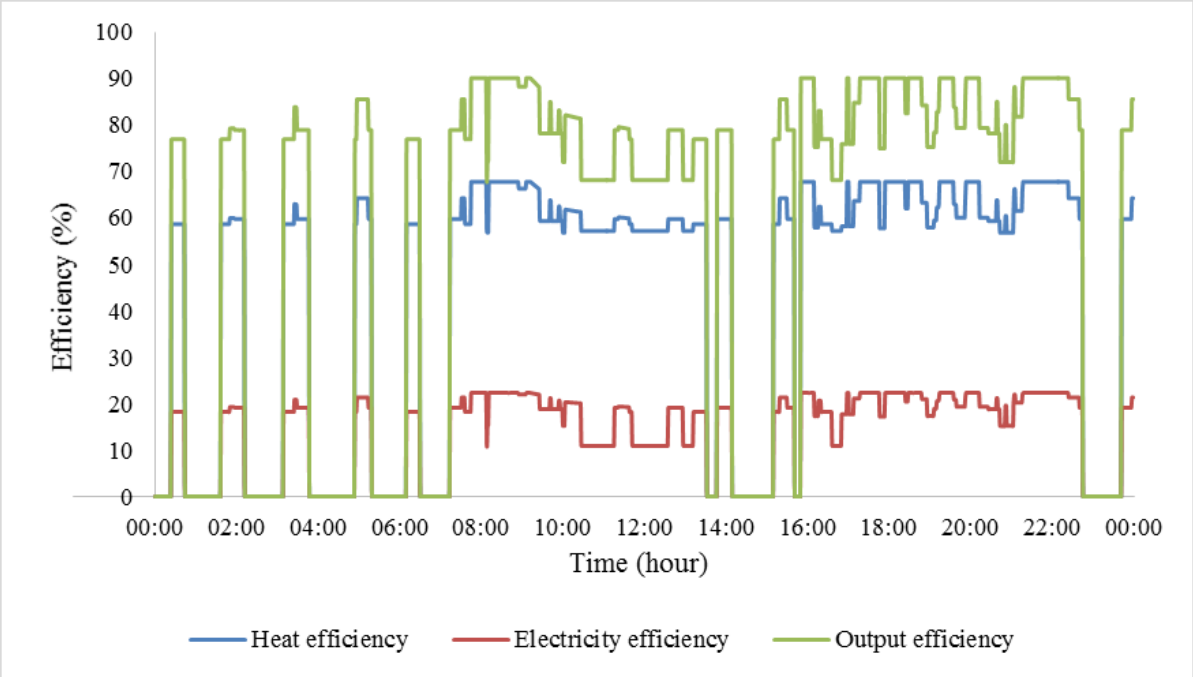

d) Spring, gas engine CHP, electricity dependant sizing CHP

Figure 3.7 CHP output efficiencies in each minute of a spring day based on different sizing criteria.

The optimization results for summer, autumn and winter will be shown in the Appendix 2. Figure 3.8 is a graph to show daily energy costs in different seasons based on different sizing criteria.

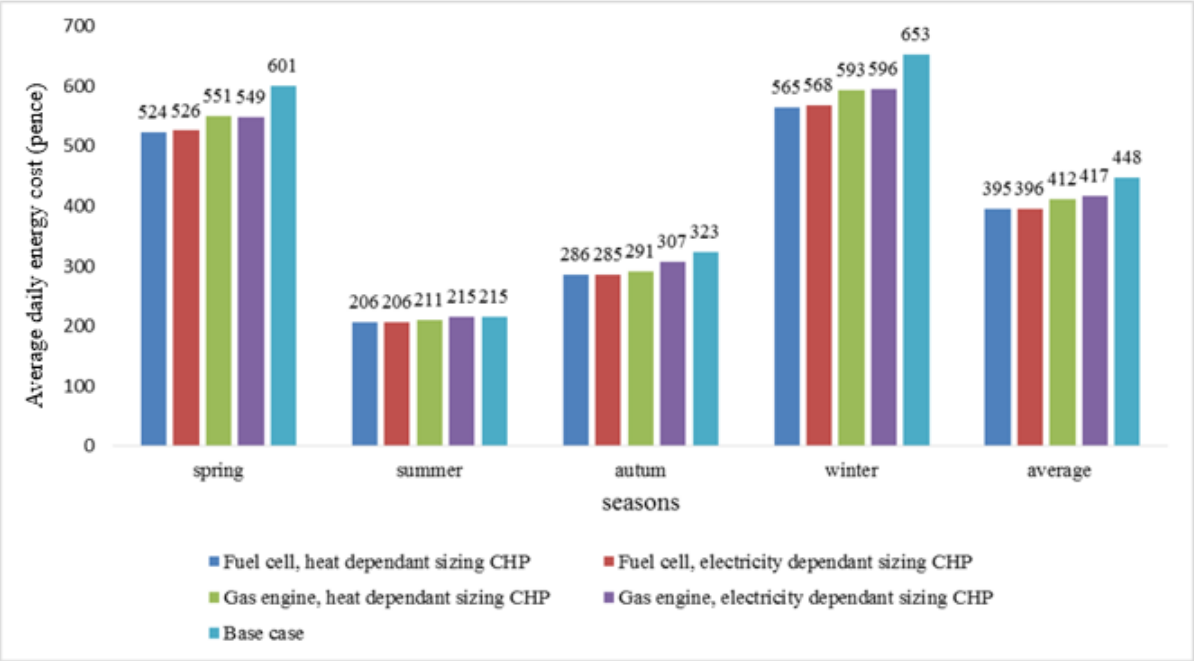

Figure 3.8 Different daily operational costs based on different optimizing criteria.

Based on this research, five conclusions can be made. First, when either heat or electricity load is used as optimizing criteria, the daily energy costs are about the same for a house which installs fuel cell CHP. But the costs will be much different for a house which installs gas engine CHP. Because for a terraced house, the optimal capacities of fuel cell CHP are nearly the same when different load curves are used as sizing criteria; however, the optimal capacities for gas engine CHP are quite different.

Then, the fuel cell CHP saves more money compared with gas engine CHP in all cases, because fuel cell CHP has higher electricity output efficiencies compared with gas engine CHP and daily electricity price is much higher than gas price.

Next, even though the CHP can be operated at low output efficiency conditions, the optimization results show that to maximize daily benefit, CHP should always be operated at high output efficiency conditions. The overall output efficiencies are normally higher than 65% for both CHP.

The forth conclusion is oversizing CHP can increase daily energy costs and reduce energy efficiency. In addition, if the rated capacity of CHP is very high, CHP will be ‘switched off’ in the most of time in a day shown in (Appendix 2. Figure A2.1 d)).

Finally, choosing electricity load curve as sizing criteria for gas engine CHP needs to be approached carefully, because gas engine CHP has a high heat to electricity output ratio. By choosing electricity load as sizing criteria for gas engine CHP, the system will generate a lot of redundant heat.

3.4.3 Theoretical best CHP capacity

This part shows the theoretical best fuel cell and gas engine CHP capacities based on the algorithm proposed in 3.3.3.

Theoretical best fuel cell CHP capacity

Figure 3.9 is a graph to show the relationship between fuel cell CHP installation capacity and average daily energy costs. Figure 3.9 reveals that the average daily energy cost for a year decreases with the increase of fuel cell CHP capacity until the CHP capacity reaching 5000 W. From Figure 3.9, the theoretical best fuel cell CHP capacity should be located between 5000 W and 5500 W. Figure 3.10 shows the average daily energy cost for different CHP installation capacities which are located within the feasible region. From Figure 3.10, the daily energy cost is at a global minimum when the capacity of the fuel cell CHP is set as 5200 W.

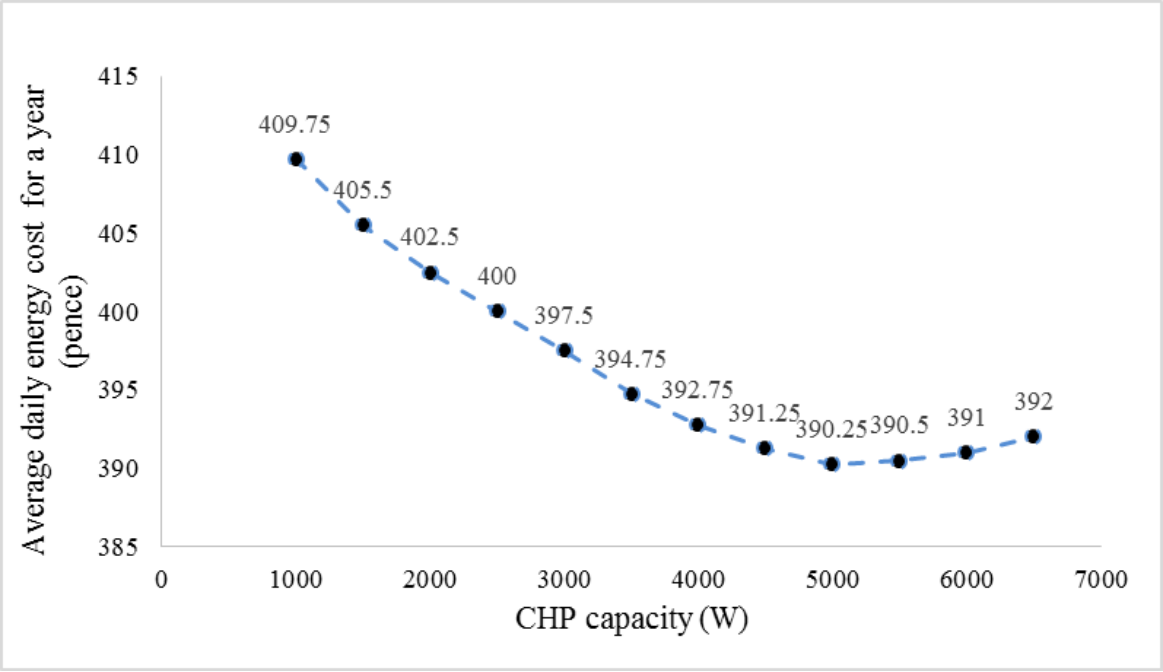

Figure 3.9 Average daily energy costs of a terraced house for installing different capacities fuel cell CHP.

Compared with optimization results acquired by the MR method in section 3.4.2, the GA method gives 5 pence extra of average daily energy cost reduction. However, to get this reduction, the fuel cell CHP capacity needs to be increased by 50%.

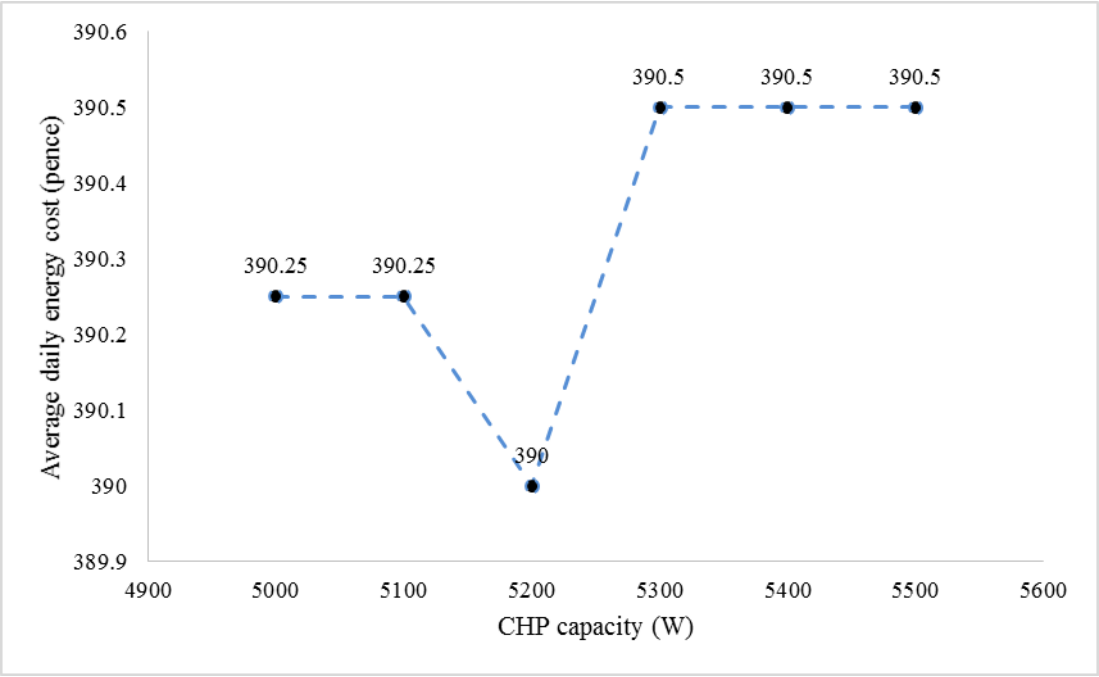

Figure 3.10 Average daily energy costs within theoretical best fuel cell CHP capacity region.

Theoretical best gas engine CHP capacity

Figure 3.11 is a graph to show the relationship between gas engine CHP installation capacity and average daily energy costs. Figure 3.11 indicates that the average daily energy cost for a year decreases with the increase of gas engine CHP capacity until the CHP capacity reaches 3500 W. From Figure 3.11, the theoretical best gas engine CHP capacity should be located between 3000 W and 3500 W.

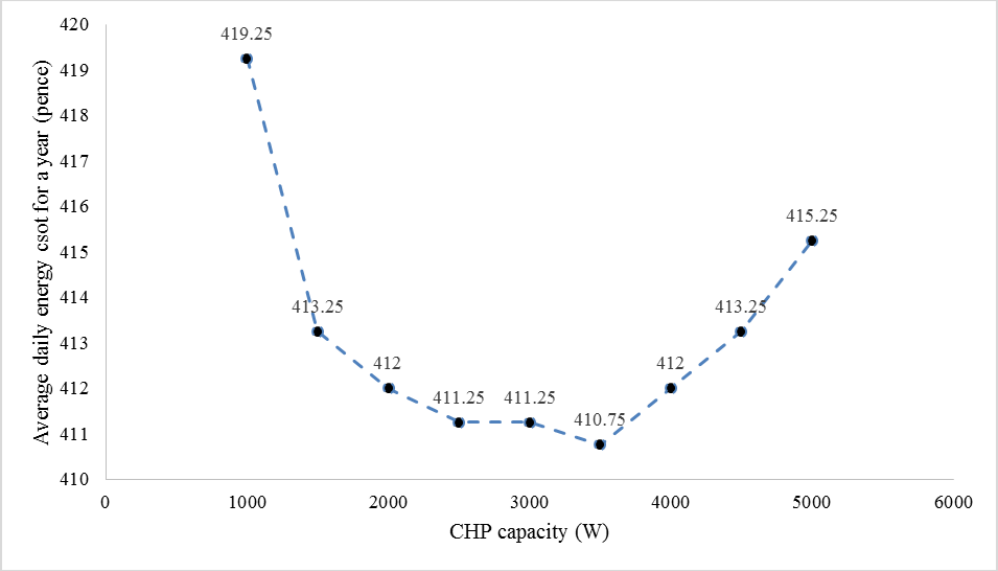

Figure 3.11 Average daily energy costs of a terraced house for installing different capacities gas engine CHP.

Figure 3.12 is plotted to show the average daily energy costs for different CHP installation capacities which are located within feasible region. From Figure 3.12, the theoretical best gas engine CHP capacity is 3500 W. Compared with the MR method, the GA method gives a further 1.25 pence daily energy cost reduction and a nearly the same optimal gas engine CHP capacity.

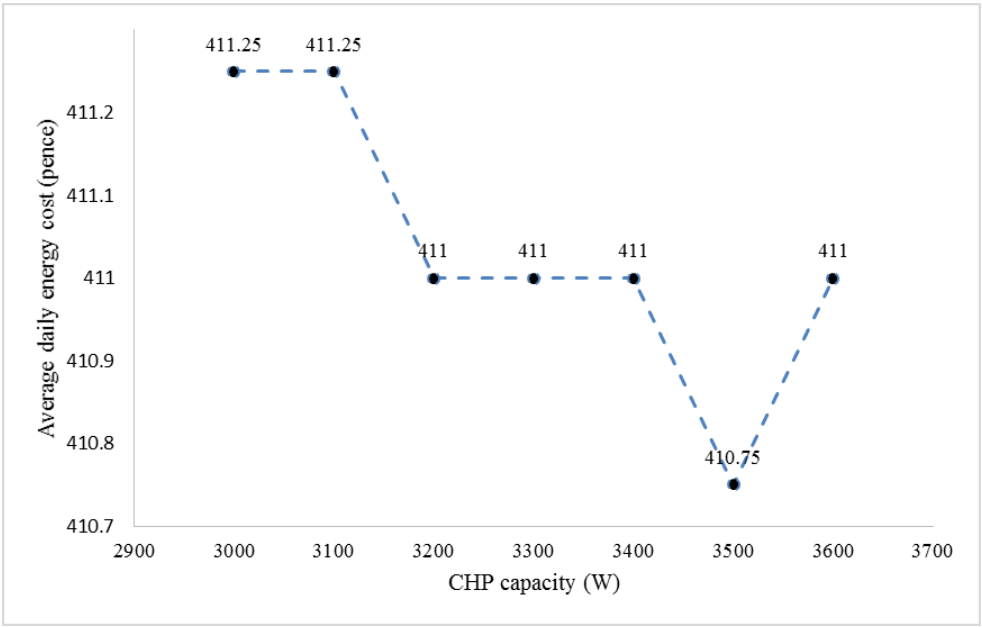

Figure 3.12 Average daily energy costs within theoretical best gas engine CHP capacity region.

The simulation results show that the fuel cell CHP and the gas engine CHP offer 13% and 8.4% of average daily energy cost reduction of a year compared to the base case defined in Chapter 2. This proves that fuel cell CHP has better performance in domestic energy cost reduction. However, to achieve the extra 4.6% energy cost reduction, the installation capacity of fuel cell CHP is 48.5% higher than gas engine CHP. Moreover, considering different manufacturing cost of two CHPs [39], the investment cost of fuel cell CHP will be 55.8% higher than gas engine CHP.

3.4.4 Effective CHP output efficiency and average input power to rated power ratio

Figure 3.13 and Figure 3.14 show the CHP installation capacity against effective CHP output efficiency and input power to rated power ratio, respectively. Both of graphs reveal that the effective CHP output efficiency and input power to rated power ratio reduce for both types of CHP when CHP installation capacity is increasing. In these two graphs, P1 and P2 are the theoretical best CHP capacity acquired by the MR method. The difference is that P1 uses the heat demand as sizing criteria and P2 uses the electricity demand as sizing criteria. P3 is the theoretical best CHP capacity acquired by the GA method.

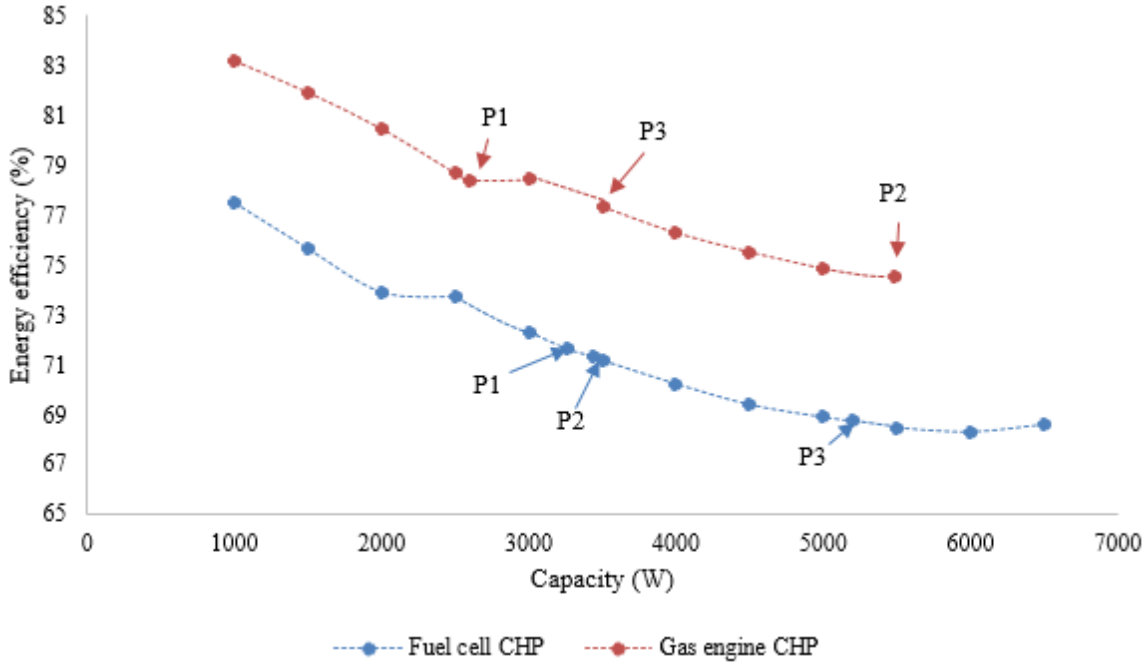

Figure 3.13 Effective CHP energy efficiency against CHP installation capacity.

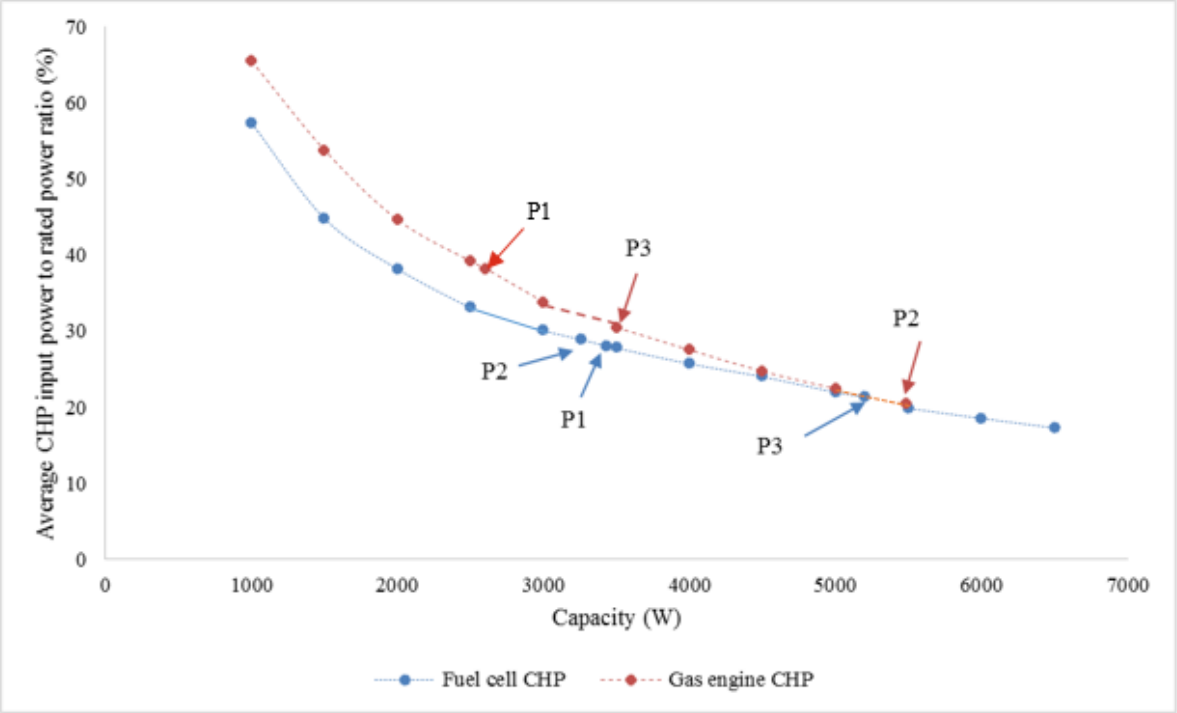

Figure 3.14 Average CHP input power to rated power ratio against CHP installation capacity.

Figure 3.13 shows that both CHP are operated at high output energy efficiency states for different CHP installation capacity. This is because that CHP is a kind of high energy efficiency generators. The graph also shows that gas engine CHP has higher effective energy efficiency compared to fuel cell CHP, the reasons being that heat demand is much higher than electricity demand in a domestic building and gas engine CHP rated energy efficiency is higher than fuel cell CHP.

Figure 3.14 indicates without an energy storage system, the capacity of CHP has not been fully utilised. For both CHP technologies, to get theoretical minimum daily energy cost, less than 30% of capacity is utilised.

3.5 Analysis and discussion

Table 3.5 is a summary of the work in this chapter. The average daily investment in this table is calculated based on the installation costs of gas engine and fuel cell CHP showing in [39]. However, the installation costs of gas engine and fuel cell CHP showing in [39] are higher than the present CHP installation costs. This is because [39]

shows CHP installation costs 7 years ago. With the development of the micro-CHP technology, the installation costs of micro-CHP have already been reduced (shown in Chapter 6.3.1). Therefore, the actual system investment should be lower than the value shown in this research and the system benefit to cost ratios obtained in Table 6.1 are conservative.

Table 3.5 A summary of the optimal results based on different CHP sizing criteria.

Sizing criteria	Type of CHP	Optimal capacity (W)	Base case average daily energy cost (pence)	Optimal average daily savings (pence)	Effective energy efficiency (%)	Average CHP input power to rated power ratio (%)	Average daily investment * (pence)
Heat	Fuel cell	3434	448	53	71.32	28.05	529
Electricity		3259		52	71.62	28.91	502
Theoretical best size		5200		58	68.73	21.39	801
Heat	Gas engine	2602		36	78.4	38.2	349
Electricity		5482		31	74.56	20.4	735
Theoretical best size		3500		37	77.34	30.47	469
Average daily investment * (pence) = (Total investment + maintenance fees) (pence) / CHP life (in days)							

First, this work proves that using heat demand as optimization criteria can obtain better optimization results compared with electricity demand. This is because average heat demand in a year is much greater than the electricity demand. Only using the heat demand as sizing criteria to size fuel cell and gas engine CHP for a terraced house which was built between 1984 and 1997 is acceptable, because compared with the theoretical best size CHP, the average daily energy savings are over 90% of

theoretical maximum savings. However using electricity as sizing criteria for gas engine CHP can cause problems, because the heat to power ratio of gas engine CHP is very high and this may cause the CHP to generate high levels of redundant heat.

Secondly, when using the MR method to size the CHP, the benefit to cost ratios are higher in most of cases compared to when the GA method is used to size the CHP. This is because the MR method tries to find the CHP capacity that can meet most of the demand in a year and this will make full use of CHP capacity. Consequently, even though the daily energy cost savings cannot achieve its theoretical maximum, the significant reduction of investment cost makes the ratio higher.

Thirdly, the optimization results show that it is difficult to deal with the conflict between operational cost, system investment and energy efficiency. The optimization results also show that to get higher daily energy savings, it is preferable to install large capacity CHP, however, this will significantly increase the investment cost and reduce energy efficiency. This is because by increasing the capacity of the CHP, more electrical demand occurring at the peak energy price time can be supplied by the CHP, and this will reduce energy costs. However, by increasing the capacity of the CHP, average CHP input power to rated power ratio is reduced, which means the CHP is always working at low input power and this will lead to energy efficiency reduction. Moreover, the low average CHP input power to rated power ratio indicates that most of CHP capacity has not been fully utilised. This is the reason why CHP investment cost is very high.

Fourthly, energy cost reduction is satisfactory in spring, autumn and especially winter. However, energy cost reduction in summer is disappointing. This is because the heat demand in summer is small compared with other seasons, therefore the electricity generated by the CHP is limited. To increase energy cost reduction in summer, CHP capacity must be reduced, however, this can reduce energy cost reduction in other seasons. In order not to reduce energy cost reduction in other seasons, extra electrical energy must be stored in advance to supply the load at peak electricity price times.

Finally, the results also show that the computation time of the MR method is much shorter than the GA method. The calculation time of the GA method normally depends on the scale of CHP capacity. Figure 3.9 and Figure 3.11 show that within the feasible

CHP capacity region, the average daily energy costs are very similar, therefore in the future work, the scale of CHP capacity in the GA method can be set as 500 W rather than 100 W and this will increase computation efficiency and reduce computation time.

3.6 Conclusion

In this Chapter, daily energy operational costs, investment costs and energy efficiency are all considered when using the MR and GA methods to size the CHP. The GA optimization results show that by installing a 5200 W fuel cell CHP, the daily energy costs can be minimized which is 13% reduction compared to base case. However, to achieve this reduction, there will be about 3% energy efficiency reduction and 7% input power to rated power ratio reduction compared to use the MR method and the heat demand to size CHP. Using the MR method and the heat demand to size the CHP is good enough because the MR method gives a higher benefit to cost ratio and energy efficiency. In addition, it makes more use of CHP capacity, even though it needs 5 pence extra to generate energy for a day. To deal with the conflict between energy efficiency, energy costs and system investments, energy storage systems may need to be installed. In the next chapter, an algorithm is proposed to size a hybrid energy storage system.

Chapter 4. Sizing hybrid energy storage systems

An important technology to improve energy efficiency and reduce energy costs for domestic buildings, hybrid energy storage systems (HESSs) are introduced in this chapter. This chapter first introduces different types of batteries and analyses all factors that can influence HESSs lifetime and improve its use. Secondly, this chapter proposes a new method to size the capacity of a battery-supercapacitor system, to design the maximum discharge current and to limit the state of charge (SOC) of the battery. At this stage, the entire problem is formulated as a function which is only related to battery capacity. This reduces the number of variables in the objective function and makes its global minimum more obvious. Then, a simple, practical control scheme is proposed to evaluate the results of formulating all variables in terms of the battery capacity. Finally, an operational region for HESSs is defined graphically, and this is very useful in avoiding battery capacity saturation, battery discharge current saturation and battery SOC saturation when sizing the battery. Regarding the domestic multi-energy system presented in Chapter 2, the daily benefit-cost ratio of the HESS is doubled compared to previous research [7].

4.1 Introduction

Battery-supercapacitor hybrid energy storage systems have an important role in increasing energy efficiency, and can help reduce the demand in electricity consumption. By reducing electricity demand, not only energy cost but also carbon emission can be reduced. Due to these reasons, HESSs are becoming a key component of future smart buildings.

Battery energy storage systems (BESSs) are an important part of HESSs and they are well suited to be installed on domestic buildings because of their relatively safe, silent, scalable, low maintenance, and efficient characteristics [7]. BESSs are widely used in domestic buildings to reduce electricity grid imports, to supply backup electric power in the form of uninterruptible power suppliers and to store redundant energy generated by any distributed energy generation system [8]. BESSs have excellent carbon emission reduction through increasing energy efficiency and can also benefit the

overall system economics [57]. In addition, BESSs improve the households' energy self-sufficiency [58]. However, inappropriate battery sizing will reduce battery lifetime, decrease system benefit and increase carbon emission [59, 60]. Also, the inappropriate control strategy of a BESS will further reduce battery lifetime and result in sub-optimal system benefits [59]. Due to the potential environmental damage arising from the full battery's life cycle, selecting the right types of battery for domestic buildings is crucial [57].

Even though inappropriate sizing, selecting and operating batteries will reduce system potential benefits, batteries are still one of the most economical ways of storing electricity [61], with the lead acid battery being the most mature battery technology. Currently, lead acid batteries are widely used in many fields, for example, in Uninterruptible Power Supply (UPS) systems and Electric Vehicle (EV) systems. For renewable power generation systems, lead acid batteries are also currently often used to store energy from PV systems [62]. On the other hand, there are many drawbacks to this type of battery, such as short lifetime, temperature limitations and current limitations [63]. Thus, many studies have analysed how to minimize the limitations of battery storage systems. The main emphasis of this research is to maximize the lifetime of battery systems without decreasing system stability and overall benefit.

Whilst the careful design of battery storage systems can increase overall energy storage system benefits, the design must also mitigate any shortcomings of the battery itself. For example, currently SOC and temperature are thought to be the two main factors that can influence the life time of batteries [62]. In this way, most battery storage systems try to avoid working at low SOC, low temperature and high temperature. In fact, there are many more factors that can influence the life time of battery storage systems, for example, irregular load and heavy discharge current are also harmful [64]. In [65], it is stated that the rated battery capacity can be reduced if the battery always discharges with heavy current. In [66], it is shown that the life span of two groups of batteries will be longer than one battery which has the same capacity as two groups of batteries. In other words, if two groups of batteries can be discharged at a suitable ratio, the life span of batteries can be further increased.

It is well known that batteries have high energy density (100 Wh/kg), but relatively low power density (<1000 W/kg) and their output cannot change rapidly. On the other hand,

supercapacitors have very high power density (<10000 W/kg), long life spans (>50000 charge cycle) and very low energy density (10 Wh/kg) [62]. Therefore it has often been proposed that a hybridised storage system could best harness the advantages of both storage technologies. With increasing interest in battery-supercapacitor hybrid energy storage systems (HESSs) at building level, the problem of how to minimise the cost (installation, maintenance and operation) without influencing the system performance becomes an important optimization issue.

Suitable energy storage equipment and an effective energy storage strategy have significant influence on a smart building's energy performance. Therefore optimizing energy storage systems at building level is a crucial research area. To the best knowledge of the author, this chapter contains the first study to optimise daily the cost benefit ration of a HESS accounting for the three key factors (SOC, maximum discharge current and HESS capacity).

The main contributions of this chapter are: 1) three key factors (SOC, discharge current and HESS capacity) are comprehensively considered for the optimization, 2) the optimization problem is formulated to a function only relating to the battery capacity, greatly simplifying the objective function, 3) An optimal operating region is defined within this objective function, which achieves the best compromise between discharge current, state of charge and battery capacity, 4) Using this approach, the daily benefit-cost ratio of the HESS is shown, in an example case study multi-energy system, to be significantly increased by a factor of two compared to the previous work [1].

The optimization results acquired in this chapter will be used in next chapter as the rated capacity of the HESS. With the optimal size of the HESS and proposed rule-based control algorithm, daily energy cost savings will be calculated in Chapter 5. Then the optimal results will be compared with Chapter 3 (domestic buildings without HESS) to discuss in Chapter 6 whether it is suitable to install HESSs at domestic building level.

4.2 The characteristics and optimal choice of batteries

With the development of battery technology, more types of batteries have been produced by manufacturers, and the prices of many batteries have decreased very

rapidly, resulting in their widespread use. Generally speaking, although batteries have quite high energy density, they tend to have fairly low power density. However, due to different characteristics of different batteries, not all of the batteries are suitable for storing energy at building level.

Currently, at least five types of batteries are widely available, including the NiCd battery, Li-Ion battery, sodium-sulphur battery, flow battery and lead acid battery. The NiCd battery is normally used in power systems with output between the ranges of 1 kW-0.5 MW. However, the power density of the NiCd battery is quite low and due to materials used in its production, it has harmful environmental consequences. Moreover, the standby loss of this type of battery is quite high, thus it is not a good choice for building level energy storage. The Li-Ion battery possesses a low discharge rate, no memory effect and high energy density. The main disadvantage of this type of battery is that because internal resistance can cause it to overheat, it needs overcurrent and overvoltage protection. Another disadvantage of this battery is its high cost. The sodium-sulphur battery is normally used in systems with output power 0.8 MW-10 MW, and the operation temperature of this battery is between 300-350 °C. For safety reasons, it is not suitable for use in buildings. The vanadium redox battery (VRB) is a typical flow battery and it is widely used in systems with output power between 10 kW-10 MW. VRBs have very long lifetimes, in the order of ten years. However, the output voltage of this battery is quite low, at approximately 1.4 V, which is why in order to acquire higher output voltages, many batteries need to be used in series. Therefore, it is advisable not to use it in buildings. The lead acid battery is currently one of the most well-established batteries, though it cannot discharge deeply and the physical size of the battery is relatively large. The technology of lead acid battery is mature, the cost is relatively cheap and the output of this battery can vary from 1 kW-10 MW, which makes it suitable for use in buildings [61]. This thesis will therefore use a lead acid battery and supercapacitor as an example energy storage system. Table 4.1 is a brief summary of different types of batteries.

Table 4.1 A summary of different types of batteries.

Type of batteries	Discharge power range	Main disadvantages
NiCd	1 kW-0.5 MW	Low power density, Environmentally unfriendly; High standby loss
Li-Ion	1 kW-1 MW	Internal resistance can cause it to overheat; High cost
Sodium-sulphur	0.8 MW-10 MW	High operation temperature (300-350°C)
Flow battery- VRB	10 kW-10 MW	Low output voltages;
Lead acid	1 kW-10 MW	Low depth of discharge; large size

4.3 Factors potentially affecting battery use

4.3.1 State of Charge (SOC)

When talking about the parameters that can influence battery lifetime, SOC is definitely one of the most important factors. SOC is a parameter that needs to be recorded every minute because it may not only influence battery lifetime, but also battery charging/discharging efficiency.

Experiment results show that the influence of discharging 1 Ah electricity at different SOCs have different impacts on battery lifetime. For example, when SOC is 100%, then discharging 1 Ah electricity is equivalent to only discharging 0.55 Ah electricity over its whole lifetime. However, if SOC is 50%, then discharging 1 Ah electricity is equivalent to discharging 1.3 Ah electricity over its whole lifetime [67]. Figure 4.1 shows the relationship between the weighting factor and the SOC of battery and suggests that in order to extend their lifetime, batteries should work at higher SOCs.

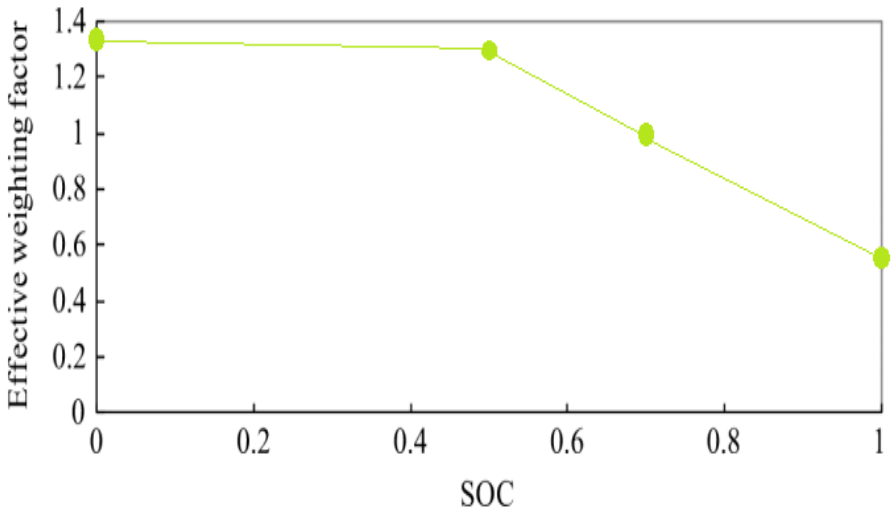

Figure 4.1 Relationship between the weighting factor and the SOC of battery [65].

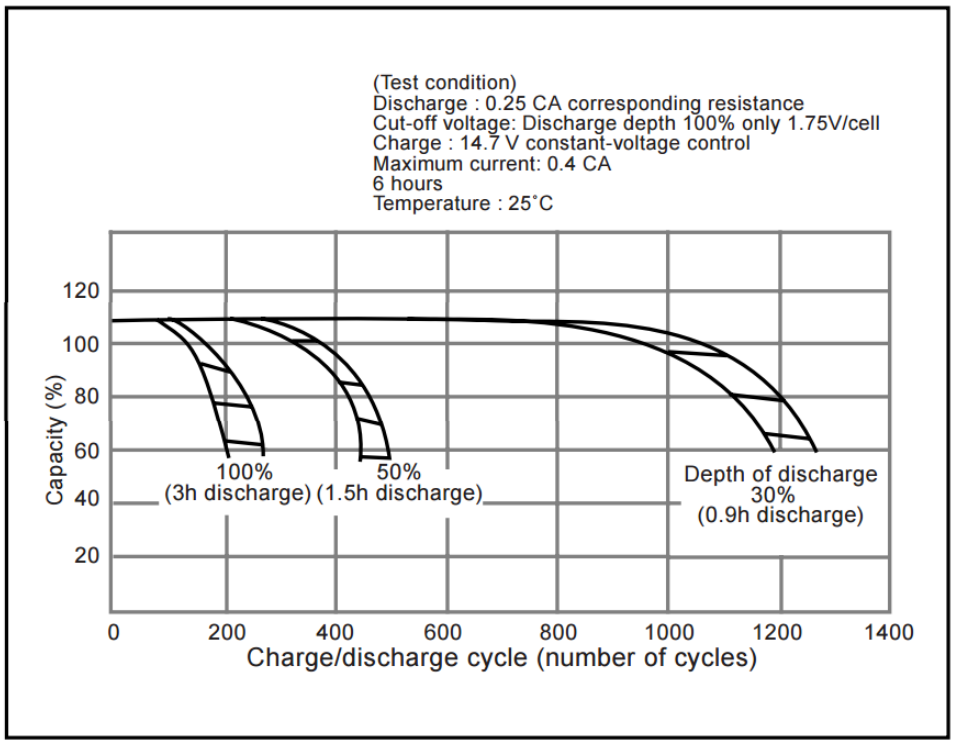

Figure 4.2 Battery cycle life against depth of discharge [68].

By limiting the depth of SOC to approximately above 60%, the battery's life cycle can be extended. Figure 4.2 is used to illustrate the life cycle of a Panasonic lead acid battery against different SOCs. By doing a simple calculation, it can be clearly shown that the accumulative battery lifetime is approximately equal to 360 to 390 times battery rated capacity when SOC is limited at 30%. However, when SOC is limited at 50%, the accumulative battery lifetime decreases to 212 to 225 times of battery rated

capacity. Thus, by limiting the depth of SOC, the accumulative lifetime of the battery can be significantly improved. Therefore, SOC will be considered when optimising the HESS in this work.

4.3.2 Battery capacity

The lifetime of the battery significantly decreases if an undersized, low capacity battery is installed in a large power system. Increasing the capacity of the battery can allow it to work at a higher SOC, which will increase battery lifetime. However, for a householder, an energy storage system is always limited by its physical size and installation capacity. Oversizing the capacity of the battery can increase the installation and maintenance cost of a storage system and increase the system standby loss. Thus careful consideration of these competing factors is necessary to maximise the lifetime of the battery and minimise the operational cost of the system. Battery capacity will be analysed later in this chapter.

4.3.3 Operating temperature

In [69], battery capacity is reduced as the operating temperature decreases and the level of reduction depends on the type of battery and on the discharge current. On the other hand, if the operating temperature (for a lead acid battery) is over 40 °C, the battery lifetime decreases and the standby loss will increase. However, in [70], it is stated that if the battery system is installed in a location where ambient temperature does not change significantly, the uncertainty of the load prediction has a stronger influence compared to the operating temperature. Thus, if the battery is installed in a ventilated room, and the ambient temperature is stable and suitable for battery operation, the influence caused by temperature can be ignored. In this work the temperature dependency of the battery is therefore excluded.

4.3.4 Maximum discharge current

Heavy discharge current has a negative effect on the effective battery capacity. In [70], the effective battery capacity is less than the rated battery capacity, if the discharging current is higher than one tenth of battery rated capacity. Also, in [65], if the battery is always operated with heavy discharge currents, the battery discharge efficiency will decrease, and the life span of battery will be reduced. Table 4.2 illustrates the relationship between discharge current and battery effective capacity, where q is

battery rated capacity. This work will limit the maximum discharge current when sizing the capacity of HESSs.

Table 4.2 Maximum battery capacity for different discharge current [70].

Discharge current (A)	Discharge time (h)	Maximum discharge capacity (Ah)	Maximum discharge capacity / Rated capacity (%)
250 (q/10)	10	2500	100
430(q/5.8)	5	2150	86
625(q/4)	3	1875	75
1300(q/1.9)	1	1300	52
2050(q/1.2)	0.5	1025	41
2700(q/0.9)	0.33	900	36
3100(q/0.8)	0.25	775	31

4.3.5 Battery output voltage imperfection

In many studies, the output voltage of the battery has been idealised. Firstly, it is always assumed that the output of the battery is a constant. Figure 4.3 is a diagram used to show the relationship between actual terminal voltage and discharge time. Secondly, even for the same type of battery, the internal resistance and output voltage of each individual battery have some variation [66], which will have a slight influence on the battery lifetime.

Mathematical models, physics models and circuit models have all been proposed in analysing battery discharge characteristics. In [71], the importance of the battery output I-V curve has been demonstrated. However, nowadays the battery output I-V curve is used to model a dynamic system, and is seldom used to analyse the economical operation of the energy storage system. Moreover, it is unrealistic to think that it is possible to build two batteries whose internal resistances and output voltages are exactly identical. Therefore, this factor is not analysed in this work.

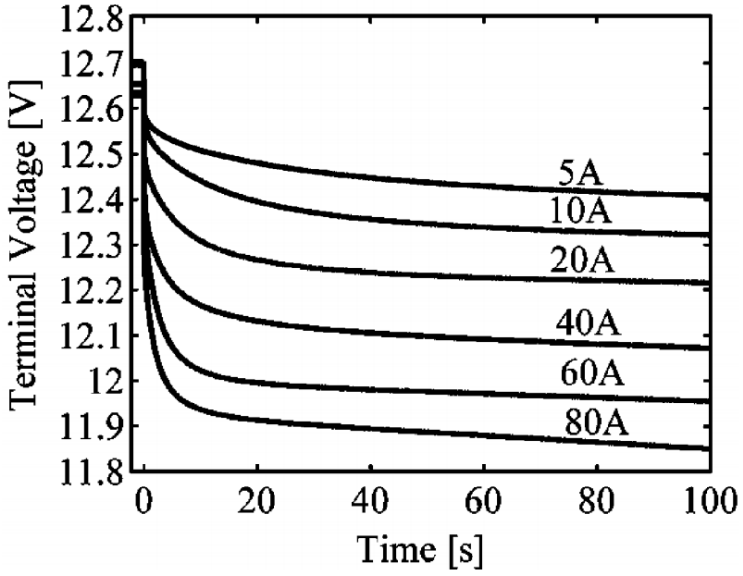

Figure 4.3 The relationship between output voltage and discharging time at different discharge current [71].

4.3.6 Battery control strategies

Different battery discharging strategies can affect the economic operation of a battery. In [69], it is proven that choosing different discharge current schemes allows the size of the battery to be changed. However, different control strategies might require a change in user behaviour, and so in order not to inconvenience users in this work, this factor will be ignored.

Another battery control strategy is to use two groups of batteries instead of one battery to meet the demand. Though this will increase battery lifetime, it is not used in this work because the physical size and installation cost of energy storage systems at building level is strictly limited.

In conclusion, this work will ignore the influences of operating temperature, imperfections of battery output voltage and battery control strategies. The most significant factors have been shown to be SOC, discharge current and battery capacity and thus, these parameters will be considered in this work when optimizing the battery storage system.

4.4 The characteristics of supercapacitors

In contrast to batteries, supercapacitors have relatively low energy density, and high power density. Supercapacitors can be used to offer pulse power in hybrid energy storage systems. The discharge/charge current of a supercapacitor can be 7 times higher than the rated charge current of battery [63].

Because no chemical reaction takes place, the lifetime of supercapacitors compared to batteries is extremely long. The life cycle of supercapacitors can reach one million cycles [72, 73]. Thus in many industry applications, the life of supercapacitors is not limited by cycling stress [73].

In addition, supercapacitors can respond very quickly to sudden changes of demand. For this reason, they are often used to smooth the load curve and let the battery discharge current change slowly. They have the benefit to improve power quality and decrease the shock on the battery system, which can extend the life of batteries [62].

Finally, the installation cost of the supercapacitor is very high, but the maintenance fee is quite low (almost zero). Sizing the capacitor is quite important, in order to make full use of the supercapacitor capacity [63, 74].

4.5 Factors potentially affecting supercapacitor lifetime

The lifetime of the supercapacitor can be defined as the time period from first use to last use. During this period, two parameters need to be monitored, which are the supercapacitor capacity and the internal resistance. Normally, a supercapacitor needs to be replaced when the capacity of the cell reduces to 80% of its initial value, or the equivalent series internal resistance increases to 200% of its initial value. The lifetime of the supercapacitor is strongly affected by temperature and operating voltage. Other factors, such as duty cycle and power flow profiles, can have subtle influences [75]. In the following subsections, the impacts caused by operating temperature and voltage will be analysed.

4.5.1 Operating temperature

[73] and [76] indicate that the lifetime of a supercapacitor will be halved if the operating temperature increases by 10°C from the ambient. Furthermore, it has been proved in

[77] that the equivalent supercapacitor's internal resistance will increase and the capacity of the supercapacitor will decrease at high temperatures.

Operating temperature encompasses ambient temperature and system temperature. In order to keep ambient temperature suitable and stable, the supercapacitor should be installed in a ventilated room. System temperature is mainly influenced by discharge current. The system temperature will be significantly increased if the supercapacitor discharges at a high current for a long time. However, in the hybrid system in this work, limiting the discharge current of battery systems will also limit the discharge current of supercapacitors. On the other hand, when the supercapacitor is used for smoothing the demand curve rather than offering high power, this also has the benefit of decreasing system temperature. Moreover, by adding a cooling system, for example small fans, the operating temperature can be limited within a suitable range, which is why this thesis will ignore the factor of operating temperature.

4.5.2 Operating voltage

If the maximum terminal voltage on the supercapacitor can be reduced by 0.2 V, the lifetime of the supercapacitor can be doubled [76]. Thus, the lifetime of the supercapacitor can be extended by adding converters to limit the operating voltage.

Previous analysis has shown that by limiting temperature and operating voltage, the life span of the supercapacitor will not be greatly influenced. Moreover, the life span of the supercapacitor is much longer than that of the battery. In this work, the lifetime of supercapacitor will not be considered. Instead, this work will focus on sizing the supercapacitor. By making full use of the supercapacitor, the average daily cost will be reduced. In this work, a supercapacitor BCAP1500 whose rated voltage and capacity are 2.7 V and 1500 F, is used as an example [78].

4.6 System control strategy

Clearly the choice of system control strategy has an effect on the daily energy cost saving. However this must be fixed in order to quantify the effect of battery capacity on daily benefit to cost ratio. This section therefore proposes a simple, practical control scheme to evaluate the results of formulating all variables in terms of the battery capacity.

4.6.1 Electricity system control strategy

As shown in Figure 2.7 in Chapter 2, in each season, there are two high electricity price periods and three low electricity price periods every day. These five time periods can be defined as: H1, H2, L1, L2 and L3, and are shown in Figure 4.4.

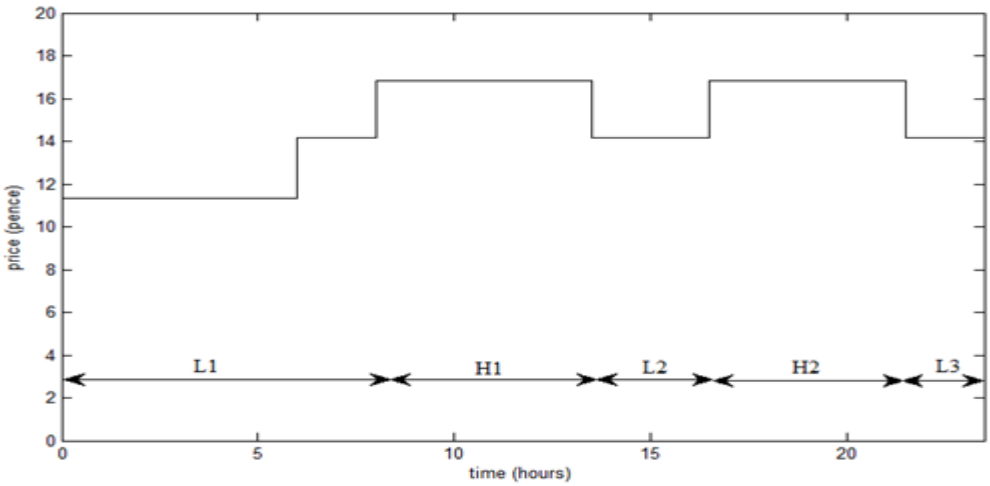

Figure 4.4 Daily electricity price diagram.

Electricity system control strategy for H1 and H2

There are two periods in a day (H1 & H2) where the electricity tariff is obviously higher than the rest of the day. In order to reduce system operational cost and maximize system benefit, there is no doubt that less electricity should be imported from the national grid at this time. So at H1 and H2, electricity should be supplied by the CHP and the HESS as much as possible. The output of the HESS can be limited by battery discharge current and minimum SOC during this time.

Electricity system control strategy for L1 and L2

On the other hand, the electricity price is quite low in L1 and L2, suggesting an ideal time to use the electricity from the grid to charge the HESS. However, in this work, instead of charging the HESS by electricity from the grid, the HESS is charged by the CHP during this time. There are two reasons for making this change. The first one is cost efficiency. Even though electricity price at L1 seems low, it is still high compared with the electricity price generated by the CHP. The second reason is to improve energy efficiency. In [79], the energy loss due to power transmission and distribution is 7%. If more energy can be generated locally by the CHP, energy loss due to power

transmission and distribution can be reduced. Moreover, the emission factor of gas is generally less than electricity in many countries due to the use of coal based generation, therefore there is also an environmental benefit. Thus, at L1 and L2, the CHP is switched on to supply the loads and charge the battery. During this period, if the demand is lower than the power generated by the CHP, the rest of energy generated by the CHP will be stored. However, if the demand is higher than the power generated by the CHP, the difference between the generated power and the demand will be supplied by the grid.

Electricity system control strategy for L3

As mentioned before, if the system's electricity demand can be supplied by the CHP rather than the grid, the electricity cost can be reduced, and system transmission and distribution loss will also be reduced. However, in order to reduce redundant electricity generated by the CHP and to make the battery discharge to the initial value at the beginning of the day, the CHP should be turned off. Thus from the start of L3 to the 40 minutes before the end of the day, the electricity control strategy is the same as H1 and H2. For the last 40 minutes, the CHP will be switched off and the electricity demand will be supplied by the HESS. In this period, if the output of the HESS is limited by the discharge current and the minimum SOC of the battery, the difference between HESS output and demand will be supplied by the grid. Table 4.3 is used to show the daily electricity operation of the system.

Table 4.3 Daily electricity control strategy in this building.

Time period		State of CHP	Possible state of the HESS	Electricity supplies' priority list
L1		ON	Charge/Standby	CHP→ Grid
H1		ON	Charge/Discharge/Standby	CHP → HESS → Grid
L2		ON	Charge/Standby	CHP→ Grid
H2		ON	Charge/Discharge/Standby	CHP → HESS → Grid
L3	Start to last 40 minutes of L3	ON	Charge/Discharge/Standby	CHP → HESS → Grid
	Last 40 minutes of L3	OFF	Discharge/Standby	HESS → Grid

4.6.2 Heat system control strategy

Heat is generated by gas in the building (no matter whether generated by CHP or boiler), and the gas price is relatively low and stable compared with the electricity price. In addition, heat storage overall efficiency is quite low and standby loss is much higher than in an electricity storage system. Thus it is preferable for the heating system to not store heat in advance. However, the CHP may generate redundant heat when it is used to generate electricity, therefore only this portion of heat will be stored. Considering the high standby loss of the heat storage system, the energy stored in the water tank should be utilized as soon as possible.

By following this system control strategy, the daily energy cost saving will be:

$$E_s = \sum_{t=1}^{t=1440}(P_E(t) \times C_e(t) + P_H(t) \times C_g(t)/\eta_B) - \sum_{t=1}^{t=1440}(P_{Ein}(t) \times C_e(t) + P_{Gin}(t) \times C_g(t)/\eta_B) - \sum_{t=1}^{t=1440}(P_{CHP} \times C_g(t) \times K(t)) \quad (4.1)$$

$$K(t) = \begin{cases} 1 & If\ the\ CHP\ is\ operated\ at\ rated\ power \\ 0 & If\ the\ CHP\ is\ switched\ OFF \end{cases} \quad (4.2)$$

In equation (4.1) and (4.2), E_s is total daily energy cost saving in pence, $P_E(t)$ and $P_H(t)$ are electricity energy demand and heat energy demand in each minute, $C_e(t)$ and $C_g(t)$ are the electricity price and gas price in each minute respectively. By applying the proposed system control strategy, $P_{Ein}(t)$ and $P_{Gin}(t)$ are energy supplied by the grid and energy supplied by the boiler in each minute. η_B is boiler's efficiency, and $K(t)$ is the state of the CHP. As mentioned in chapter 3, when a CHP is working at low input power, the electricity output efficiency of this CHP is much less than its rated value. Thus, in the calculations of this chapter, the CHP can only work at 'rated power' or 'switch off'.

4.7 Battery system optimization

4.7.1 Optimization function for battery systems

The battery's installation cost and maintenance cost are directly proportional to the capacity of the battery and inversely proportional to the battery lifetime. The average daily cost of battery storage system can be written as:

$$C_b = (C_{bi} + C_{bm} \times Y) \times q_b / T_L \quad (4.3)$$

In equation (4.3), C_b is average daily cost of battery storage system, C_{bi} is the unit price of the battery, which is 0.8 US$/ Wh (approximately 0.534 £/Wh) and C_{bm} is the annual maintenance cost of battery, which is 0.2283 US$/ kWh (equals to 0.1522 £/kWh.) [63]. Y is the life span of the HESS in years, and q_b is the battery capacity in Ah. T_L is the life span of the HESS in days.

In Chapter 4.3.1, it has been mentioned that the life span of battery can be greatly influenced by the battery's minimum SOC and battery minimum SOC can be influenced by battery installation capacity. So the life span (Y & T_L) will be a function of a function of battery installation capacity. On the other hand, with the increase of discharge current, the effective battery capacity will be reduced. In other words, the battery capacity q_b will increase as well. Different constraints will lead to different optimization results.

4.7.2 Constraints

Discharge current

As shown in Table 4.2, when the discharge current is greater than one tenth of battery capacity, the ratio of maximum discharge capacity and rated capacity will be less than 100%. The relationship between installation battery capacity q_b and effective battery capacity q_{eb} can be summarised as:

$$q_b = q_{eb} / \alpha \quad (4.4)$$

α is a scaling factor of effective battery discharge capacity and battery rated capacity. The value of α can be acquired from Table 4.2 for different maximum discharge current. In this work, seven discrete maximum discharge currents (listed in Table 4.2) will be used to analyse how battery discharge currents affect battery system average daily cost.

SOC and battery capacity

Instead of influencing battery effective capacity, these two factors have an influence on the battery life span. Normally battery life span in days can be expressed as:

$$T_L = q_a / q_d \tag{4.5}$$

where q_a is the accumulative capacity of batteries, q_d is the daily effective battery capacity consumption. SOC will affect q_a and battery capacity can have an influence on q_a and q_d.

As mentioned in Chapter 4.3.1, the accumulative capacity of batteries can be significantly improved by limiting the depth of SOC. Thus q_a is a function of battery capacity and depth of SOC. Therefore,

$$q_a = \beta \times q_b \tag{4.6}$$

In (4.6), β is a scaling factor of battery accumulative capacity and battery rated capacity. From Figure 4.2, the cycle numbers of a lead-acid battery are 200 to 225, 425 to 450 and 1200 to 1300 when the minimum SOC is limited as 0%, 50% and 70%, respectively. In this work, the number of cycles of a lead-acid battery for deep discharge (Minimum SOC=0), medium discharge (Minimum SOC=50%) and light discharge (Minimum SOC=70%) are set as: 225, 450 and 1300. The scaling factor β can be represented as:

$$\beta = \int_{SOC=i\%}^{SOC=100\%} q(SOC)dSOC \times \mathrm{N} \tag{4.7}$$

In (4.7), i is used to represent the type of discharge, for example, if i= 70, the battery is operated as a light discharge model and the minimum SOC of battery is 70%. Another variable N, in (4.7), is the number of discharge cycles at given i. $q(SOC)$ is a function of the effective weighting factor of the battery at different SOC. From Figure 4.1, $q(SOC)$ can be approximately modelled as:

$$q(SOC) = \begin{cases} -1.5 \times SOC + 2.05 & if\ SOC > 50\% \\ 1.3 & if\ SOC < 50\% \end{cases} \tag{4.8}$$

Similar to equation (4.6) and (4.7), the daily effective battery capacity consumption can be expressed as:

$$q_d = \int_{SOC=i\%}^{SOC=peak\%} q(SOC)dSOC \times n \times q_b \tag{4.9}$$

In (4.9), n is the number of full discharge cycles in a day, and normally this is equal to 1, but in some extreme cases, n can be very large (for example, if the battery

installation capacity q_b is very small). This is not practical for HESSs in a building, so it will not be analysed. $SOC{=}peak\%$ is the maximum SOC that the battery can reach. When the battery capacity increases beyond a certain point, the battery cannot be fully charged and will always work at a relatively low SOC, which will increase daily effective battery capacity consumption. Figure 4.5 demonstrates how battery capacity affects system operation.

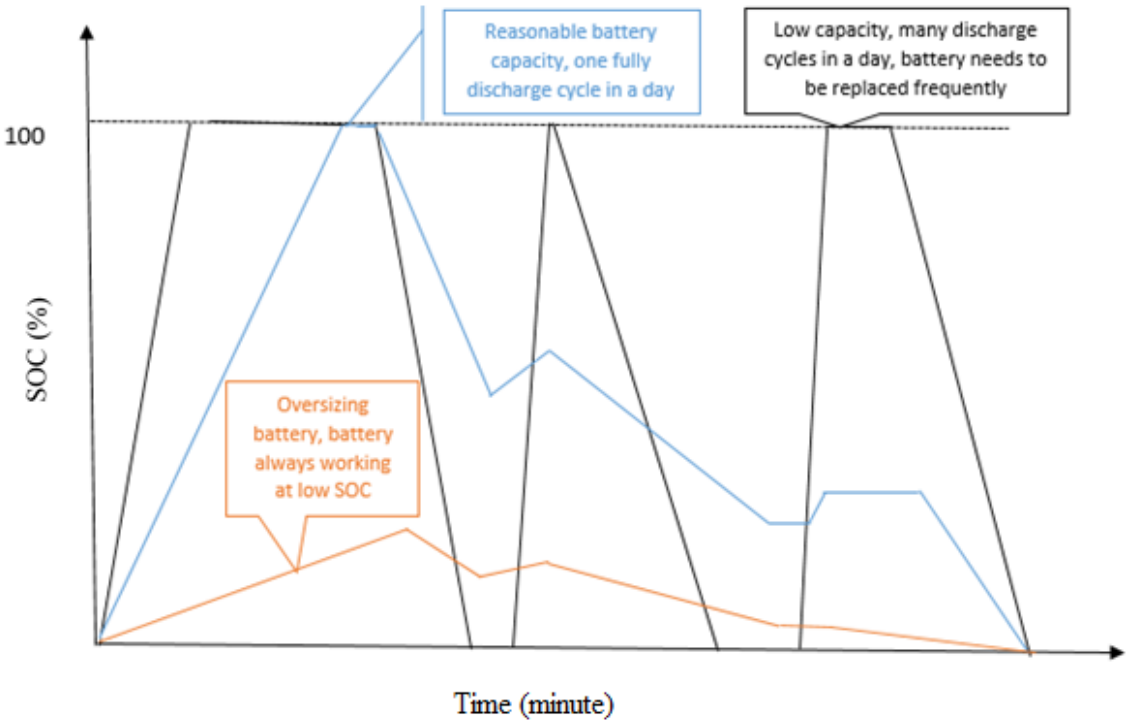

Figure 4.5 Daily battery SOC curves for different Battery Capacity Levels.

By combining equation (4.3) to (4.9), the average daily cost of the battery storage system can be derived as:

$$C_b = (C_{bi} + C_{bm} \times \frac{N \times \int_{SOC=i\%}^{SOC=100\%} q(SOC)dSOC}{365 \times n \times \int_{SOC=i\%}^{SOC=peak\%} q(SOC)dSOC}) \times \frac{q_{eb}}{\alpha} \times \frac{n \times \int_{SOC=i\%}^{SOC=peak\%} q(SOC)dSOC}{N \times \int_{SOC=i\%}^{SOC=100\%} q(SOC)dSOC} \quad (4.10)$$

Now, the average daily cost of the battery storage system can be formulated as a function of only the battery capacity for a given SOC and discharge current.

4.8 Supercapacitor system optimization

Like the battery storage system, the supercapacitor can be used to supply energy for electrical systems. However, the installation cost of the supercapacitor system for per unit energy is much higher than the battery system. Therefore, it is not suitable to store large amounts of energy using the supercapacitor. Instead, the supercapacitor can be used to smooth load curve and have a fast response to load changing.

To give a longer time for the battery to reach a new balance, the supercapacitor should have the ability to offer the same level of power as the battery for a short period of time. The maximum output power that the battery can offer is:

$$P_{max} = V_b \times I_{max} \tag{4.11}$$

where P_{max} is the maximum output power of the battery, V_b is the battery output voltage and I_{max} is the maximum discharge current of the battery. As mentioned in the previous section I_{max} is a function of battery installation capacity, which can be represented as:

$$I_{max} = q_b/\mu \tag{4.12}$$

In (4.12), μ is a time scaling factor. Thus, the maximum output power of the supercapacitor should be equal to the maximum output power of the battery, which is:

$$P_{max} = V_b \times q_b/\mu \tag{4.13}$$

The capacitance of the supercapacitor (q_s) can be written as [78]:

$$q_s = \frac{i}{dV} \times (dt + \tau) \tag{4.14}$$

In (4.14), i is the average current, dV is the difference between maximum supercapacitor operation voltage and minimum supercapacitor operation voltage. dt is the discharge time and τ is the time constant for the supercapacitor. For BCAP1500, τ is 0.7 seconds [78]. To be more specific:

$$\mathrm{i} = \frac{i_{maxs}+i_{mins}}{2} = (\frac{P_{max}}{V_{min}} + \frac{P_{max}}{V_{max}})/2 \tag{4.15}$$

$$\mathrm{dV} = V_o - V_{min} \tag{4.16}$$

In (4.15) and (4.16), i_{maxs} and i_{mins} are the maximum output current of the supercapacitor and the minimum output current of the supercapacitor. V_{max} and V_{min} are the maximum output voltage and the minimum output voltage of the supercapacitor. V_o is the HESS operation voltage.

When sizing the supercapacitor chosen in this HESS (BCAP1500), all the parameters will be constants except for the supercapacitor's maximum output power. In this way, the size of the supercapacitor is directly proportional to its maximum output power. However, the maximum output power of the supercapacitor system can be influenced only by the battery installation capacity at the given maximum battery discharge current. Thus the size of the supercapacitor only depends on the battery installation capacity when the type of the supercapacitor, HESS and the maximum battery discharge current are given.

The average daily cost of the supercapacitor system is proportional to the total cost of the supercapacitor and inversely proportional to the lifetime of HESSs, so the average daily cost of supercapacitor (C_s) can be expressed as:

$$C_s = (C_{si} + C_{sm} \times Y) \times q_s / T_L \tag{4.17}$$

In (4.17), C_{si} and C_{sm} are the unit installation cost of the supercapacitor and the annual maintenance cost of the supercapacitor. At current exchange rates (£ against $), C_{si} is 0.5 £/F and C_{sm} is 0.007 £/F [63]. Q_s is the supercapacitor installation capacity, which is proportional to the battery installation capacity. Y and T_L is life span of the HESS in years and in days. The values of Y and T_L depend on the life span of battery system, because the life span of the supercapacitor system is much longer than that of the battery. So the average daily cost of supercapacitor (C_s) only relates to battery capacity (q_b).

Therefore, finding the minimum average daily system cost (Min C) at the given total daily energy cost saving, E_s becomes the whole system optimization problem. The objective function is:

$$\text{Min C} = C_s + C_b \tag{4.18}$$

The analyses above show that the minimum average daily cost will only be influenced by battery capacity if the type of supercapacitor, maximum battery discharge current and minimum battery SOC are given.

The battery output voltage and the maximum supercapacitor output voltage are set to be 24 V, which is equal to the HESS operation voltage. The minimum supercapacitor output voltage is set as 12 V. The maximum discharge time for the supercapacitor is 10 s. The type of supercapacitor is BCAP1500, with a time constant of 0.7 s. Twenty-one different scenarios (3 types of SOCs and 7 types of maximum discharge currents) are tested to show how SOC, discharge current and battery capacity affect the average daily cost of the HESS. The best system data setting can be acquired by comparing these different cases.

4.9 Results

4.9.1 Daily energy cost saving

Figures 4.6, 4.7 and 4.8 show the daily energy cost saving with the control strategy mentioned in Chapter 4.6. However, the depth of battery discharge is different in the three figures. Figures 4.6, 4.7 and 4.8 are used to model deep discharge (Minimum SOC=0%), medium discharge (Minimum SOC=50%) and light discharge scenarios (Minimum SOC=70%).

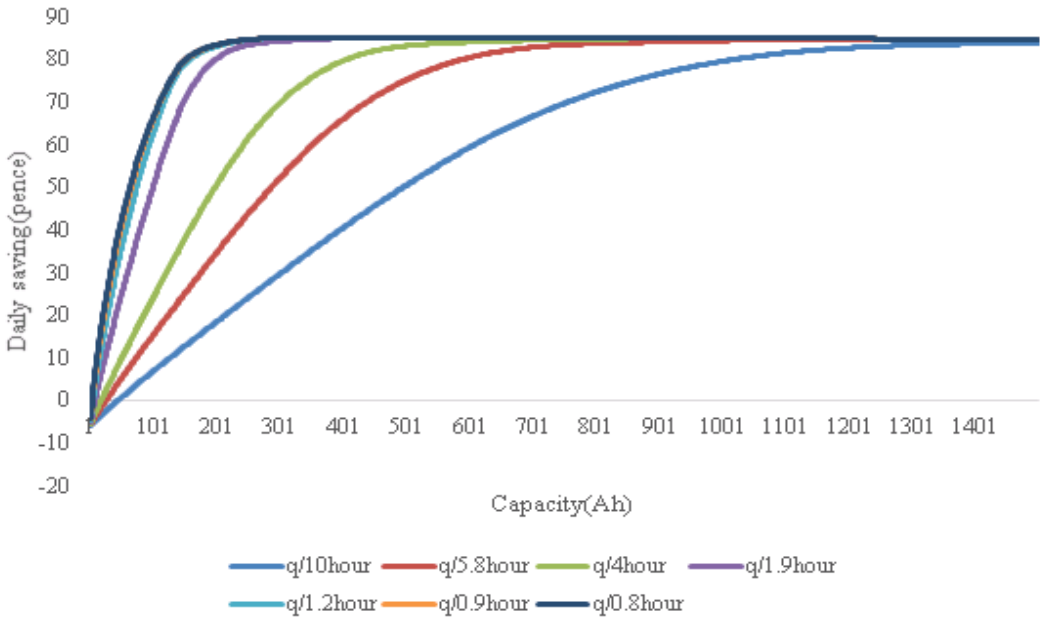

Figure 4.6 Daily energy cost saving VS battery capacity at different discharge currents (Deep Discharge).

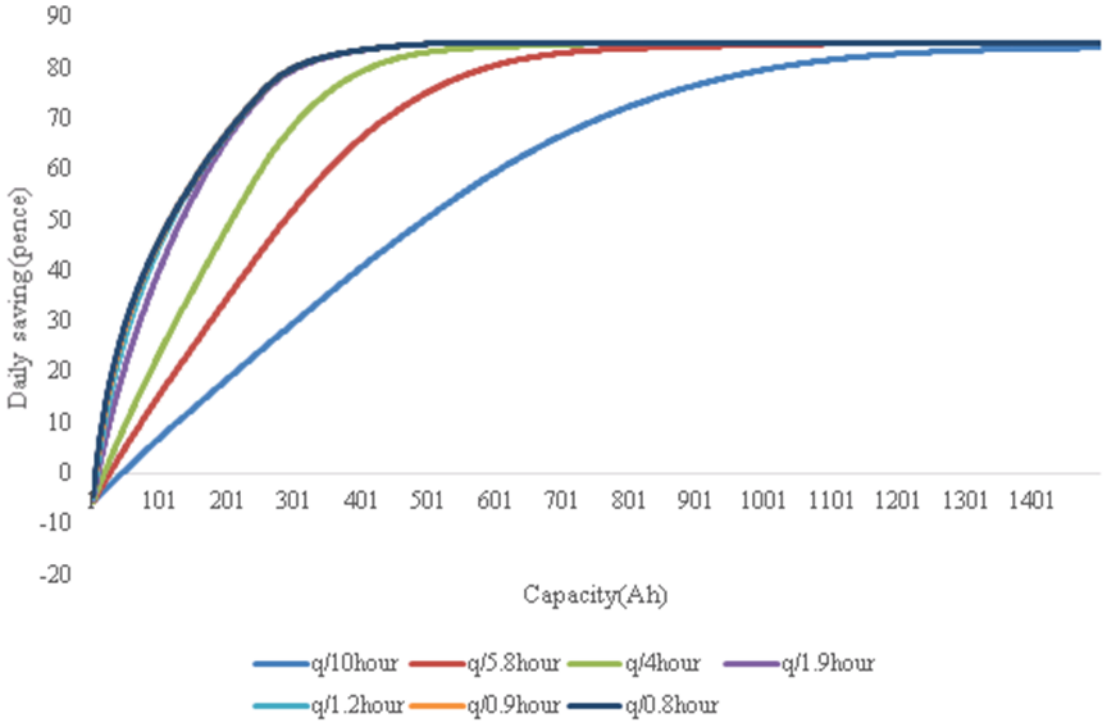

Figure 4.7 Daily energy cost saving VS battery capacity at different discharge currents (Medium Discharge).

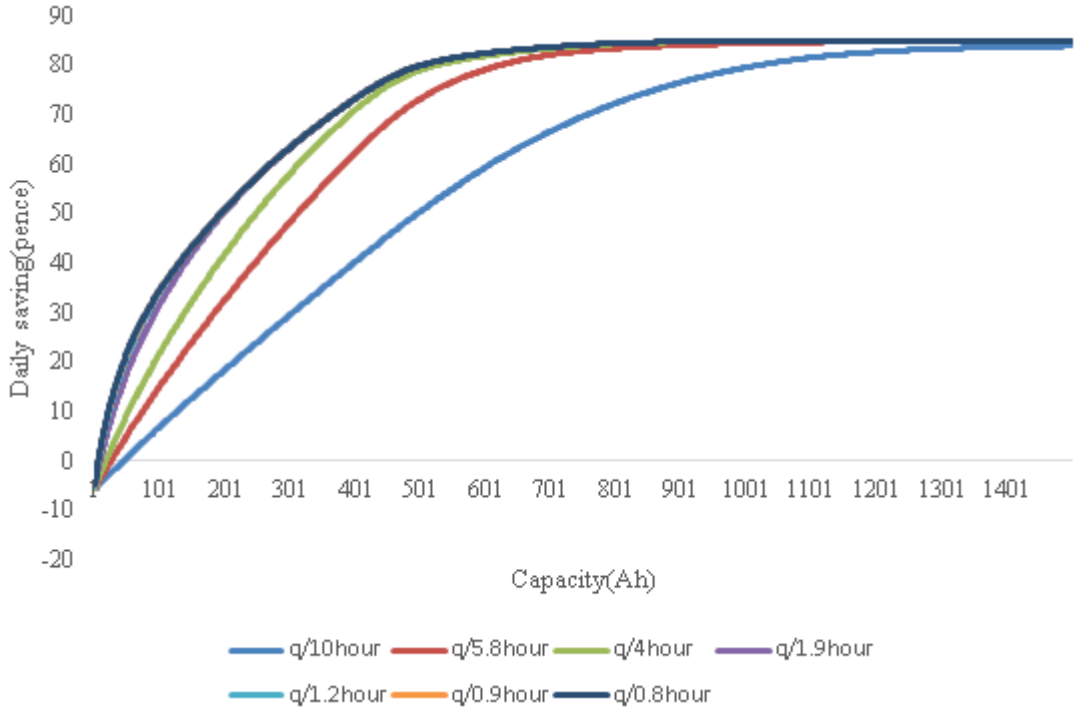

Figure 4.8 Daily energy cost saving VS battery capacity at different discharge currents (Light Discharge).

Capacity saturation

Figures 4.6-4.8 show that with the increase of the battery capacity the average daily energy saving will reach the saturation point. This saturation value, whereafter it is not influenced by the SOC and maximum discharge current, is the maximum daily energy saving. For the same system control strategy, the saturation value of daily energy saving will be the same. In this case, the maximum daily energy saving is 84.7 pence. In order to improve the daily energy saving saturation value, a more advanced control strategy should be applied to the system.

SOC saturation

By comparing Figures 4.6-4.8, the average daily saving curves are the same for different SOC tests, if the discharge current is set as one tenth of the battery capacity. However, with the increase of the discharge current, the average daily saving curve will be different. In order to solve the SOC saturation problem, the system needs to operate at a higher discharge current.

Discharge current saturation

In Figure 4.8, when the discharge currents are higher than $Q/1.9$ and the battery capacities are higher than 216 Ah, the average daily saving is the same at different discharge currents. At this time, the best way to solve discharge current saturation is to decrease system minimum SOC. If system minimum SOC is decreased to 50%, the saturation value of the discharge current becomes 259 Ah.

Figure 4.9 shows the limitation of HESS operation. To make optimal use of the battery, an effective HESS should work in the operation area but avoid the saturation area.

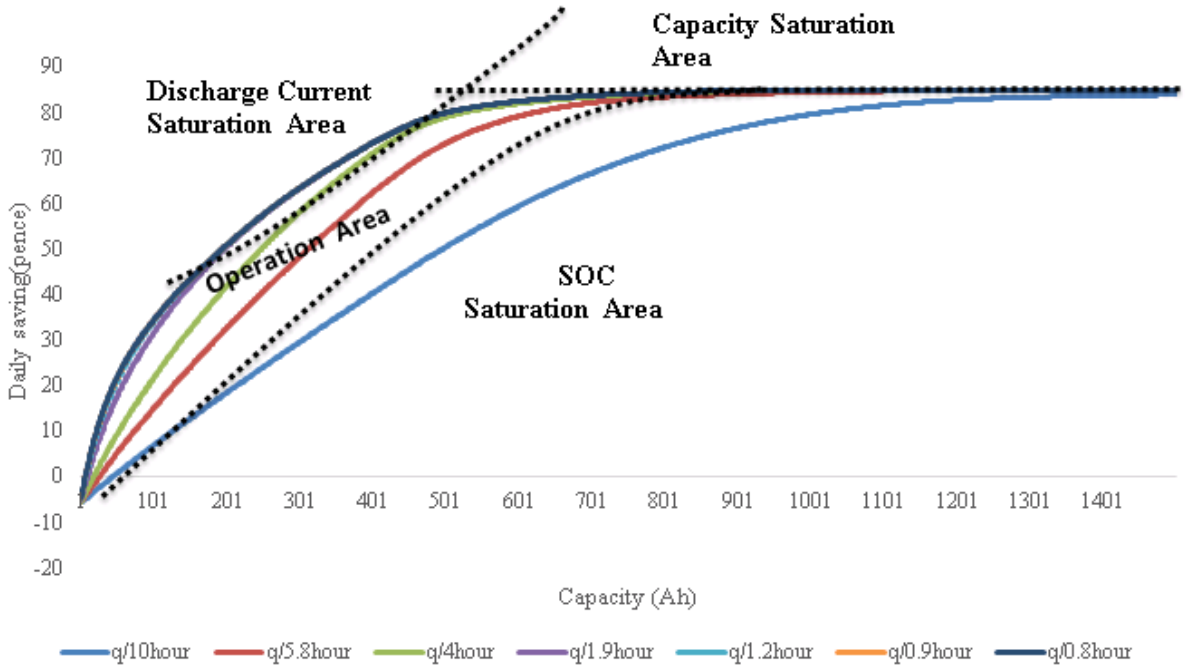

Figure 4.9 The limitation of HESS operation system.

4.9.2 Average daily HESS cost

It is well known that because of the manufacturing of the current technology, the average daily cost of HESSs is much higher than the average daily saving. In [6] the average daily cost of HESSs is about 14.5 times higher than the average daily saving. Because HESSs can reduce the burden of the grid at peak demand time, and increase the allowable penetration of fluctuating renewable generation, governments are likely to increasingly subsidise building level storage, such as the domestic HESSs. Moreover, with the improvement of energy storage technology, the installation cost of the overall system will significantly decrease in the future, and with effective control schemes it is likely to go beyond breakeven point.

To balance maximum daily energy saving and the battery operation cost, this thesis will attempt to optimize the battery capacity when average daily energy saving is 95% of its maximum value, which is 80 pence. Table 4.4 shows the average daily cost of different discharge currents in the case of light discharge. In order to illustrate how SOC influences system operate, Table 4.5 shows the optimized HESS at different SOCs.

Table 4.4 Average daily HESS cost for discharge currents (SOC=70).

Discharge current (A)	q/10	q/5.8	q/4	q/1.9	q/1.2	q/0.9	q/0.8
Average daily energy saving (£)	0.8						
Effective battery capacity (Ah)	1022	624	527	504	504	504	504
Installation battery capacity (Ah)	1022	726	703	969	1229	1400	1626
Average daily cost of battery system (£)	9.29	6.83	6.86	9.54	12.10	13.78	16.00
Supercapacitor capacity (F)	137	144	176	355	562	749	843
Average daily cost of supercapacitor(£)	0.05	0.06	0.07	0.14	0.23	0.30	0.34
Average daily cost of the HESS (£)	9.34	6.89	6.93	9.68	12.33	14.08	16.34

Table 4.5 Optimized results of daily cost of the HESS at different SOCs.

SOC (%)	0	50	70
Average daily energy saving (£)	0.8		
Best discharge current (A)	q/1.9	q/4	q/5.8
Effective battery capacity (Ah)	199	416	624
Installation battery capacity (Ah)	382.7	555	726
Average daily cost of battery system (£)	18.25	15.12	6.83
Supercapacitor capacity (F)	141	136	144
Average daily cost of supercapacitor (£)	0.26	0.15	0.06
Average daily cost of the HESS (£)	18.51	15.27	6.89

Table 4.4 demonstrates that for the light discharge scenario, the minimum average daily cost of the HESS can be acquired when the maximum discharge current is set as $q/5.8$. At this time, the effective battery capacity is 624 Ah and installation battery capacity is 726 Ah. The Supercapacitor Capacity is 144 F. The average daily cost of the battery system and of the supercapacitor system are £6.83 and £0.06 per day. The average daily cost of the HESS mainly depends on the battery system. From Table 4.4, it is also obvious that when the discharge current is greater than $q/1.9$, the effective battery capacity is the same, which is due to discharge current saturation.

The results in Table 4.5 show that the best discharge current for the HESS is different for different SOCs. This means that in order to get the global minimum average daily cost for the HESS, both the discharge current and SOC should be adjusted. In this case, for a small building, the global minimum average daily cost of the HESS is £6.89. The depth of discharge of the battery is light and the best discharge current is $q/5.8$.

4.10 Conclusion

In this chapter, a hybrid energy storage system at building level has been investigated, the factors that can influence HESSs economical operation have been analyzed, and a battery SOC and discharge currents control model has been proposed. By applying this model, the daily investment of a HESS is reduced to 7.6 times (based on Table 4.5) of the HESS daily benefit, a twofold improvement on a smart building with battery storage system only and local energy generation. Even so, the daily cost of the system currently outweighs the benefits, by a factor of almost 8. However, when accounting for government subsidies and ongoing improvements in HESS technology, the economic case for storage at building level will rapidly become favourable.

The proposed optimization model for a HESS first shows three saturation factors that can influence system average daily saving. These three factors are battery capacity, maximum discharge current and SOC. To deal with battery capacity saturation, a more precise system control strategy is required. To deal with battery maximum discharge current saturation, the battery system needs to reduce the minimum SOC. To solve the SOC saturation, the battery system needs to increase the maximum discharge current. It has been concluded that a successful design should make full use of battery

capacity and attempt to make the battery system work in an operational area without saturation caused by capacity, discharge current or SOC.

The proposed HESS optimization model also shows that for a given daily energy cost saving, different depth of battery discharges will lead to different optimized system discharge currents and different average daily HESS costs. For a small building, the best HESS operation for the battery is light discharge and keeping the maximum discharge current at about one sixth of the battery capacity.

This chapter has proven that HESSs optimization can be used to balance maximum battery discharge current, minimum SOC and battery capacity. The maximum discharge current can have an influence on battery effective capacity, the minimum SOC and the capacity can have an influence on the battery's lifetime. By optimizing the HESS, its average daily cost can be significantly reduced.

Chapter 5. Rule-based control algorithm operational cost optimization of domestic buildings

This chapter presents a novel control algorithm for optimising operational costs of a combined domestic micro-CHP, boiler, battery and heat storage system. In this chapter, a minute by minute basic time-step is used to predict the loads and then based on the predicted loads, a simple and computationally efficient rule is developed to control CHP in two binary states, which aims to maximise CHP efficiency, and give the algorithm increased real world feasibility. In addition, a novel application of a dual battery system is proposed to support the micro-CHP. Each battery supplies just one of the distinctive morning and evening electrical load peaks, and thus inherently improves overall battery system lifetime.

A case study is presented where the algorithm is shown to yield up to approximately 20% energy cost savings above the base case, which is similar to the previous research done by M.C. Bozchalui, and 98.3% of the theoretical minimum cost. The theoretical minimum cost is calculated with conservative assumptions of perfect load prediction and ideal CHP operation at rated efficiency. In general, the algorithm is shown to always yield better than 88% of the theoretical minimum cost (except for summer days). This is a ratio that will be considerably higher when real-world CHP limitations are factored into the theoretical minimum calculation.

5.1 Introduction

In order to reduce daily energy cost and carbon emissions, renewable energy has been deployed in an increasingly localised and decentralised manner, in the form of distributed generation (DG). Distributed generation has the added advantage of increasing system robustness and reducing transmission losses [80]. At building level this takes the form of micro-generation, reducing the reliance on the grid. Energy independence can be increased still further with appropriate energy storage at building level so that local renewably generated energy can be stored until it is required. Moreover, with increasing uptake of SG technologies (especially smart meter technology), electrical power in buildings can be consumed more efficiently compared

with conventional buildings, through change in user behaviour and automation of building services, such as lighting [18]. These technologies play important roles to optimize electricity consumption at building level, however they have less impact on other forms of energy use, such as gas space heating and domestic hot water.

Researchers have therefore recently begun to focus on synergies between various kinds of energy carriers such that a holistic treatment can minimise the total overall energy use. In this context, a concept which was described in Chapter 2 called ‘Energy Hub’ (EH), was proposed to model various forms of energy transformation, conversion and storage considered holistically in a single entity [17]. The EH model is commonly used in recent literature to model the aforementioned technologies in a domestic setting and thus solve household energy optimization problems.

In [81], an application of multi-agent systems for cyber-enabled energy management of building structures (CEBEMS) is investigated; the CEBEMS models the building cooling, heat and power zones and finally energy zones, coordinates local generation to optimise building energy usage. In [82], the Monte Carlo valuation method for Energy Hubs is proposed. Together with DSM, this method solves the system uncertainty problem and improves system flexibility. However, in [81, 82], system scheduling and optimization are only based on heat demand, and electricity demand is neglected.

A multi-time scale structure rule is built to optimize a micro-grid energy system in [83]. [83] also claims that rule-based optimizations for energy systems are preferable to algorithm-based optimizations, because they are computationally more efficient and easier to implement in real-world applications. The types and capacity of DG and storage devices are optimised in [84] using a number of hybridised techniques. By defining sensitive loads as loads that must always be met under any conditions and non-sensitive loads as loads that may be interrupted under some conditions, [84] also develops an operational energy management strategy in micro-grids. However in both approaches described in [83] and [84] , the householder’s comfort may be compromised; due to requirements of DR in [83] and considering the non-sensitive load in [84].

In [11], a smart Energy Hub is modelled and multi-energy networks based on an integrated demand side management technique are proposed. Similar to [85, 86], the simulation time period for this work is one hour, which does not sufficiently consider dynamic changes of the EH modelled at domestic level.

For integrated energy systems, combined heat and power (CHP) can be used to couple the heat and electricity carriers. Residential buildings can benefit from Micro-CHP to simultaneously generate heat and power, and thus provide energy services at increased overall efficiency. Based on [87], the overall capacity for Micro-CHP is normally below 15kW. In some work, for example, [11] and [88], the heat efficiency and electricity efficiency of CHP are assumed to be constant. However, chapter 3 has clearly demonstrated that since the output of most micro-CHP may be varied, the efficiency also varies with any dynamic operation. Additionally, a CHP system requires some ramp up time to reach a steady state after it switched on or to match actual output after a set point is changed [89]. Finally micro-CHP presents the problem of whether to best schedule the output to meet electricity demand, heat demand or a compromise between the two.

In most work on building level Energy Hub optimisation, instead of attempting to predict load, it is assumed systems have perfect forecasts and so know energy demand in advance [5, 88]. However load prediction at building and micro-grid level can require long computation time and often performs poorly (an average error of 4.8% is given in [90] based on a number studies including [91-93]). It is therefore important to include improved load prediction in future work, and always take into account its performance and computation time in the context of overall optimisation.

In this chapter, a rule-based system optimization model will be proposed. Moreover, considering the difficulties to precisely predict heat and electricity load at building level, this chapter proposes a ‘CHP switch’ (CHPS) algorithm to control energy generation. This algorithm simultaneously considers the heat load and electricity load, which reduces the errors caused by energy prediction. The system time step is set as one minute, and thus will better track the true dynamic changes of the hybrid energy system. The optimization model presented here reduces energy cost, up to 19.8% compared to 20% in [18]. However, the proposed algorithm is more realistic and therefore more

straightforward to implement in a real world context. Moreover, the proposed algorithm will not affect household comfort level because loads are not constrained in any way.

The major contributions of this chapter are: 1) developing the rule-based control method; 2) reducing the simulation time step to one minute; 3) constructing a 'CHP switch' algorithm; 4) introducing dual battery operation in this context and 5) considering the re-start time of the CHP system and making CHP work in a more constraint aware way. The overall optimization algorithm for the Energy Hub at building level proposed in this thesis is summarised in Figure 5.1. In this Chapter, electricity load can be supplied by CHP, a HESS and electricity grid. Heat load can be supplied by CHP, a heat storage and boiler. Electricity grid and boiler are used as energy suppliers to meet to load when other energy suppliers cannot meet the demand.

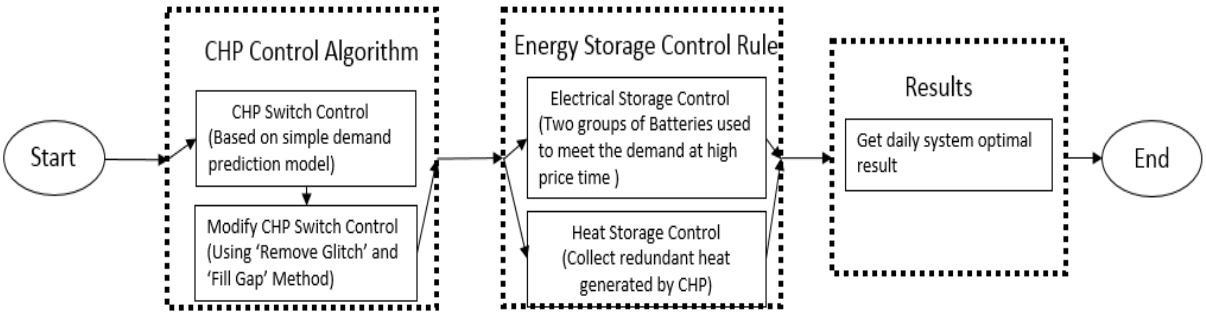

Figure 5.1 Rule-based Energy Hub optimization algorithm proposed in this chapter.

5.2 Optimization methods

5.2.1 CHP switch (CHPS) algorithm

As mentioned in the Chapter 5.1, energy prediction at building level has an average error of approximately 5% [90] whilst the short-term prediction level has worse performance. This suggests that a more precise model should be proposed to control the power generation system (CHP system).

Close study of household electrical demand has revealed that it usually changes rapidly and after changing will remain in the same state for several minutes or longer. However the heating demand fluctuates more smoothly and on slower time scales. After careful study of these two time series, [94] found that the electricity consumption

and heat consumption in every minute can thus be effectively predicted with the following simple equations:

$$P_{pE}(t+1) = P_E(t) \tag{5.1}$$

$$P_{pH}(t+1) = \sum_{i=t}^{i=t-9} P_H(t)/10 \tag{5.2}$$

In Equation (5.1) and (5.2), $P_{pE}(t+1)$ and $P_{pH}(t+1)$ represent the predicted electricity demand and heat demand in $(t+1)^{th}$ minute, respectively. $P_E(t)$ is the electricity consumption in the t^{th} minute and $P_H(t)$ is the heat consumption in t^{th} minute. In order to evaluate the accuracy of this load prediction approach, more than a hundred sets of daily load time series were been tested. This data showed that on a minute by minute bases 90.5% of the time the electrical demand is identical to the previous minute.

Clearly there will be some errors between the predicted demands and actual demands by using equation (5.1) and (5.2). This is shown in [94]. However, this has a very small influence if heat and electricity generation are considered together. Moreover, the main novelty of [94] is that this paper treats the predicted demands as a reference input just to control the CHP binary switch, whereas other studies, use more sophisticated statistical methods to predict demands. Then the predicted demands are used to deal with the whole system's optimization. Used specifically to control the switching of CHP, equations (5.1) and (5.2) yield a very low error rate of 3%, and have vastly reduced computation times and complexity compared to statistical methods.

After calculating the predicted demands, the benefit that CHP will give in the next minute can be expressed as:

$$B_{CHP}(t) = H_{CHP}(t) \times \frac{C_g(t)}{\eta_B} + E_{CHP}(t) \times C_e(t) \tag{5.3}$$

In (5.3), $B_{CHP}(t)$ is the benefit, in monetary terms that CHP can generate at the t^{th} minute if it is switched 'on'. $H_{CHP}(t)$ and $E_{CHP}(t)$ are the effective value of heat and electrical power contribution due to CHP in the t^{th} minute. $C_e(t)$ and $C_g(t)$ represent the gas and electricity prices in the t^{th} minute, respectively. η_B is gas to heat transfer efficiency, which equals to boiler's output efficiency. The cost to implement CHP in the next minute can be written as:

$$C_{CHP}(t) = P_R \times C_g(t) \tag{5.4}$$

where $C_{CHP}(t)$ is the cost of implementing CHP in the t^{th} minute and P_R represents the rated power (including heat power, electrical power and losses) of the CHP system. By comparing with the benefit that CHP can generate and the cost of implementing CHP, the state of CHP can be decided.

This algorithm significantly reduces the error introduced by energy prediction. Because this algorithm uses the predicted heat demand and electricity demand together to control the 'CHP switch'. The heat output of CHP is normally much greater than the electricity output (two to four times higher), and the errors of heat prediction are relatively small. This will reduce the error of 'CHP switch' model to some extent. Additionally, when the capacity of CHP is carefully designed and considering the fact that the domestic electricity price is usually much higher than the domestic gas price, the state of CHP is influenced by the benefit that CHP can yield. As long as the benefit of implementing CHP is greater than the operation cost of CHP, CHP will be switched on. This means, the CHP control system does not need to know the exact heat and electricity demand. Instead, it only needs to know whether the benefit of implementing CHP is greater than the cost, which further reduces the errors introduced by energy prediction. Finally, the short-term prediction is only used in CHP switch control and not for other parts of the system.

5.2.2 Modified 'CHP switch' algorithm

The CHPS algorithm offers a new way to control the 'CHP switch', however, the states of CHP may be changed very frequently in a short time period. Considering the fact that the state of CHP cannot be changed too frequently due to operational restrictions such as ramp up time, a modified 'CHP switch' algorithm is proposed in this part to reduce the switching frequency of CHP. This algorithm ideally requires the load to be recorded for at least a year a beforehand. If this data is not available then the daily load can be approximated using heating degree days and total aggregated energy bills, or the load simulators such as those used in this thesis [21] .

There are two ways to reduce CHP switching frequency. The first one is to keep CHP on when it should be off, defined in this chapter as 'Fill gap', and the second way is to keep CHP off when it should be on, defined in this chapter as 'Remove glitch'.

Figure 5.2 shows the ‘Fill gap’ and ‘Remove glitch’ methods. The ‘Fill gap’ method is normally used when the CHP is switched off in a short time period and at that time the energy price is relatively high. On the contrary, the ‘Remove glitch’ is normally used when the CHP is switched on for a very short time period and the energy price is relatively low at that time. By using both the ‘Fill gap’ and the ‘Remove glitch’, the switching frequency can be reduced, which mitigates the cycling stress on the CHP unit and allows it to reach a steady state with maximum operating efficiency. However, for those short periods, the CHP will generate surplus energy in the ‘fill gap’ and fail to meet load in the ‘remove glitch’ mode. These models will decrease the energy efficiency slightly, but they can be mitigated with energy storage, and supplemented by the grid if necessary.

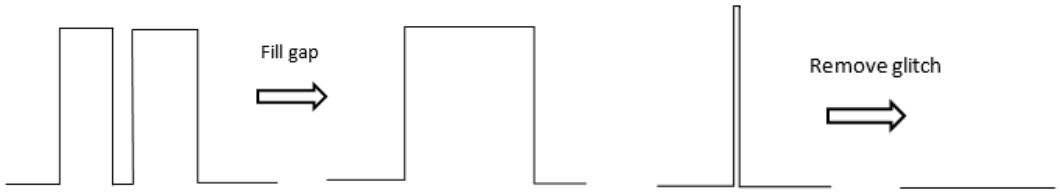

Figure 5.2 ‘Fill gap’ and ‘Remove glitch’ method

When using the ‘Fill gap’ or the ‘Remove glitch’ to reduce CHP switching frequency, it is necessary to have knowledge of the states of CHP in next few following minutes. To obtain states of the CHP in the next few more minutes, ‘probability of CHP switch on’ at each minute in a day is calculated based on historical data.

To get the ‘probability of CHP switch on’ in a day, four steps are required. First, select all the relevant recorded daily energy consumption data from the last year as sampling data i.e. data from the corresponding month of the previous year(s). Second, data that covers unusual events need to be removed from the sampling data (for example, days in which the occupants were absent or there was increased occupancy). When combined with occupancy data, for example from occupancy sensors, this process can be easily automated. If this leaves insufficient data to analyse, more data can be acquired from the year before last year or the load can be estimated, as mentioned before, through simulation and analysing historical weather data. The third step is to record the states of CHP switch in every minute for all sampling data. This is obtained using the previous year’s recorded demand and calculated using the basic control

described in chapter 5.2.1. The last step is to calculate the 'probability of CHP switch on' in each minute in a day using the following equation:

$$P_{on}^{t} = \frac{N_{on}^{t}}{N'} \tag{5.5}$$

In (5.5), $P_{on}{}^{t}$ is the 'probability of CHP switch on' in the t^{th} minute, $N_{on}{}^{t}$ is the number of days that CHP is switched on in the t^{th} minute and N' is total days in the sampling data.

After getting the 'probability of CHP switch on' in each minute in a day, CHPS algorithm can be modified as:

Step 1: Using Equation (5.1) and (5.2) to predict the next minute's electricity demand and gas demand.

Step 2: Comparing the benefit and cost of CHP in the next minute. If the benefit is greater than the cost, the state of CHP is set as 'possible on' and if the benefit is less than the cost, the state of CHP is set as 'possible off'.

Step 3: If the switch is 'on' at present and the state of CHP in the next minute is predicted as 'possible on', the CHP is kept 'on' in the next minute. On the other hand, if the switch is 'on' at present and the state of CHP in the next minute is predicted as 'possible off', the state of CHP in the next minute will depend on the possible state of CHP in the next few minutes (10 minutes are used here). If in the next ten minutes, 'the probability of CHP switch on' is less than 50% for every individual minute - CHP will be shut down; otherwise CHP will be kept 'on'.

Step 4: If the switch is off at present and the state of CHP in the next minutes is predicted as 'possible off' the CHP will be kept 'off' in the next minute; however, if the state of CHP in the next minute is 'possible on'; two situations should be taken into account. If the 'probability of CHP switch on' is less than 20% in all of the next ten individual minutes, this 'possible on' will be treated as a 'glitch' and will be held in the off state. Otherwise CHP will be switched on in the following minute. To attempt to make full use of CHP, in this case, 'probability of CHP switch on' is set as 20%, rather than 50% as in step 3.

It is important to note that for all cases, the CHP cannot be switched on, if 'switch off' time between two 'switch on' times is shorter than CHP re-start time. Figure 5.3 is a flow diagram to show modified CHPS algorithm.

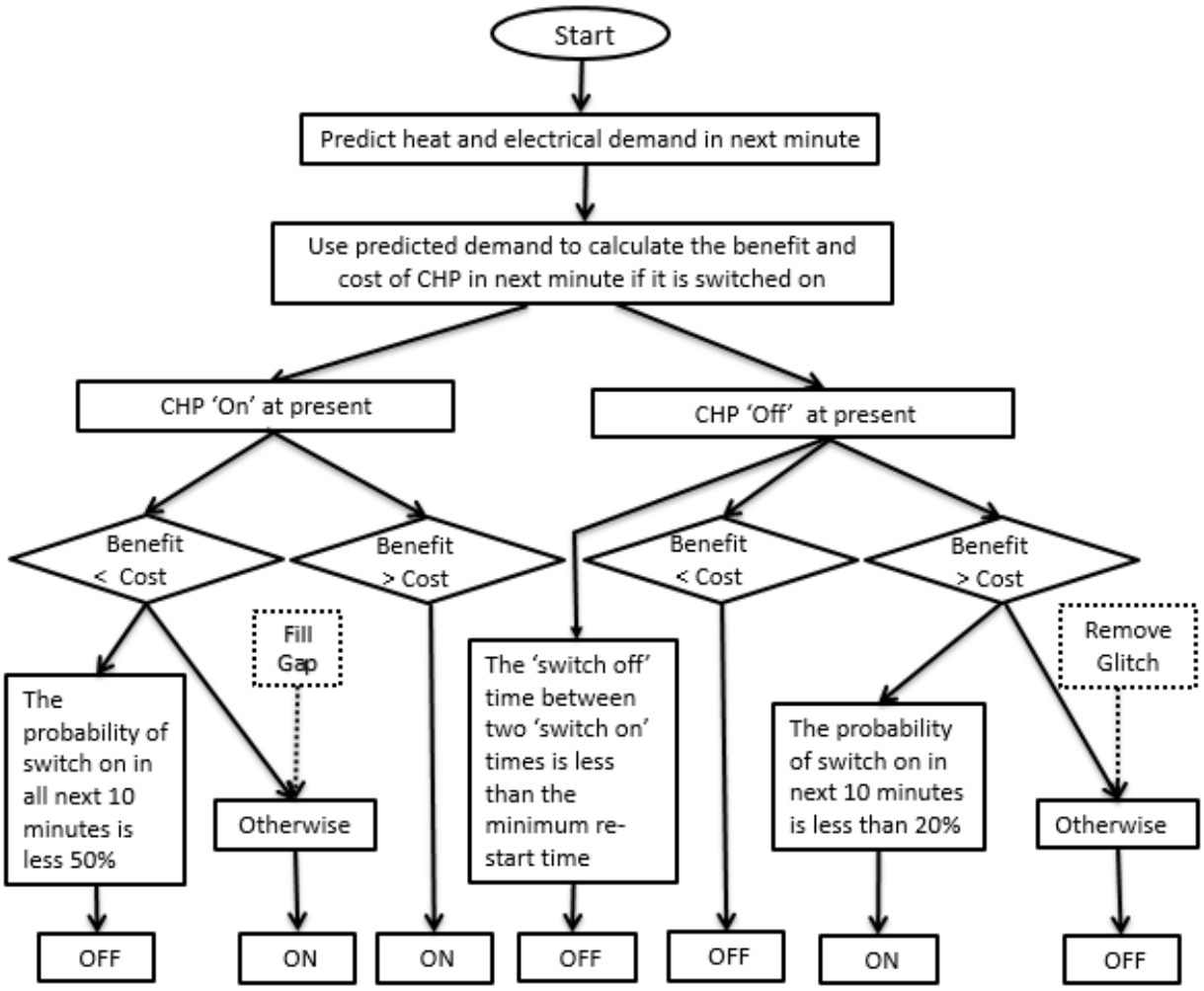

Figure 5.3 Modified CHPS control model.

5.2.3 Energy storage systems control rule

Storage systems play an increasingly important role in modern energy systems. By regulating demand, they improve energy efficiency and thus reduce emissions. The energy cost can be greatly reduced, provided energy storage systems can be operated optimally. Moreover, storage technology has improved very quickly in recent years, specifically, in terms of smaller and lighter physical footprints and reduced cost [61], making them more practical in the domestic context. However, with the addition of a

storage system, the energy systems' complexity is greatly increased. With the inclusion of storage, the EH model requires a time domain treatment such that the full charge cycle of storage is considered, greatly increasing computational complexity. Additionally, a storage system needs many converters, transformers and switches to connect energy storage systems to the main energy system, thus giving a more complex system topology.

Electrical storage systems (ESSs) control rule

The purpose of the ESS is to support the CHP by reducing the reliance on grid imports during peak price periods and storing the surplus energy from the CHP switching, thus reducing the overall running cost of meeting the loads. However, this requires a precise control rule. Two things need to be considered carefully in advance: the amount of energy required to meet each electrical peak demand and the exact time to begin charging.

An ESS normally consists of a group of batteries, but in an Energy Hub system at building level, it is desirable to have more than one group of batteries due to the high frequency of charge cycles required. Compared with large electrical systems, the electricity demand at building level has higher uncertainty, thus the states (charging and discharging) of ESSs may need to be changed very frequently. However, the life span of batteries will be significantly reduced if the states of batteries are changed too frequently. In [95], the authors describe that a simple two-battery system has a longer life span compared with a single battery system which has the same capacity.

In this chapter, the ESS consists of two groups of batteries, and two batteries are used separately to supply the electrical load at the two daytime peak demands (shown in Figure 5.4).

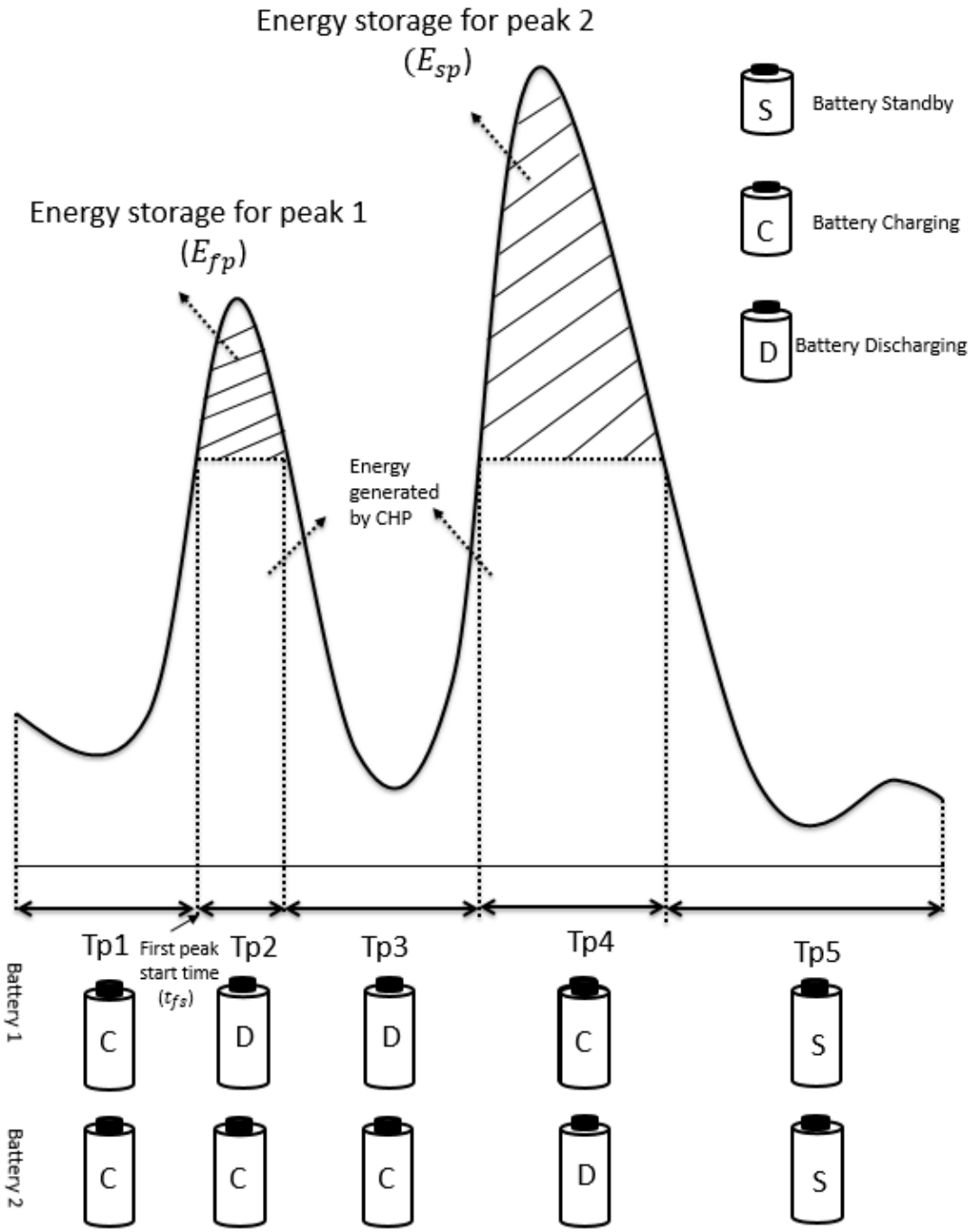

Figure 5.4 Two-battery storage system control rule.

In Figure 5.4, the first battery is charged before the morning peak, TP1, and discharged to compensate energy shortage for the first peak demand time TP2. (The energy shortage in the first peak demand time is the difference between electrical energy generated by CHP and the building's electrical demand.) The second battery is charged from very early in the morning to the beginning of the second peak, TP1 to TP3, and then discharged to compensate energy shortage for the second peak, TP4.

The electricity used to charge batteries is normally the surplus electricity generated by the CHP system. Very occasionally, electricity from the grid is used to charge the battery. The two-battery storage system control algorithm is shown in the flowchart in Figure 5.5 and is as follows:

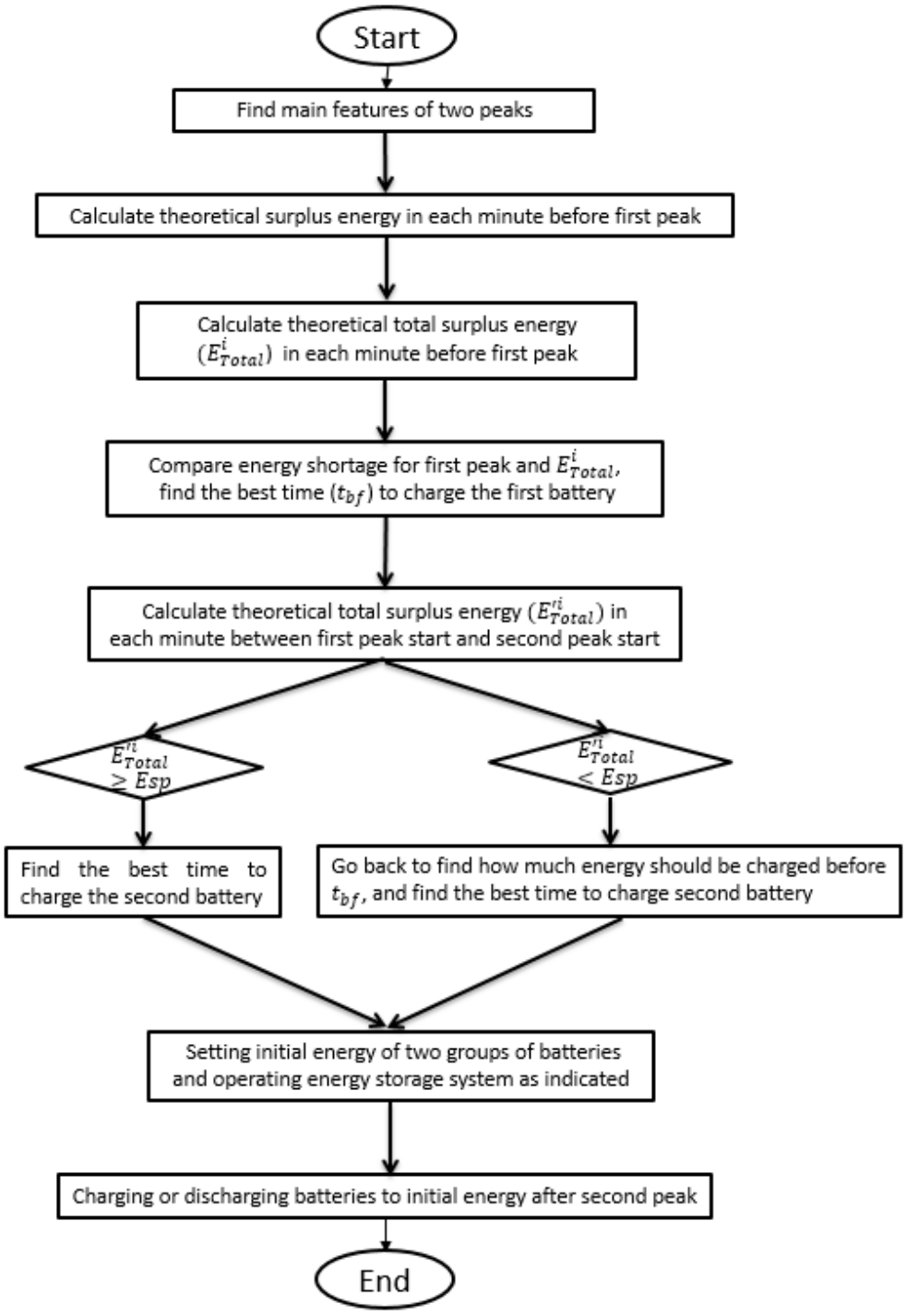

Figure 5.5 Electrical energy storage system control rule.

Step 1: Find each of the two daily peak demand start and end times and calculate how much energy should be stored in advance for each peak. This can be done by analysing the historical data from the same month of the previous year and using the curve fitting algorithm described in [96].

Step 2: After finding the first peak demand start time (t_{fs}), and the amount of energy shortage for the first peak demand (E_{fp}), the amount of theoretical surplus electrical energy ($E_{Theo}{}^{i}$ in kilowatt hour) generated in each minute before the first peak can be calculated.

$$E_{Theo}^{i} = (P_R \times \eta_{CHPE} \times t - E_{his}^{i})/(1000 \times 60) \quad (5.6)$$

In equation (5.6), P_R is CHP rated power in Watts, η_{CHPE} is CHP electrical efficiency, t is time in minutes and E_{his}^{i} is the average historical electricity consumption in the i^{th} minute, in Joules. E_{Theo}^{i} is the theoretical surplus electrical energy that can be stored in the i^{th} minute.

Step 3: Then, the E_{Theo} vector needs to be modified to get the total surplus electrical energy (E_{Total}) in each minute generated by CHP before the beginning of the first peak. To be specific, this means changing all the values in the E_{Theo} vector whose value is less than zero to zero, and keeping other terms the same, producing a modified vector E'_{Theo}. The formula of E_{Total} in the i^{th} minute can be written as:

$$E_{Total}^{i} = \sum_{t=i}^{t=first\ peak\ start\ time} E'^{i}_{Theo} \quad (5.7)$$

Step 4: Comparing E_{Total}^{i} and E_{fp}, to find the highest value of i that makes E_{Total}^{i} greater than E_{fp}. Record the value of i which is the best time to charge the first battery (t_{bf}).

Step 5: Use the same method to calculate the total theoretical surplus electrical energy E'^{i}_{Total} in each minute generated by the CHP between the start of the first peak and the start of the second peak. Compare E'^{i}_{Total} with energy shortage for the second peak (E_{sp}), if E'^{i}_{Total} is greater than E_{sp}, record the value of i', which is the theoretical best time to charge the second battery. However, if E'^{i}_{Total} is less than E_{sp}, calculate the difference between the two values and record it as E'_{sp}, and then calculate the total

theoretical surplus electrical energy E''^{i}_{Total} in each minute generated by CHP before the best time to charge the first battery(t_{bf}). Comparing E''^{i}_{Total} and the E'_{sp}, find the maximum value of i'' and that is the theoretical best time to charge the second battery.

Step 6: Set the initial energy of the two groups of batteries. By carefully choosing the battery initial energy, ESSs efficiency can be improved. On the one hand, if the initial energy in batteries is too high, the standby loss will be greater; on the other hand, if the initial energy is very low, the life span of battery will be reduced and less energy can be used as backup energy when the peak demand time extends or it comes earlier. This step is empirical and dependent on the particular system parameters, as shown in the example in Chapter 5.4.3.

Step 7: After the end of the second peak, both batteries need to be charged or discharged to the initial value. This usually involves charging both batteries since they have previously supplied the two load peaks. Therefore even if the CHP cannot be used to recharge the batteries, this approach uses cheaper grid electricity during the cheaper night time period.

Heat storage systems (HSSs) control rule

Compared with ESSs, the Heat Storage System (HSS) has lower overall efficiency (i.e. charging efficiency and discharging efficiency), and a higher standby loss as quantified in Chapter 2. In addition, gas price is likely to remain static on an hourly basis whereas domestic electricity price will soon become dynamic in most developed countries. Despite this, static gas price is likely to remain always cheaper for some time. Therefore, under these conditions, the use of a boiler to heat water in advance is not justified. For HSSs control, the HSS is only charged by the redundant heat generated by CHP and discharged when it is required. Heat is then dispatched when it is needed, from the supplies with the following priority order 1. CHP (if it is 'ON'), 2. HSS, 3. Gas via the boiler.

5.2.4 Effective CHP energy efficiency and Average CHP input power to rated power ratio

As mentioned in Chapter 3, inappropriate CHP sizing and control will reduce system benefit to cost ratio and system energy efficiency. Two parameters, effective CHP energy efficiency and average CHP input power to rated power ratio, are defined in

Chapter 3 to test the performance of CHP, and these two parameters will be used in this chapter to show the CHP performance for the new CHP control algorithm. Equation (5.8), (5.9a) and (5.9b) are used to show effective CHP energy efficiency and average CHP input to rated power ratio.

$$\widetilde{\eta_{CHP}} = \eta_{CHPR} \tag{5.8}$$

$$h_{CHP} = \sum_{t=1}^{t=L}(K(t))/L' \tag{5.9a}$$

$$K(t) = \begin{cases} 1 & If\ the\ CHP\ is\ operated\ at\ rated\ power \\ 0 & If\ the\ CHP\ is\ switched\ OFF \end{cases} \tag{5.9b}$$

In (5.8), $\widetilde{\eta_{CHP}}$ is effective CHP energy efficiency and η_{CHPR} is CHP rated overall output efficiency. In (5.9a) and (5.9b), h_{CHP} is the average CHP input power to rated power ratio, $K(t)$ is the state of CHP in t^{th} minute and L' is the number of samples. Considering the fact that CHP can only be operated in two states: ON and OFF, the effective CHP output efficiency is equal to CHP rated overall output efficiency. Moreover, average CHP input power to rated power ratio is only related to the time that CHP is switched ON.

5.2.5 Theoretical minimum daily operation cost

To evaluate the performance of the proposed EH optimization, the following work will introduce a method to calculate the theoretical minimum daily operation cost for the EH shown in Chapter 2. This calculation assumes the system has perfect load predication, the CHP output can be varied from 0 to its maximum rated output, the efficiency at any output is its rated efficiency and there is no delay between the set point and actual output. Therefore it gives the most conservative base case against which to evaluate the efficacy of the algorithm proposed in this chapter.

This calculation consists of five steps. First, compare the electrical demand and maximum electrical output of CHP, to find the first and last time that the electrical demand is greater than CHP electrical output in each high/intermediate price time. The high/intermediate price time are H1 and H2/L2 and L3 which are shown in Figure 4.4, respectively. Calculate the amount of electrical energy shortage (EES) during each high price time and intermediate price time based on equation (5.10):

$$E_{sn} = \sum_{t=ns}^{t=ne} P_E(t) \times t - P_R \times \eta_{CHPE} \times T \tag{5.10}$$

In (5.10), E_{sn} is EES for n^{th} high/intermediate price time. $\sum_{t=ns}^{t=ne} P_E(t) * t$ is the sum of the electrical energy consumption calculated during the n^{th} high/intermediate price time when electrical energy generated by CHP is less than the demand and T is the total time that electrical energy generated by CHP is less than the demand during n^{th} high/intermediate price period. This assumes that the CHP capacity is rated such that at certain peak times of electrical demand it will not be able to meet the demand.

Second, calculate redundant electrical energy that can be stored during n^{th} high/intermediate price period if the CHP is working at rated power.

$$E_{nstore} = (P_R \times \eta_{CHPE} \times T' - \sum_{t=ns}^{t=ne} P_E(t') \times t') \times \eta_b \qquad (5.11)$$

where, E_{nstore} is total electrical energy that can be stored for n^{th} high/ intermediate price time. $\sum_{t=ns}^{t=ne} P_E(t') \times t'$ is the sum of the electrical energy consumption calculated during the n^{th} high/intermediate price time when electrical energy generated by CHP is greater than electrical demand and T is the total time that electrical energy generated by CHP is greater than demand during n^{th} high/intermediate price period. η_b is battery-supercapacitor system overall efficiency.

The third step is to find the differences between EES in step 1, and redundant energy that can be stored during n^{th} high/ intermediate price period from step 2. Using the same method as proposed in the 'electrical storage system control rule' part, find the best time that CHP needs to work at rated power to charge the battery. Using the maximum CHP output here avoids storage standby losses as much as possible because charging occurs at the latest possible period before the energy is required.

After finding the time that CHP should work at rated power, the next step of this calculation is to control the output power of CHP at other times of day. At these times, if the electrical demand is greater than CHP electrical power generation, CHP must work at its rated power. If the electrical demand is less than the rated CHP electrical output, CHP output power should just meet the electrical demand. This step considers the relationship between energy tariff and battery-supercapacitor system overall efficiencies. Also at this step, redundant heat generated by CHP can be stored by the heat storage system and when the CHP output cannot meet the heat demand, the heat storage system will be prioritized to supply the heat load.

Finally, calculate the electricity and the gas bought from the grid. The gas price contains two components: gas used to supply the boiler and gas used to supply the CHP. The theoretical minimum operation cost of an Energy Hub can be written as:

$$C_{Theo} = C_{grid} + C_{chp} + C_{boiler} \tag{5.12}$$

In (4.12), C_{Theo}, C_{grid}, C_{chp} and C_{boiler} are the theoretical minimum operation cost, electricity costs bought from grid, CHP operation cost and boiler operation cost. In the following section a case study will be used to illustrate the aforementioned methodology and compare it against the minimum theoretical cost.

5.3 A case study

In this chapter, a terraced house built in the UK between 1984 and 1997, which was occupied by four people, will be used as an example to test the proposed optimization rules. The electricity loads and heat loads were generated by the CREST and Strathclyde model, which were mentioned in Chapter 2. In order to simulate statistically realistic historical data, 50 groups daily electricity demand data need to be generated in each month.

From Chapter 3, in a terraced house, gas engine CHP has a higher effective energy efficiency and average CHP input power to rated power ratio compared with fuel cell CHP, if their installation capacity is the same. Meanwhile, the installation cost of gas engine CHP is much lower compared with fuel cell CHP. The only weakness of the gas engine CHP is that it needs to cost more to supply daily heat and electricity demand. However, this can be compensated by adding an energy storage system.

Chapter 3 also shows that when the gas engine CHP capacity is set as 3500 W, the system can obtain theoretical daily minimum operation cost. Considering the fact that the energy storage system has the ability to shift the loads, in this chapter, a 3 kW gas engine CHP is installed in the domestic building.

In Chapter 4, a hybrid electrical energy storage system has been designed, and in this chapter, to test its performance, the optimal battery and supercapacitor capacity obtained in Chapter 4 will be tested. In this chapter, the total battery installation capacity is 726 Ah and 24 V, and the total supercapacitor capacity is 144 F. Other parameters can be found in Chapter 2, Table 2.1.

In the next section, a spring day's energy data is used as an example to show how the proposed algorithm works. Figure 5.6 and 5.7 are the daily energy tariffs and demand in a typical spring (April) day.

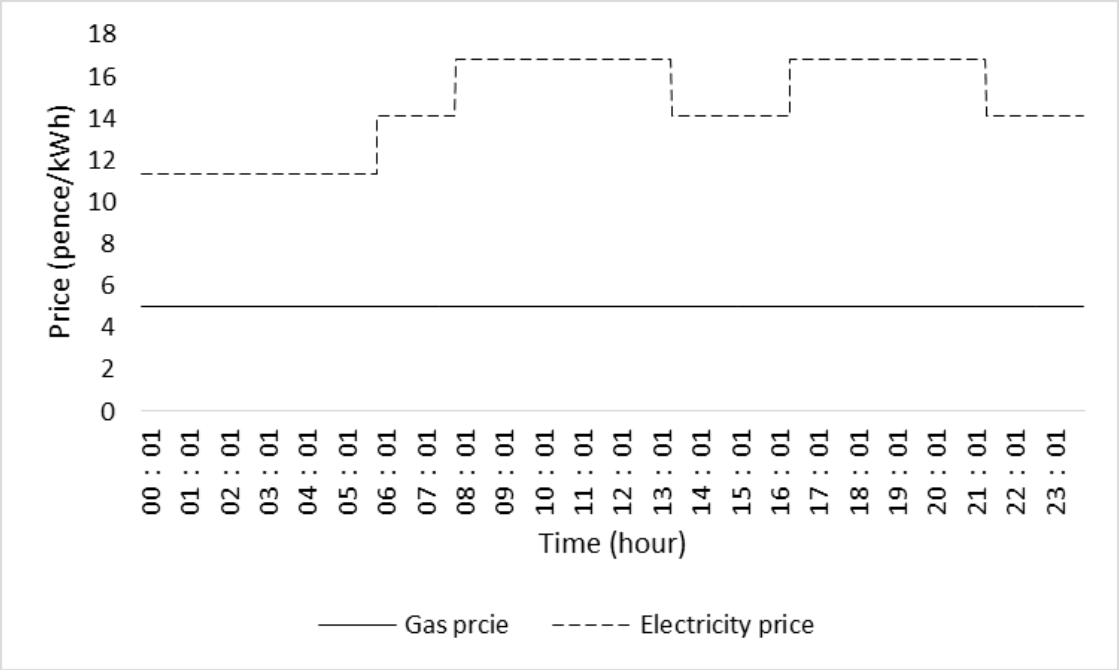

Figure 5.6 Electricity and gas tariffs in spring.

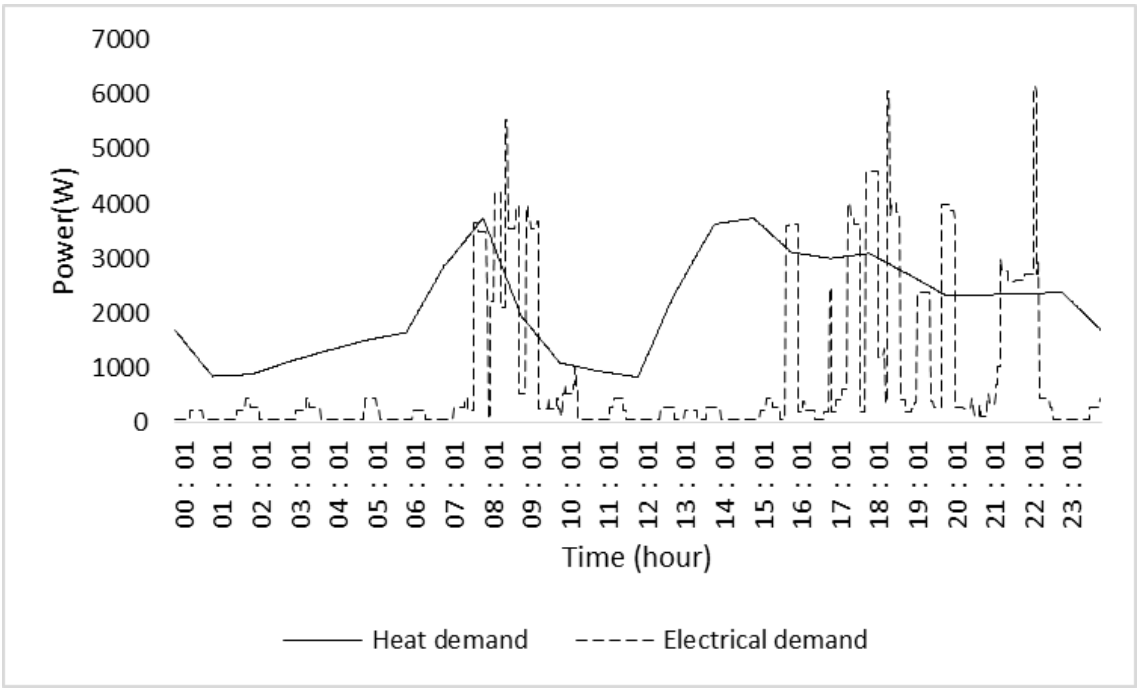

Figure 5.7 An example of daily heat and electrical demand in spring [21, 23].

5.4 Optimization results

For a domestic building, the energy tariffs and demands which are shown in Figure 5.6 and Figure 5.7, yield a daily gas cost of 293 pence and a daily electricity cost of 308 pence. In this case, the daily operational cost for a domestic building is 601 pence without any optimization algorithm. The following section will show daily operational cost based on the CHP control algorithm.

5.4.1 CHP control algorithm optimization

To get a more precise CHP control result, load prediction plays a crucial role. Based on the simple load prediction rule proposed by equation (5.1) and (5.2), Figure 5.8 shows the differences between the actual demands and the predicted demands. Figure 5.8 reveals that the electrical demand prediction error can be very high compared to the heat demand prediction error. However, when using the predicted demands just to control binary CHP, as discussed in Chapter 5.2.1 and shown in [94], this approach gives a surprisingly low error rate, which is 2.9% in this particular case study. Figure 5.9 shows the times that the CHP control algorithm generates errors in the typical day.

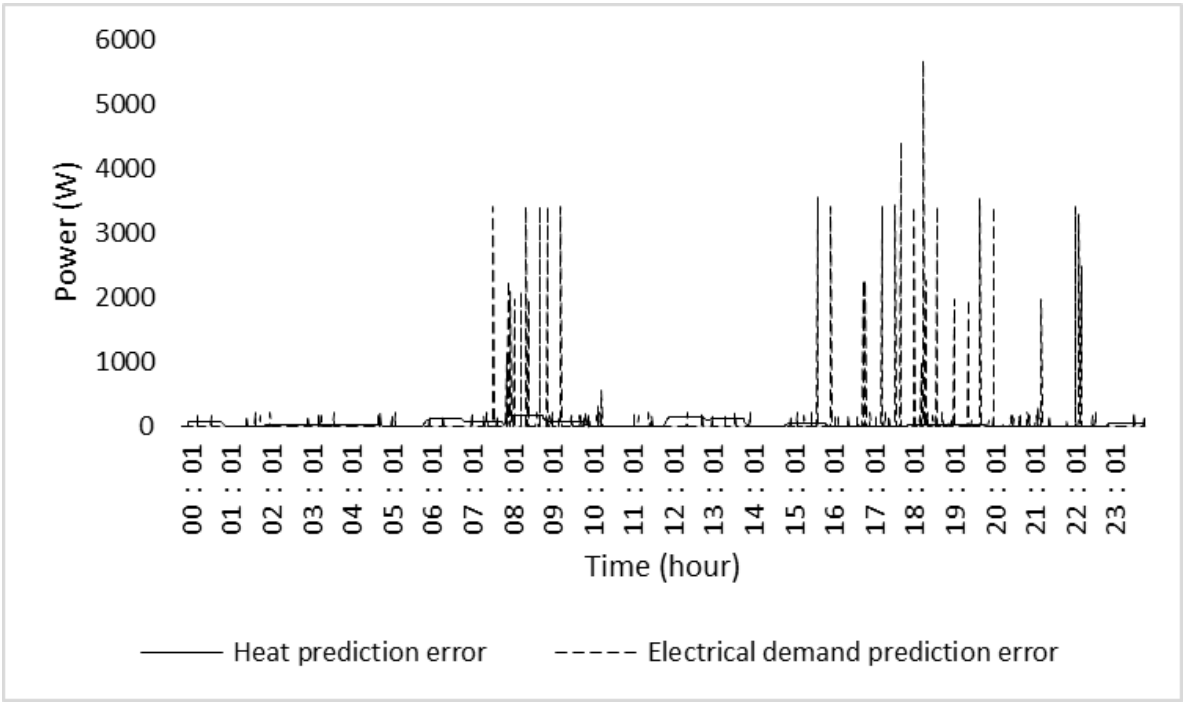

Figure 5.8 Heat and electrical demand prediction errors by using the proposed prediction algorithm.

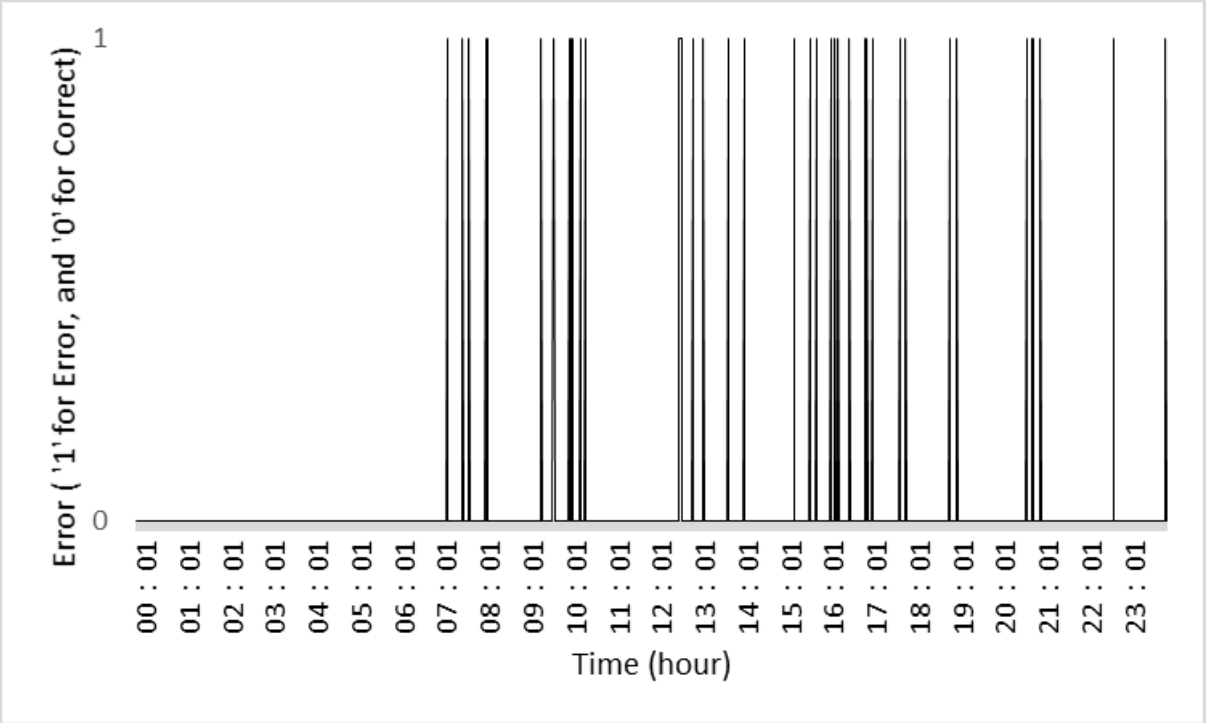

Figure 5.9 The CHP control algorithm errors in a sampling date.

By applying the CHP control algorithm, the domestic building energy operational cost is reduced to 563 pence, which offers 38 pence saving a day. However, by applying this algorithm, the state of CHP changes very frequently, especially at night peak demand time. This is shown in Figure 5.11. In Figure 5.11, the dotted line shows the state of CHP in a day with the CHP control algorithm. To reduce dynamic ramp up times and cycling stress on the CHP, it is necessary to reduce CHP switching frequency.

5.4.2 Modified CHP control algorithm

To reduce CHP switching frequency, ‘Remove glitch’ and ‘Fill gap’ methods are used in this section, as described in Chapter 5.2.2. In order to distinguish a CHP state signal as ‘glitch’ or ‘gap’, the probability of CHP ‘switch on’ in each minute needs to be acquired in advance. Figure 5.10 shows the probability of CHP ‘switch on’ of all the days in April averaged. After getting the probability of CHP ‘switch on’, the modified CHP switch state can be acquired and it is shown in Figure 5.11, where the solid line shows the modified CHP state in that day.

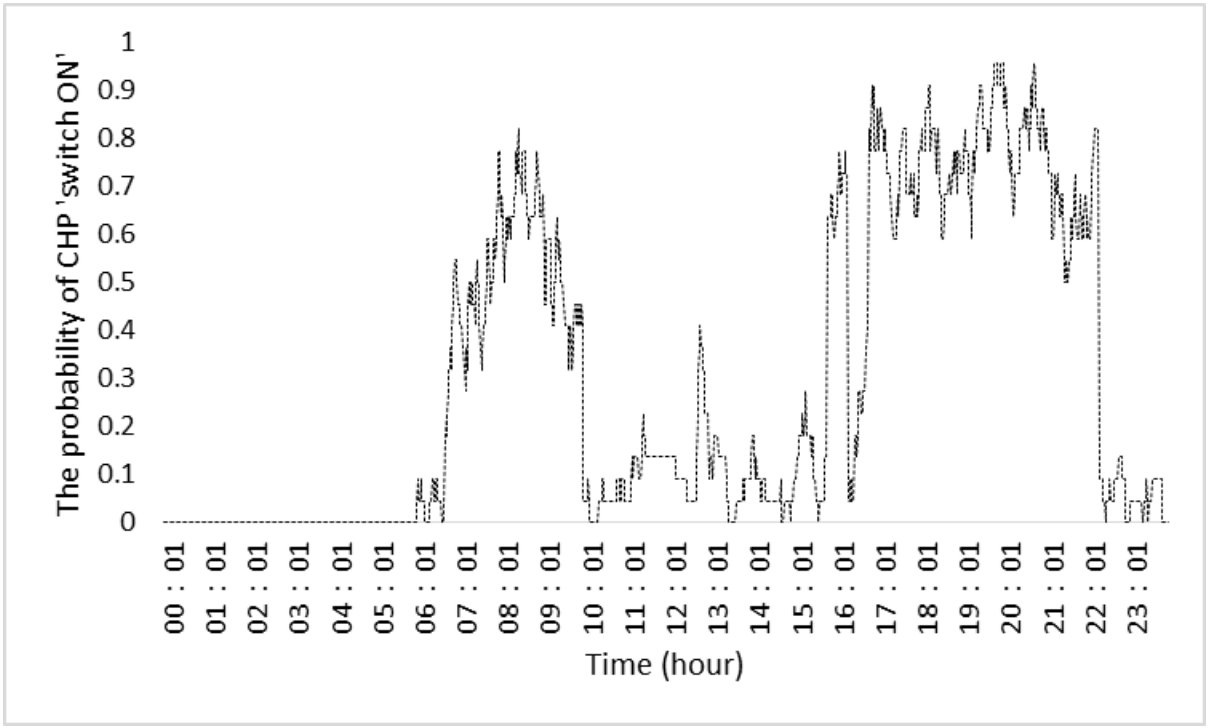

Figure 5.10 The probability of CHP 'switch ON' in April.

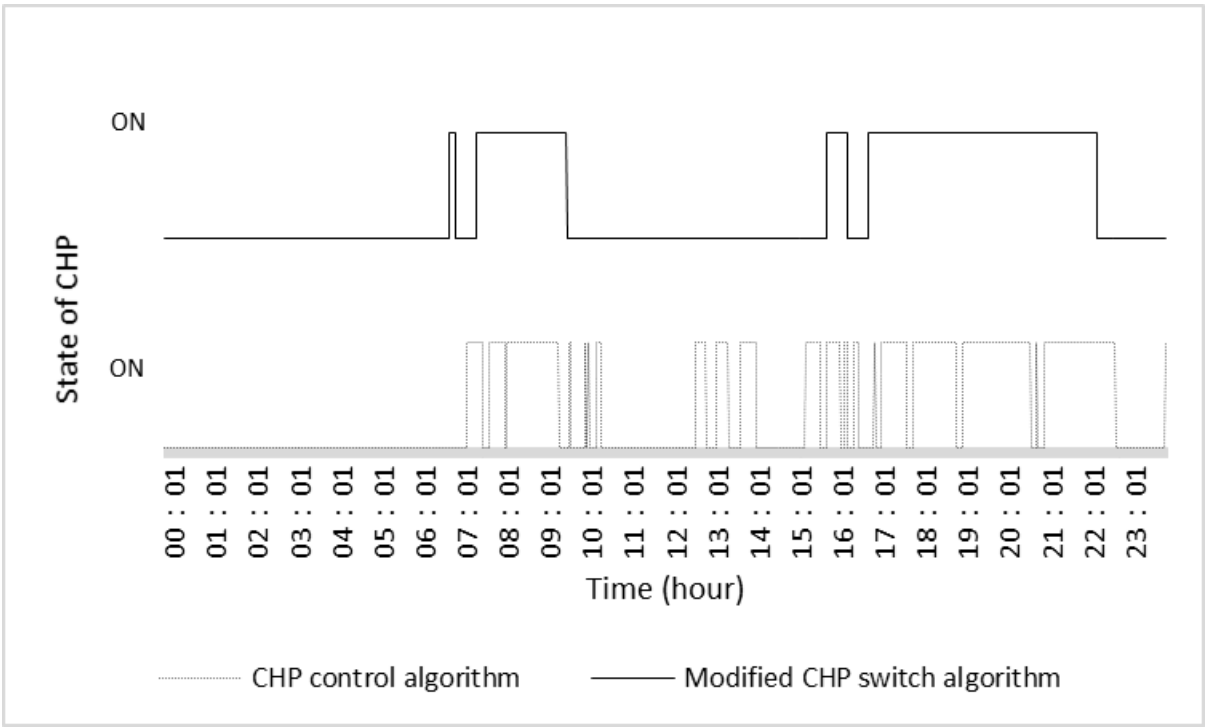

Figure 5.11 The states of CHP by applying CHP control algorithm and modified CHP control algorithm.

Compared to the standard CHP control algorithm, the modified CHP switch algorithm has successfully reduced switching frequency through ‘Fill gap’ and ‘Remove glitch’. However, ‘Fill gap’ and ‘Remove glitch’ increase the system operational cost slightly to 566 pence, which is about 3 pence higher than the CHP control model. Simply using the CHP control model can reduce the energy cost for the domestic building; however, energy efficiency is reduced due to the redundant energy generated by the CHP. Figure 5.12 shows the total electrical energy and heat energy that can be stored if the energy storage system is available. After calculation, total redundant heat generated by the CHP is 0.197 kWh and the redundant electricity is 1.33 kWh.

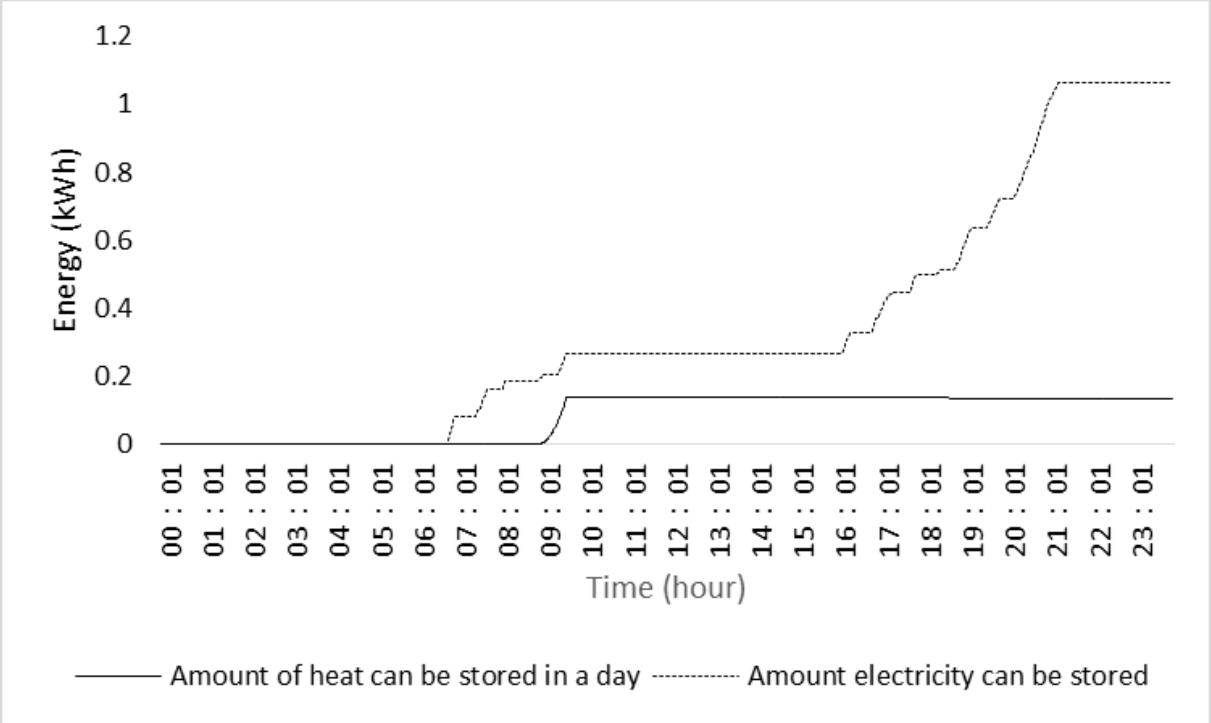

Figure 5.12 The accumulative redundant energy stored in the energy storage system by applying the modified CHP control algorithm.

5.4.3 Energy storage system

The importance of using an energy storage system was mentioned previously. A robust and intelligent energy storage system can save the operational cost of an Energy Hub and reduce carbon dioxide emission. However, inappropriate design may waste more energy and cause system instability.

In Figure 5.13, the black points in the graph represent the average of the electricity used in each minute in April 2013 and the blue curve indicates the distribution of

electricity consumption in April 2013. Assuming that the pattern of the household's energy consumption does not change much, the blue curve can offer some help when designing the energy storage system in April 2014. Figure 5.14 and Figure 5.15 show the two peaks in Figure 5.13 in more detail. Compared with Figure 5.14, Figure 5.16 has changed its matching factor to 1.0.

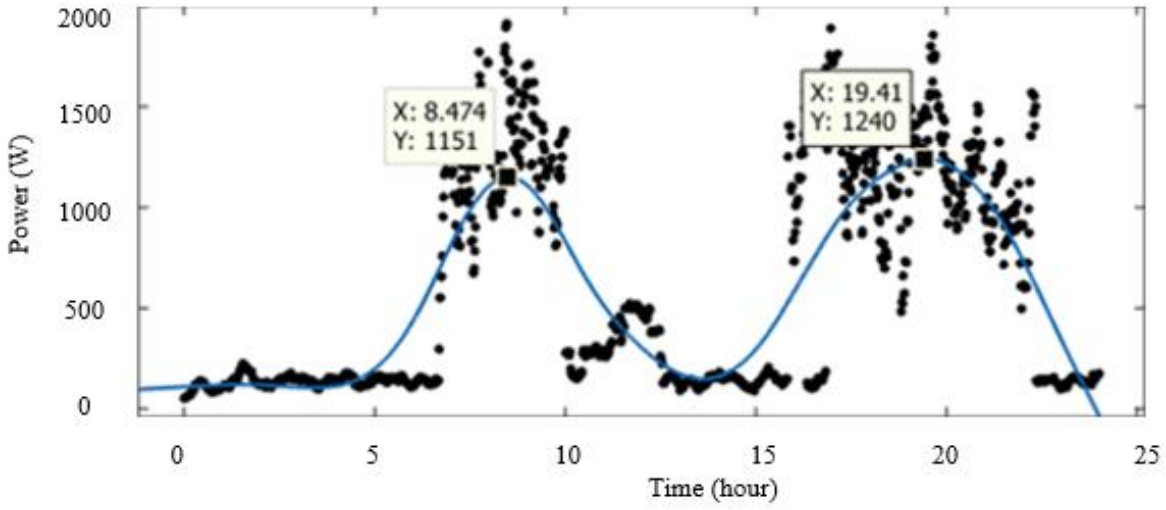

Figure 5.13 Electricity consumption distribution in April 2013 (matching factor 0.85).

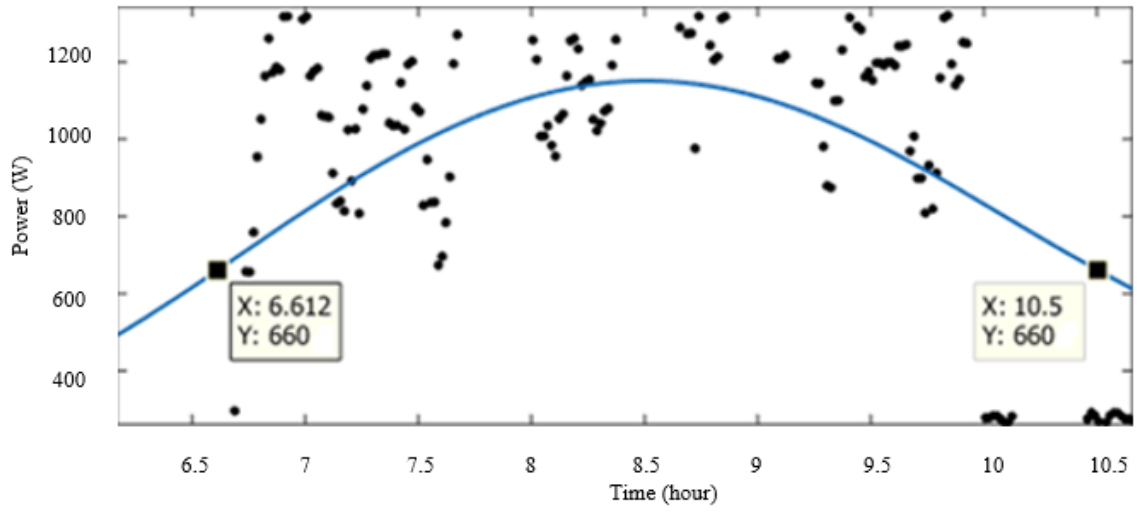

Figure 5.14 Morning peak boundary condition.

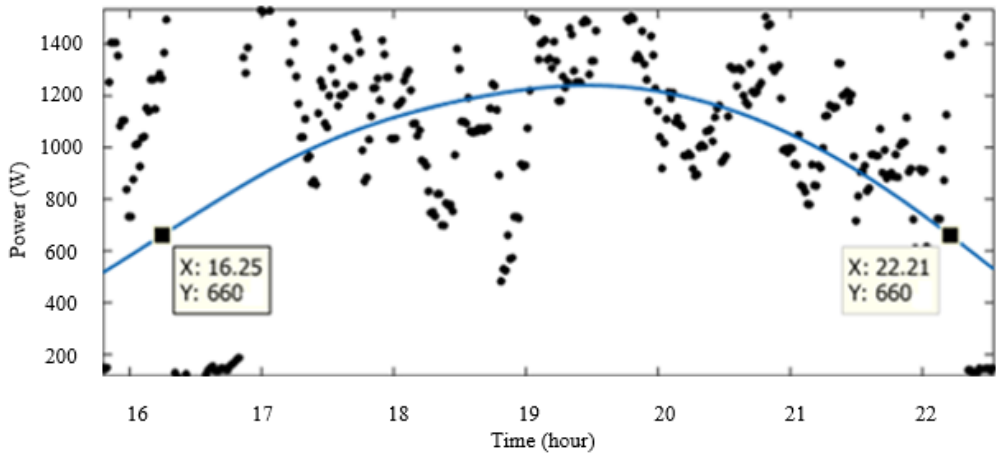

Figure 5.15 Evening peak boundary condition.

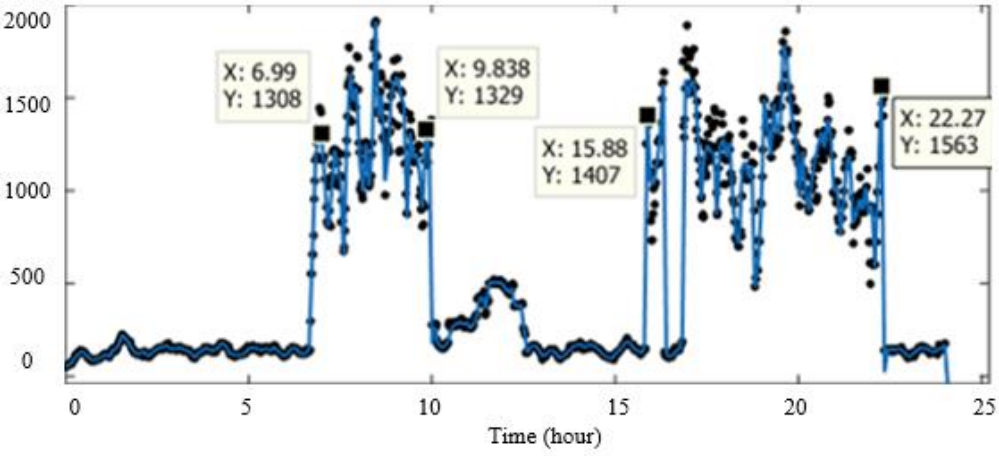

Figure 5.16 Electricity consumption distribution in April 2013 (matching factor 1.0).

By analysing Figures 5.13 to 5.16, some useful information may be identified as shown in Table 5.1.

Table 5.1 2013 April electricity consumption situation.

2013 April household electricity use situation (Weekday)			
Morning peak	**Start: 06:37:00 am**	**End: 10:30:00 am**	**Duration: 3hour57mins**
Electricity to be stored	**2.417 kWh**		
Evening peak	**Start: 4:15:00 pm**	**End: 10:13:00 pm**	**Duration: 5hour58mins**
Electricity to be stored	**3.417 kWh**		
Getting up time	**06:59:00 am**	Bed time	**10:16:00 pm**
Average use per minute	**567.8 W**	Total electricity consumption	**299.8 kWh**

Table 5.1 can be used to illustrate how much electricity should be stored in each month, the time to charge and discharge the batteries and the household's living habits.

Similar work has been done by the author to show electricity consumption in other months of 2013 in the same house. By comparing all 12 months' results, average electricity consumption per minute in 12 months can be shown in Figure 5.17 and the maximum energies that need to be stored in 12 months are shown in Figure 5.18.

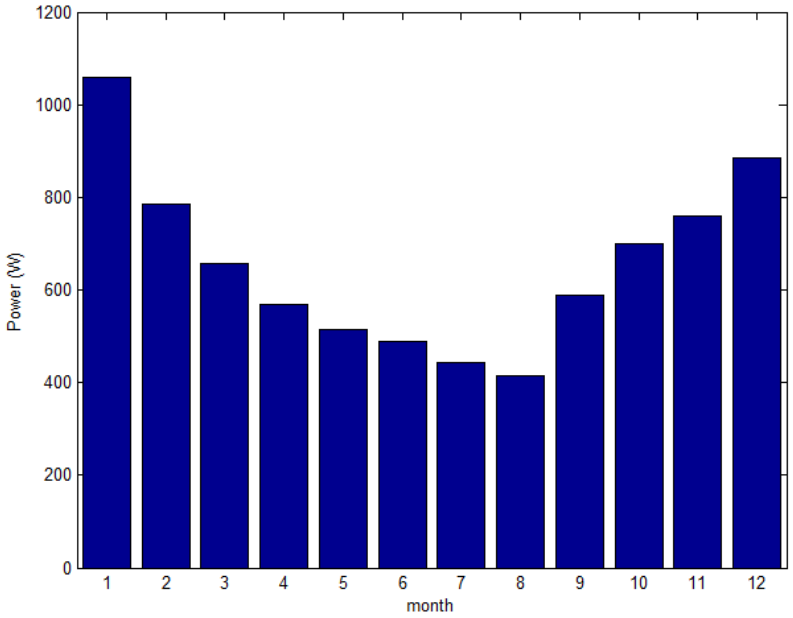

Figure 5.17 Average electricity consumption in 12 months.

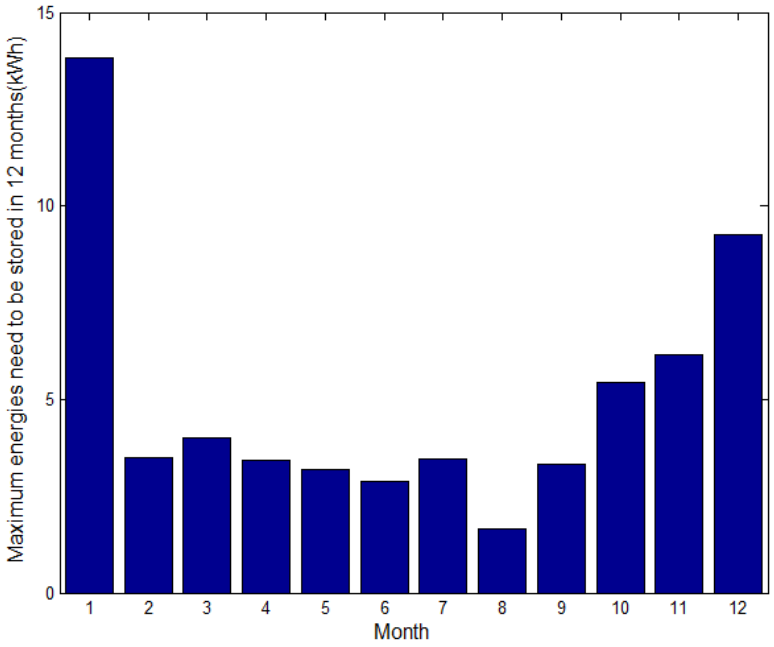

Figure 5.18 Maximum energies to be stored in 12 months.

Figure 5.17 shows that the maximum average electricity consumption is 1058 W/min in January and the minimum average electricity consumption is 431.4 W/min in August. Figure 5.17 demonstrates that large differences of average electricity consumption make it difficult to size the CHP. Also, Figure 5.18 shows a great differences of maximum energy to be stored in 12 months, which further complicates the process of sizing the energy storage equipment.

Aforementioned in Chapter 5.2.3, by carefully choosing the initial value of the energy storage system, the operational cost can be reduced to some extent. Considering the high standby loss of the heat storage system and the flat rate of gas price, it is preferable not to store heat in advance. Thus, the initial heat in HSS is set to 0 kWh. However, considering the fact that the electricity tariff can change significantly in a day and the standby loss for electrical storage system is relatively small, storing a reasonable amount of electrical energy in advance can improve overall system cost. Figure 5.19 shows the electricity cost of the domestic building against initial energy stored in the electrical storage system. This was produced using a fixed base case combining the overall management system shown in Figure 5.1 and the initial parameters in Chapter 2.

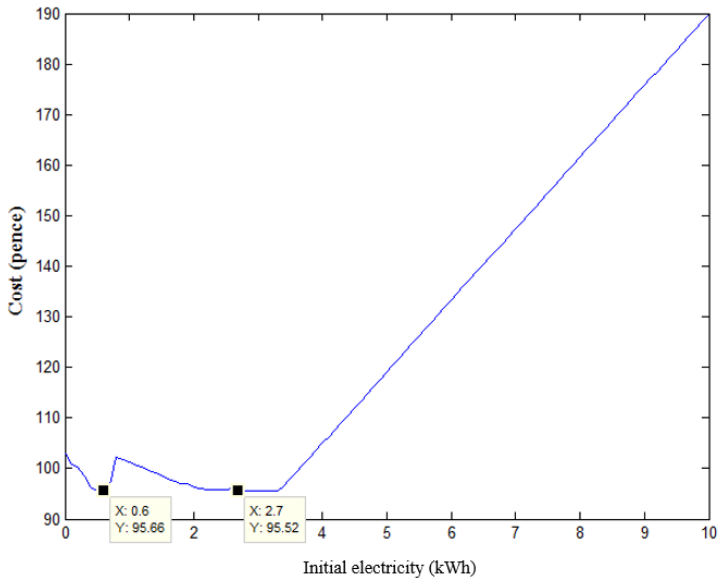

Figure 5.19 Battery initial energy in (kWh) vs domestic building daily electricity cost.

From Figure 5.19, there are two initial electricity values that can generate minimum daily electricity costs. Even though the global minimum cost can be acquired by setting

initial electricity as 2.7 kWh, this chapter will choose 0.6 kWh as initial electricity. This is because the battery charging power can reach 35 kW at the end of day if the initial electricity is set as 2.7 kWh. This has great influence on battery life time, therefore the initial electricity of the battery is set as 0.6 kWh. After setting the initial energy for the energy storage system and operating it as demonstrated in Chapter 5.2.3, the amount of imported gas, electricity and the state of CHP can be acquired. Figure 5.20 shows the state of CHP, the amount of imported gas and electricity in a day based on the proposed Energy Hub optimization rules in this thesis. Figure 5.21 shows the amount of energy which is stored in battery one, battery two and the hot water tank respectively.

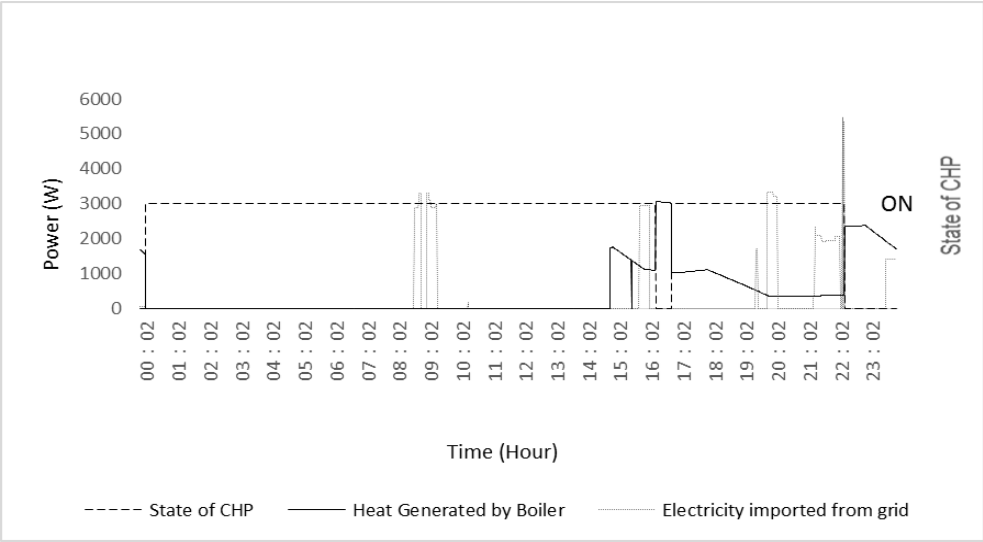

Figure 5.20 The state of CHP and the amount of imported gas and electricity in a day.

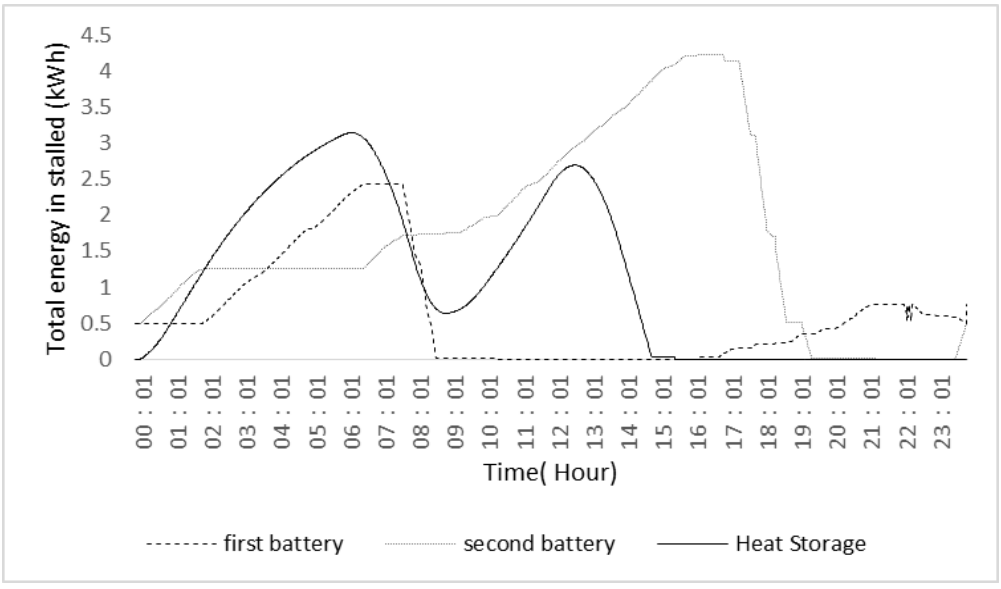

Figure 5.21 Energy stored in hot water tank and batteries.

With the installation of the energy storage system, the daily energy cost can yield a further reduction. Based on the control algorithm, total operational cost now reduces to 482 pence, which saves £1.19 a day. Specifically, the cost of electricity imported from the grid is 96 pence, the gas used to supply heat demand is 62 pence and the remaining cost of 324 pence is used to import gas to supply the CHP. With the proposed optimization rules, the total cost reduction is 19.8%, which is very similar to the simulation result (reduces cost by 20%) shown in [18]. However, compared with [18], the proposed method will not affect the householder's comfort.

5.4.4 Effective CHP energy efficiency and Average CHP input power to rated power ratio

As mentioned in Chapter 5.2.4, the CHP only has two states: 'ON' and 'OFF'. Therefore, according to the function of the effective CHP energy efficiency, which is shown in equation (5.8), the effective CHP energy efficiency is equal to CHP rated capacity. Thus, the effective CHP energy efficiency equals to gas engine CHP rated capacity, which is 88%. In this case study, the CHP switch has been switched on for 1299 minutes in the test day, and according to equations (5.9a) and (5.9b), average CHP input power to rated power ratio equals 90.2%.

In the test day, effective CHP energy efficiency and average CHP input power to rated power ratio are both improved compared with the experiment results shown in Chapter 3. The binary CHP switch control rule proposed in this chapter plays an important role in improving effective CHP energy efficiency. Meanwhile, the energy storage system has a strong ability to shift the load which can reduce CHP installation capacity and increase average CHP input power to rated power ratio.

5.4.5 Theoretical minimum

As shown in Table 5.2, using the calculation in Chapter 5.2.5, the theoretical minimum operation cost for the sampling day is 474 pence. To get the theoretical minimum, the cost of electricity imported from the grid is 78 pence, the gas that is used to supply the heat demand is 36 pence and the remaining cost of 360 pence is used to import gas to supply the CHP. Comparing the optimization results with theoretical minimum, it is easy to find that the cost from the combined hub control algorithm is very close to the theoretical minimum, and the ratio of cost from the theoretical minimum to the combined hub control algorithm cost is approximately 98.3%. This ratio varied from

88.8% to 99% after testing the whole year's data (except summer days) and clearly strongly depends on the daily load profile. If the daily average electrical load is very high, the CHP may need to operate at the rated power for the whole day, and this will reduce the difference between the proposed algorithm's cost and theoretical minimum. Thus, in this case the ratio is very high and the proposed method is very effective. However, it is worth noting that the theoretical minimum is calculated using conservative assumptions such as perfect CHP efficiency and instantaneous output. Therefore the whole range of ratios will be somewhat improved when real world imperfections are accounted for. It can thus be stated with some confidence that the algorithm presented here always yields better than 88% of the theoretical minimum cost.

Table 5.2 Energy cost in case study without algorithm, proposed algorithm and theoretical minimum

Price / Algorithm	Gas price (Pence)		Electricity price (pence)	Total price (pence)
	Gas used for CHP	Gas used for Heat		
No algorithm	293		308	601
Proposed algorithm	324	62	96	482
Theoretical minimum	360	36	78	474

5.4.6 Energy Hub optimization results in different seasons

To evaluate the performance of the proposed algorithm in different seasons, Table 5.3 is used to summarize the optimization results of the proposed algorithm. Compared Table 5.3 with optimization results (theoretical best size for fuel cell CHP) shown in Chapter 3, the daily energy cost saving increases by 18.5 pence which is about 32 percent higher. Moreover, effective CHP efficiency and average CHP input power to rated power ratio have improved, especially the average CHP input power to rated power ratio which has tripled. However, to get these benefits, the average daily investment should be increased to 1091 pence which is about 36% higher.

The proposed algorithm successfully reduces average daily energy cost in spring, however, its performance in summer and winter is not as good. This is because energy demands are very low in summer, especially in terms of heat demand, which will reduce CHP operation time. During winter, however, system energy cost saving is mainly limited by the capacity of CHP.

Table 5.3 Different seasons' system optimization results.

	No algorithm cost (pence)	Proposed algorithm cost (pence)	Effective CHP efficiency (%)	Average CHP input power to rated power ratio (%)	Average daily investment (pence)
Spring	601	482	88%	90.2	1091
Summer	215	204		21.9	
Autumn	323	261		71.8	
Winter	653	539		92.0	
Average	448	371.5		69.0	

5.5 Conclusion

The proposed rule-based Energy Hub optimization algorithm reduces the complexity of computation, improves system dynamic performance (the time step in this work is one minute compared to previous work which is an hour or half an hour) and reduces system operational cost up to 19.8% a day in spring which is similar to previous work. However, the present work increases customers' comfort level by removing the concept of non-sensitive loads (i.e. treating all load as critical). The optimization approach is more real world feasible, because it is assumed in this thesis that CHP has binary states of operation. This assumption reduces the time delay between set points and actual output arising from dynamic operation of CHP, therefore reducing inaccuracy in the optimization when deployed in the real world. Also, it maximizes the CHP efficiency, reducing energy loss since when in operation the plant operates for longer at full capacity. Finally, the modified CHP control algorithm reduces the cycling stress on the CHP, extending the plant's lifetime. For the first time in the context of

domestic CHP, dual battery storage systems are deployed together to store surplus electricity thus extending the life time of each battery.

The average daily energy cost of a year from the combined hub control algorithm is 371.5 pence, which gives about 76.5 pence energy saving a day. In the present case study that uses conservative theoretical minimum assumptions, the ratio between the control algorithm's savings and the theoretical minimum savings are always higher than 88% for a whole year's data (except summer days). This clearly shows that this is a very powerful algorithm to optimize energy consumption in a domestic building.

To further increase daily energy cost saving, there are three suggested approaches. The first one is to increase cost from the combined hub control algorithm to theoretical minimum ratio. To increase this rate, a more precise 'gaps' and 'glitches' diagnostic system is required. However, this will significantly extend computation time and system complexity. The second way is to reduce the theoretical minimum cost itself which can be achieved by improving storage system efficiencies and by improving CHP generation efficiencies. This will happen as individual technologies improve. Finally, further reducing of summer energy costs is needed, because the energy cost reduction in this season is less than 6 percent. This is due to the fact that because heat and electricity demand is extremely low in summer, CHP cannot be fully utilised. To solve this problem, combining the rule based and the algorithm based control scheme in a reasonable way is necessary. Also, if a tap changing CHP can be designed, the daily operational cost can be further reduced. These are the most promising ways to reduce optimal operational cost and the further work to achieve this will be addressed in Chapter 7.

Chapter 6. Results and analysis

This chapter compares optimization results of Chapter 3 and Chapter 5 to show the monetary and efficacy performance of the houses only installed with CHP and the houses installed with CHP and HESSs. By analysing the daily energy cost saving, daily benefit to cost ratio, effective energy efficiency of CHP and average CHP input power to rated power ratio between two different houses, this chapter shows the importance of the HESSs and gives suggestions to households on selecting CHP and HESSs.

6.1 Monetary related optimization results

Table 6.1 summarizes monetary related optimization results which were acquired by methodology proposed in Chapter 3 and Chapter 5. From Table 6.1, it is obvious that the average daily energy cost can be further reduced if energy storage systems can be installed. Meanwhile, in most cases, CHP installation capacity can be reduced if energy storage systems can be installed. This is because energy storage systems can shift loads and store redundant energy generated by CHP, and by doing this CHP can be fully exploited.

Table 6.1 Monetary related optimization results between the houses only installed with CHP and the houses installed with CHP and HESSs.

	Base case	Heat dependant sizing CHP		Electricity dependant sizing CHP		Theoretical best CHP size		Proposed control algorithm
Type of CHP	No (Case 0)	Gas engine (Case 1)	Fuel cell (Case 2)	Gas engine (Case 3)	Fuel cell (Case 4)	Gas engine (Case 5)	Fuel cell (Case 6)	Gas engine (Case 7)
Energy storage system installation	NO							YES

Type of CHP	NO (Case 0)	Gas Engine (Case 1)	Fuel Cell (Case 2)	Gas Engine (Case 3)	Fuel Cell (Case 4)	Gas Engine (Case 5)	Fuel Cell (Case 6)	Gas Engine (Case 7)
CHP installation capacity (kW)	0	2.602	3.434	5.482	3.259	3.5	5.2	3
Average daily investment (p)	0	349	529	735	502	469	801	1091
Average daily energy cost in spring (p)	601	551	524	549	526	545	505	482
Average daily energy cost in summer (p)	215	211	206	215	206	213	211	204
Average daily energy cost in autumn (p)	323	291	286	307	285	297	295	261
Average daily energy cost in winter (p)	653	593	565	596	568	588	549	539
Average daily energy cost saving of a year (p)	0	36	53	31	52	37	58	76.5
Average benefit to cost ratio	0	10.3%	10.0%	4.2%	10.4%	7.9%	7.2%	7.0 %

6.1.1 Average daily energy cost saving

Without the HESS, the maximum average daily energy cost saving is 58 pence (case 6), which is approximately 12.7% of energy cost reduction compared with the base case. In this case, the daily installation cost of CHP system is 801 pence, which gives a 7.2% benefit to cost ratio. However, if HESSs are installed (case 7), the average daily energy cost saving can further increase to 76.5 pence, which yields another 4.4% energy cost reduction. In this case, the daily CHP installation cost reduces to 402 pence, which is nearly half of case 6. However, it needs additional 689 pence to install and maintain HESS on a daily basis. Therefore, the benefit to cost ratio in this case is 7%. Comparing case 7 with case 6, the daily energy cost reduction ratio has significantly improved without having great impact on the benefit to cost ratio. This proves HESSs and proposed rule base control algorithm have good performance on reducing average daily energy cost. In order to reduce energy cost, installing HESSs is a good option.

6.1.2 Average benefit to cost ratio

Without HESSs, the maximum average daily benefit to cost ratio is 10.4% (case 4), which is 3.4% higher than a terraced house which is installed with HESSs (case 7, benefit to cost ratio is 7%). The daily energy cost saving of case 7 is 47.1% higher than that in case 4, while the daily investment cost of case 7 is more than doubled compared with case 4. Considering the fact that the investment and maintenance costs of CHP in both cases are similar, (CHP installation and maintenance costs in case 7 and 4 are 402 and 502 pence respectively.), the increase of installation and maintenance costs of case 7 is mainly caused by the HESS. Therefore, the benefit to cost ratio of case 7 is heavily restricted by the installation and maintenance costs of HESSs if energy tariffs remain the same. To improve average benefit to cost ratio, one of the most effective ways is to reduce the manufacturing cost of HESSs. If this cost can be reduced, the advantages of installing HESSs and proposed control algorithm will be increased.

6.1.3 Energy cost saving in different seasons

Compared with other six cases (case 1 to 6), case 7 is more sensitive to seasonal change, showing that HESSs have excellent performance on shifting loads and reducing daily energy cost in spring and autumn, with energy cost reduction ratios

being over 19%. However, energy cost reduction ratios are less obvious in summer and winter. Energy cost reduction ratios in these two seasons are approximately 5.1% and 17.5%.

The key factors that can limit the summer energy cost reduction of the EH system are energy demands and the system control algorithm. Due to extremely low energy demands in summer, especially heat demand, CHP operation time reduces. Meanwhile, the proposed rule based control algorithm can reduce potential EH benefit by cutting CHP operation time when energy demands are low. To increase the daily energy cost saving in summer, it is more preferable to sell energy to neighbours, since this can increase CHP operation time, with more electricity and heat generated by the cheaper energy source.

The most important factor that constrains the winter energy cost reduction of the EH system is battery and CHP installation capacities. Considering the fact that energy demands in winter is much higher than other seasons, the CHP and HESS cannot meet the heat and electricity demand at high price time. Therefore, a small proportion of high price electricity is directly imported from the grid. However in summer, increase of CHP and HESSs installation capacities will significantly elevate investment costs and reduce the energy cost saving. For these reasons, to balance system benefits in different seasons and to improve the benefit to cost ratio, rather than increase CHP and HESSs installation capacities, it is more advisable to improve CHP and HESS efficiencies.

In conclusion, HESSs and the proposed rule base control algorithm have outstanding performance in reducing daily energy costs, and the benefit to cost ratio of HESSs is mainly limited by the manufacturing price of HESSs. In addition, HESSs are very sensitive to seasonal change. To reduce impacts caused by seasonal change for HESSs, CHP and HESSs efficiencies need to be improved, and energy sharing may be required in summer.

6.2 Efficacy related optimization results

Table 6.2 shows efficacy related optimization results which were acquired by Chapter 3 and Chapter 5. From Table 6.2, HESSs and the proposed rule base control algorithm

improve the effective energy efficiency and average CHP input to output ratio. By improving these two parameters, carbon emissions can be reduced and CHP can be more fully exploited. Meanwhile, seasonal impacts have been compensated by HESSs to some extent.

Table 6.2 Efficacy related optimization results between the houses only installed with CHP and the houses installed with CHP and HESSs.

		Heat dependant sizing CHP		Electricity dependant sizing CHP		Theoretical best CHP size		Proposed control algorithm
Type of CHP		Gas Engine (Case 1)	Fuel Cell (Case 2)	Gas Engine (Case 3)	Fuel Cell (Case 4)	Gas Engine (Case 5)	Fuel Cell (Case 6)	Gas Engine (Case 7)
Energy storage system installation		NO						YES
CHP installation capacity (kW)		2.602	3.434	5.482	3.259	3.5	5.2	3
Spring	Effective CHP output efficiency	81.0%	74.2%	77.2%	74.6%	80.7%	72.3%	88%
	Average CHP input to output ratio	44.9%	33.6%	26.8%	34.1%	38.2%	27.7%	90.2%
Summer	Effective CHP output efficiency	71.7%	65.8%	71.3%	66.2%	71.3%	62.8%	88%
	Average CHP input to output ratio	14.5%	11.2%	1.1%	12.2%	7.1%	5.8%	21.9%

Type of CHP		Gas Engine (Case 1)	Fuel Cell (Case 2)	Gas Engine (Case 3)	Fuel Cell (Case 4)	Gas Engine (Case 5)	Fuel Cell (Case 6)	Gas Engine (Case 7)
Autumn	Effective CHP output efficiency	78.5%	70.4%	73.0%	71.0%	76.8%	66.7%	88%
	Average CHP input to output ratio	38.6%	25.8%	19.5%	27.1%	28.9%	18.3%	71.8%
Winter	Effective CHP output efficiency	85.7%	74.9%	76.8%	74.7%	80.5%	72.8%	88%
	Average CHP input to output ratio	54.8%	41.6%	34.3%	42.3%	47.6%	33.8%	92%
Year	Effective CHP output efficiency	78.4%	71.3%	74.6%	71.6%	77.3%	68.7%	88%
	Average CHP input to output ratio	38.2%	28.1%	20.4%	28.9%	30.5%	21.4%	69%

6.2.1 Effective CHP output efficiency

Because CHP is a kind of high energy efficiency generator, average effective CHP output efficiencies of a year are always higher than 68% for different optimization situations. With the proposed algorithm and HESSs (case 7), the average effective CHP output efficiency of a year can be maximized to 88% which is normally more than 10% higher than systems without installing HESSs, and compared with case 6, this value can be 20% higher. In this way, system energy efficiencies can be improved. From Table 6.2, it is also obvious that gas engine CHP has a higher effective output

efficiency compared with fuel cell CHP. The reasons are: gas engine CHP has higher rated output efficiency and the average yearly heat demand is much higher than electricity demand. For the same type of CHP, the effective CHP output efficiency is inversely proportional to the CHP installation capacity, if HESSs are not installed. Therefore, Table 6.2 reveals that the effective CHP energy efficiency of an EH system can be improved by installing HESSs and using the binary switch control algorithm.

6.2.2 Average CHP input to output ratio

Average CHP input to output ratio is defined to test to what extent the CHP capacity is fully exploited. From Table 6.2, without HESSs, the average CHP input to output ratios are less than 30% in most cases. However, with installing HESSs, this ratio is doubled. This is because HESSs can shift loads and reduce CHP installation capacity, making full use of CHP. Similar to the effective CHP output efficiency, the average CHP input to output ratio is inversely proportional to CHP installation capacity if HESSs are not installed. Moreover, this ratio is proportional to CHP operation time and input power of CHP. Therefore, to increase this ratio, it is necessary to reduce the CHP installation capacity, extend CHP operation time and operate CHP at its rated power, which may generate redundant energy. As a result, to store redundant energy generated by CHP and improve system energy efficiencies, HESSs are extremely important.

6.2.3 Seasonal impacts

From Table 6.2, both effective CHP output efficiency and average CHP input to output ratio can be affected by seasonal change. However, unlike monetary optimization results, efficacy optimization results show that HESSs can reduce seasonal impacts. Even though, seasonal impacts can be compensated by installing HESSs to some extent, the EH system efficacy (including energy efficiency and extent of CHP exploitation) differences among different seasons are still obvious. As demonstrated before, to improve the effective CHP output efficiency and to make full use of CHP, the best way is to reduce the CHP installation capacity and extend CHP operation time. To achieve these, HESSs need to be installed to shift loads and store redundant energy generated by CHP.

In conclusion, the proposed control algorithm and HESSs have outstanding performance in improving the effective CHP output efficiency and average CHP input

to output ratio by extending CHP operation time (shifting loads) and reducing CHP installation capacity. Moreover, efficiency optimization results show that seasonal impacts can be compensated by installing HESSs to some extent. These prove that installing HESSs is a useful way to improve energy efficiency and to make full use of CHP.

6.3 Suggestions on selecting CHP and HESSs

At present, system benefit to cost ratios of case studies are always lower than 11%. In other words, investment and maintenance costs are 10 times higher than benefits. As seen in Table 6.1, in most cases the addition of the HESS will decrease this ratio due to its high cost. In this situation, householders have less preference for installing CHP and HESSs in domestic buildings without subsidies from the governments. However, it is necessary to install CHP and HESSs in domestic buildings as they can improve energy efficiency and reduce carbon emissions.

With the development of CHP and HESSs technologies, the manufacturing and maintenance costs of CHP and HESSs will be significantly reduced. In addition, energy tariffs are likely to increase their present upward trend. Moreover, technology development can also improve HESSs overall efficiency and extend battery lifetime. Last, more research funding has been allocated to research committees to reduce energy costs in summer by energy sharing. All of these factors together may soon lead to a favourable benefit/cost ratio for CHP that is further improved by HESSs in domestic buildings.

6.3.1 CHP manufacturing and maintenance costs reduction

In [36], it is predicted that by the end of 2015 the capital cost of a CHP system will be reduced to €374/ kW. Similar to the prediction results shown in [36], the micro-CHP installation costs in 2016 is £300 /kW [37]. In this case, the installation cost of CHP becomes one seventeenth of the value used in this simulation work. Therefore, without installing HESSs, the system benefit to cost ratio can be greater than 170% for the best case. In other words, without subsidies and HESSs, households can achieve over 70% benefit if fuel cell CHP is installed and the electricity load is used as CHP sizing criteria. In this situation, households are willing to install CHP to supply heat and electricity demands.

6.3.2 Energy tariffs increase

As it is predicted in [97], oil and gas tariffs in 2050 will be 2.5 times of present value. This means if other costs (CHP and HESSs' installation and maintenances costs) have not changed significantly, the system energy cost saving can increase by 150%. In this case, the system benefit to cost ratio can increase to 26% in the best case. This suggests that without technology improvement (i.e. reducing CHP and HESSs manufacturing costs) only increasing energy tariffs will not produce a favourable case for household CHP and HESSs.

6.3.3 HESSs technology improvement

As shown in this thesis, the investment cost of EH system is restricted by HESSs, especially BESSs. The relatively high manufacturing price of BESSs reduces potential benefits of the overall system. However, as it is reported in [98], the battery market price reduced by 92% percent, between 1991 to 2005. Also, with the advance of technology, battery overall efficiency has been greatly improved. In addition, different types of batteries have been produced and some of them have relatively long lifetime, all of which suggest that, in future, lead acid batteries can be replaced by other cheaper, more efficient and longer-lasting batteries.

From the previous analysis, if the battery manufacturing prices can be further reduced to 90%, overall efficiencies can increase to 90% and lifetime can be doubled in next fifteen years, making it feasible to install HESSs in domestic buildings. Because with the proposed control algorithm, if battery overall efficiencies can be improved to 90%, system can acquire 3% extra benefit. Moreover, if the battery manufacturing price reduces to 10% of present value, and battery lifetime can be doubled, the installation and maintenance costs of battery system will reduce to 5% of present value, which is approximately 35 pence. In this case, the investment and maintenance costs of EH systems will be limited by CHP systems.

6.3.4 Algorithm development

As it is mentioned in Chapter 6.1.3, the daily energy cost reduction is 5.1% at present, which is extremely low compared to other seasons (19% in spring and autumn). In future, if this value can be improved to 19% by energy sharing, the average daily energy cost saving of a year can increase to 84 pence which is about 10% growth. But,

this is still very low compared to the average daily investment and maintenance costs, which is 1091 pence. Therefore, the most effective way to increase the system benefit to cost ratio is to reduce CHP and HESSs manufacturing price.

6.3.5 Technology improvement, energy tariffs increase and algorithm development

In the future, it is more likely that technology improvement, energy tariffs increase and algorithm development will take place in parallel. Therefore, based on aforementioned assumptions, the daily installation and maintenance costs of HESSs and CHP will reduce to 58 pence. In contrast, due to increasing tariffs and algorithm improvement average daily costs saving can increase to 216 pence. In this case, the benefit to cost ratio of overall system is 372%. Therefore, the author has confidence that the combination of domestic CHP, HESS and the proposed rule based control algorithm will soon yield a positive monetary benefit.

In conclusion, the proposed rule based control algorithm and the HESSs- CHP EH system have already improved energy efficiency. However, at present, the proposed rule based control algorithm and the HESSs- CHP EH system have not achieved monetary benefit due to high manufacturing CHP and HESS costs. It is difficult to precisely predict the energy price, HESS and CHP investment costs in future, but by analysing the factors that can potentially affect system benefit to cost ratio (shown in Chapter 6.3),the author has confidence that the benefit to cost ratio of overall system will rise to 300% in the middle of the century.

Chapter 7. Conclusions and further work

This chapter summarizes the work completed, with the main contributions and important results of this thesis firstly discussed, followed by limitations of the present work and recommended future work.

7.1 Thesis summary

This thesis attempts to optimize domestic building daily energy cost, and to identify ways of reducing the installation and maintenance costs of all domestic energy infrastructure. Considering general energy conversion, storage and transmission in domestic buildings, there are two key parts in this thesis. The first key part (Chapter 3) is to size a combined heat and power (CHP) unit based on the Maximum Rectangle (MR) method and use the Genetic Algorithm (GA) method to optimize daily energy cost for a building without an energy storage system. The second key part of the thesis (Chapter 4 and Chapter 5) is to size a hybrid energy storage system (HESS) and develop a new rule-based energy control rule to optimise energy costs for a building with an energy storage system.

In Chapter 3, daily energy operational costs, investment costs and energy efficiency are all considered when using the MR and GA methods to size the CHP. The GA optimization results show that by installing a 5200 W fuel cell CHP, the daily energy costs can be minimized which would lead to a 13% reduction compared to base case. However, to achieve this reduction, there would be about 3% energy efficiency reduction and 7% input power to rated power ratio reduction compared with using the MR method and the heat demand to size fuel cell CHP. Using the MR method and the heat demand to size the CHP is sufficient because the MR method gives a higher benefit to cost ratio and energy efficiency. In addition, it makes fuller use of CHP capacity, even though it needs 5 pence extra to generate energy for a day.

In Chapter 4, a hybrid energy storage system at building level has been investigated, the factors that can influence HESSs economical operation have been analyzed, and a battery SOC and discharge current control model has been proposed. By applying this model, the daily investment of the HESS reduces to 7.6 times as many as that in the HESS daily benefit, a twofold improvement on a smart building with only a battery

storage system and local energy generation. Even so, the daily cost of the system currently outweighs the benefits, by a factor of almost 8.

The proposed optimization model for a HESS firstly shows three saturation factors that can influence the system's average daily saving. These three factors are battery capacity, maximum discharge current and SOC. To deal with battery capacity saturation, a more precise system control strategy is required. To deal with battery maximum discharge current saturation, the battery system needs to reduce the minimum SOC. To solve the SOC saturation, the battery system needs to increase the maximum discharge current. It has been concluded that a successful design should fully exploit battery capacity and attempt to make the battery system work in an operational area without saturation caused by capacity, discharge current or SOC. And this chapter is the fundamental work for the subsequent research of Chapter 5.

In Chapter 5, the proposed rule-based EH optimization algorithm reduces the complexity of computation, improves system dynamic performance (the time step in this work is one minute compared to previous work which was an hour or half an hour) and reduces system operational costs up to 19.8% a day in spring which is similar to previous work. However, the present work increases customers' comfort level by removing the concept of non-sensitive loads. In other words, in this system all loads is deemed as critical and met at all times. The optimization approach is more real world feasible, because it is assumed in this thesis that CHP has binary states of operation. This assumption reduces the time delay between set points and actual output arising from dynamic operation of CHP, therefore reducing inaccuracy in the optimization when deployed in the real world. Also, it maximizes the CHP efficiency, reducing energy loss since when in operation the plant operates for longer at full capacity. Finally, the modified CHP control algorithm reduces the cycling stress on the CHP, extending the plant's lifetime. For the first time in the context of domestic CHP, dual battery storage systems are deployed together to store surplus electricity thus extending the life time of each battery.

Compared to the GA and MR methods which are demonstrated in Chapter 3, the rule based EH optimization algorithm is more computationally efficient and more feasible. The reason for this is the proposed rule based control algorithm is not necessary for exact loads to be known in advance. In addition, by setting the binary control algorithm,

energy efficiencies can be improved and the CHP can be fully exploited. In addition, the proposed rule based control algorithm can reduce potential benefits of an EH system by reducing CHP operation time when energy demands are low, which is one of the most important reasons for its low energy cost reduction ratio.

In comparison with Chapter 5 and Chapter 3, the average daily energy cost has an extra 47% reduction, when the HESS is installed. From an economic perspective, it is also obvious HESSs and the proposed rule base control algorithm have outstanding performance in reducing daily energy costs. However, when the HESS is installed, the benefit to cost ratio of the HESS- CHP EH reduces to 7%. The key factor that currently limits the benefit to cost ratio of a HESS is its manufacturing price. In addition, HESSs are very sensitive to seasonal change. To reduce impacts caused by seasonal change for HESSs, CHP and HESSs efficiencies need to be increased, and energy sharing may be required in summer.

From an efficacy perspective, the proposed control algorithm and the HESS have outstanding performance in improving the effective CHP output efficiency and average CHP input to output ratio by extending CHP operation time (shifting loads) and reducing CHP installation capacity. Moreover, efficiency optimization results show that by installing HESSs, seasonal impacts can be reduced to some extent. These prove that installing HESSs is a useful way to improve energy efficiency and to make full use of CHP.

In conclusion, the proposed rule based control algorithm and the HESSs- CHP EH system have already improved energy efficacy. However, at present, system benefit to cost ratios of case studies are consistently lower than 11%, which reduces the possibility to widely install the HESSs-CHP EH system. But with technology improvement, energy tariffs increase and algorithm development in the near future, it is estimated that the benefit to cost ratio of the overall system will be higher than 300% in the middle of 21st century.

7.2 Limitations of the work

As described in previous chapters, system potential benefits can greatly increase by technology improvement, for example, HESSs and CHP manufacturing price reduction, battery overall energy efficiency improvement and tap changing CHP installation. But

in the following parts, the author has attempted to increase system benefits by analysing the limitations of the proposed rule based EH control algorithm. From the optimization results, three important factors that can reduce the potential benefits of the present work are: accuracy of energy prediction, maximum battery input and output power and the flexibility of the proposed rule based EH control algorithm.

7.2.1 Accuracy of energy prediction

As mentioned in Chapter 5, the proposed rule based control algorithm does not need exact loads in advance, which is one of most important contributions of this thesis. But in Chapter 3, it is assumed the loads can be perfectly predicted in advance. Therefore, in order to achieve optimization results shown in Chapter 3, load prediction algorithms need to be studied, especially short term load prediction. In addition, accurate load prediction models can be used to diagnose ‘gaps’ and ‘glitches’ for the proposed rule based EH algorithm, and this can further reduce system cost. However, to promote the accuracy of energy prediction, computation time and system complexity will be also increased.

7.2.2 Maximum battery input and output power

As shown in Chapter 5.4.3, if the initial energy of BESSs can be set as 2.7 kWh, system daily energy cost reduction can be improved. But in this case, the maximum input power of BESSs can reach 35 kW, which can significantly decrease BESSs lifetime, and increase the average daily investment cost of the HESS. Therefore, to reduce the maximum battery input power, the initial energy of BESSs is set as 0.6 kWh in Chapter 5. However, the simulation results show that by doing this, potential system benefits will reduce. Moreover, limiting the maximum output power (discharge current) of BESSs can also reduce the average daily system benefit, which has been clearly demonstrated in Chapter 4.

7.2.3 The flexibility of the proposed rule based EH control algorithm

The optimization results in Chapter 6 show that the rule based EH control algorithm has the potential to reduce system benefits by reducing CHP operation time when the energy demands are low. This proves that the proposed algorithm cannot adapt itself when the energy demands are low, and the main reason for this is that the flexibility of the rule based control algorithm reduces as opposed to algorithm based control

algorithm. This is because by using the rule based control algorithm to control an EH system, the system needs to be strictly followed by the proposed rule after the rule is set.

7.3 Further work

Perhaps the most important areas for the further work are to increase the accuracy of energy prediction, to improve maximum battery input and output power and to promote the flexibility of the proposed rule based EH control algorithm.

To increase accuracy of energy prediction, a short term load prediction model should be established. And this model should be simple, accurate and computationally efficient. To improve maximum battery input and output power, analysing the characteristics of other batteries or finding the substitutes of battery is quite useful. To deal with low flexibility of the proposed rule based EH control algorithm, two things can be done. The first one is to increase loads by sharing energy with neighbours, and establishing an integrated two-house EH model. While the other is to combine the rule based control algorithm with algorithm based control algorithms to promote the flexibility of EH systems and extend battery lifetime. Moreover, more types of domestic buildings may need to be used as examples to test the generality of the proposed algorithm.

Besides the aforementioned further work, uncertainty analysis of the proposed rule-based control algorithm is important. For the proposed rule-based control algorithm, the uncertainty can be energy tariffs, domestic buildings' energy consumption patterns and energy generator efficiencies. As mentioned in Chapter 6.3.2, energy tariffs will increase rapidly in the next couple of decades and the electricity to gas tariff ratio will also be changed. Therefore, analysing energy tariffs uncertainty impacts on the operation of the proposed energy system is necessary. Also, the proposed rule-based control algorithm only considers two or less peak demand time in a day; the uncertainty analysis can be number of peak demand time in a day. Last, with the development of CHP, boiler and HESS technologies, it is worth to be considered the impacts caused by efficiency improvement of energy generators.

References

[1] S. Chu and A. Majumdar, "Opportunities and challenges for a sustainable energy future," *Nature,* vol. 488, pp. 294-303, Aug 16 2012.

[2] P. Sporn, "Centralized power generation," *Electrical Engineering,* vol. 65, pp. 105-107, 1946.

[3] S. Le Blond, R. Li, F. Li, and Z. Wang, "Cost and emission savings from the deployment of variable electricity tariffs and advanced domestic energy hub storage management," in *PES General Meeting | Conference & Exposition, 2014 IEEE*, 2014, pp. 1-5.

[4] M. C. Bozchalui, C. A. Canizares, and K. Bhattacharya, "Optimal Energy Management of Greenhouses in Smart Grids," *Smart Grid, IEEE Transactions on,* vol. 6, pp. 827-835, 2015.

[5] O. Erdinc, N. G. Paterakis, T. D. P. Mendes, A. G. Bakirtzis, and J. P. S. Catalao, "Smart Household Operation Considering Bi-Directional EV and ESS Utilization by Real-Time Pricing-Based DR," *Smart Grid, IEEE Transactions on,* vol. 6, pp. 1281-1291, 2015.

[6] A. Mishra, D. Irwin, P. Shenoy, J. Kurose, and Z. Ting, "GreenCharge: Managing RenewableEnergy in Smart Buildings," *IEEE Journal on Selected Areas in Communications,* vol. 31, pp. 1281-1293, 2013.

[7] J. Leadbetter and L. Swan, "Battery storage system for residential electricity peak demand shaving," *Energy and Buildings,* vol. 55, pp. 685-692, 2012.

[8] D. Setlhaolo and X. Xia, "Optimal scheduling of household appliances with a battery storage system and coordination," *Energy and Buildings,* vol. 94, pp. 61-70, 5/1/ 2015.

[9] P. P. Predd, "A Power Plant for the Home," *Spectrum, IEEE,* vol. 44, pp. 14-15, 2007.

[10] A. J. WOOD, "Power Generation, Operation and Control," *by John Wiley & Sons,* 2005.

[11] A. Sheikhi, M. Rayati, S. Bahrami, and A. Mohammad Ranjbar, "Integrated Demand Side Management Game in Smart Energy Hubs," *Smart Grid, IEEE Transactions on,* vol. 6, pp. 675-683, 2015.

[12] P. K. Singhal and R. N. Sharma, "Dynamic programming approach for solving power generating unit commitment problem," in *Computer and Communication Technology (ICCCT), 2011 2nd International Conference on*, 2011, pp. 298-303.

[13] T. Senjyu, K. Shimabukuro, K. Uezato, and T. Funabashi, "A fast technique for unit commitment problem by extended priority list," in *Power Engineering Society General Meeting, 2003, IEEE*, 2003.

[14] M. Govardhan and R. Roy, "Evolutionary Computation based Unit Commitment Using Hybrid Priority List Approach," *2012 Ieee International Conference on Power and Energy (Pecon),* pp. 245-250, 2012.

[15] M. Geidl, "Integrated modeling and optimization of multi-carrier energy systems," *PhD Thesis, ETH,* 2007.

[16] Martin Geidl, Gaudenz Koeppel, Patrick Favre-Perrod, Bernd Klöckl, Göran Andersson, and K. Fröhlich, "The Energy Hub – A Powerful Concept for Future Energy Systems," *Third Annual Carnegie Mellon Conference on the Electricity Industry,* 2007.

[17] M. Geidl, G. Koeppel, P. Favre-Perrod, B. Klockl, G. Andersson, and K. Frohlich, "Energy hubs for the future," *Ieee Power & Energy Magazine,* vol. 5, pp. 24-30, Jan-Feb 2007.

[18] M. C. Bozchalui, S. A. Hashmi, H. Hassen, C. A. Canizares, and K. Bhattacharya, "Optimal Operation of Residential Energy Hubs in Smart Grids," *Smart Grid, IEEE Transactions on,* vol. 3, pp. 1755-1766, 2012.

[19] J. Chunlian, L. Shuai, L. Ning, and R. A. Dougal, "Cross-market optimization for hybrid energy storage systems," in *Power and Energy Society General Meeting, 2011 IEEE*, 2011, pp. 1-6.

[20] E. FABRIZO, "Modelling of multi-energy systems in buildings," *PhD Thesis, SCUDO,* 2008.

[21] R. Y. a. K.Steemers, "A method of formulating energy load profile for domestic buildings in the UK," *Energy and Buildings,* pp. p. 663-671, 2005.

[22] A. Capasso, W. Grattieri, R. Lamedica, and A. Prudenzi, "A bottom-up approach to residential load modeling," *Power Systems, IEEE Transactions on,* vol. 9, pp. 957-964, 1994.

[23] M. T. I. Richardson, D.Infield, and C.Clifford, "Domestic electricity use: A high-resolution energy demand model," *nergy and Buildings,* pp. p. 1878-1887, 2010.
[24] J. Paatero; and P. Lund, "A model for generating household electricity load profiles," *International Journal of Energy Research,* vol. 30, pp. pp.273-290, 2006.
[25] M. Stokes, "Removing barriers to embedded generation: a fine-grained load model to support low voltage network performance analysis," *Ph.D. Thesis, Institute of Energy and Sustainable Development, De Montfort University, Leicester,* 2005.
[26] M. Armstrong, M. Swinton, H. Ribberink, I. Beausoleil-Morrison, and J. Millette, "Synthetically derived profiles for representing occupant-driven electric loads in Canadian housing," *Journal of Building Performance Simulation,* pp. 15-30, 2009.
[27] W. Zhimin, G. Chenghong, L. Furong, P. Bale, and S. Hongbin, "Active Demand Response Using Shared Energy Storage for Household Energy Management," *Smart Grid, IEEE Transactions on,* vol. 4, pp. 1888-1897, 2013.
[28] N. Neyestani, M. Y. Damavandi, M. Shafie-khah, J. P. S. Catalao, and G. Chicco, "Modeling the carrier dependencies on demand-side in a smart multi-energy local network," in *Smart Grid Conference (SGC), 2014*, 2014, pp. 1-6.
[29] X. P. Chen, Y. D. Wang, H. D. Yu, D. W. Wu, Y. Li, and A. P. Roskilly, "A domestic CHP system with hybrid electrical energy storage," *Energy and Buildings,* vol. 55, pp. 361-368, 2012.
[30] A. Sheikhi, A. M. Ranjbar, and H. Oraee, "Financial analysis and optimal size and operation for a multicarrier energy system," *Energy and Buildings,* vol. 48, pp. 71-78, 2012.
[31] S. K. Kollimalla, M. K. Mishra, and N. L. Narasamma, "Design and Analysis of Novel Control Strategy for Battery and Supercapacitor Storage System," *Sustainable Energy, IEEE Transactions on,* vol. 5, pp. 1137-1144, 2014.
[32] J. Fan, S. Furbo, and H. Yue, "Development of a Hot Water Tank Simulation Program with Improved Prediction of Thermal Stratification in the Tank," *Energy Procedia,* vol. 70, pp. 193-202, 2015.
[33] A. Mishra, D. Irwin, P. Shenoy, J. Kurose, and Z. Ting, "GreenCharge: Managing RenewableEnergy in Smart Buildings," *Selected Areas in Communications, IEEE Journal on,* vol. 31, pp. 1281-1293, 2013.
[34] R. Jablko, C. Saniter, R. Hanitsch, and S. Holler, "Technical and economical comparison of micro CHP systems," in *Future Power Systems, 2005 International Conference on*, 2005, pp. 6 pp.-6.
[35] M. Tasdighi, H. Ghasemi, and A. Rahimi-Kian, "Residential Microgrid Scheduling Based on Smart Meters Data and Temperature Dependent Thermal Load Modeling," *Smart Grid, IEEE Transactions on,* vol. 5, pp. 349-357, 2014.
[36] O. A. Shaneb, G. Coates, and P. C. Taylor, "Sizing of residential μCHP systems," *Energy and buildings.,* vol. 43, pp. 1991-2001, 2011.
[37] E. International, "Commercial and Environmental Benefit Calculator, Which availables at: http://www.energyinternational.co.uk/CHPCalculator1.htm," ed, 2016.
[38] H. Aki, "The Penetration of Micro CHP in Residential Dwellings in Japan," in *Power Engineering Society General Meeting, 2007. IEEE*, 2007, pp. 1-4.
[39] H. Ren and W. Gao, "Economic and environmental evaluation of micro CHP systems with different operating modes for residential buildings in Japan," *Energy and Buildings,* vol. 42, pp. 853-861, 2010.
[40] M. Pehnt, M. Cames, C. Fischer, B. Praetorius, L. Schneider, K. Schumacher*, et al.*, "Micro Cogeneration: Towards Decentralized Energy Systems," *Berlin, Germany: Springer-Verlag,* 2006.
[41] J. Tant, F. Geth, D. Six, P. Tant, and J. Driesen, "Multiobjective battery storage to improve PV integration in residential distribution grids," in *Power and Energy Society General Meeting (PES), 2013 IEEE*, 2013, pp. 1-1.

[42] Y. H. Song and Q. Y. Xuan, "COMBINED HEAT AND POWER ECONOMIC DISPATCH USING GENETIC ALGORITHM BASED PENALTY FUNCTION METHOD," *Electric Machines & Power Systems,* vol. 26, pp. 363-372, 1998/05/01 1998.

[43] A. A. Abou El Ela, A. Zein El-Din, and S. R. Spea, "Multi-objective genetic algorithm to improve the power system operation using distributed generation," in *Power Systems Conference, 2006. MEPCON 2006. Eleventh International Middle East*, 2006, pp. 612-619.

[44] D. Haeseldonckx, L. Peeters, L. Helsen, and W. D'haeseleer, "The impact of thermal storage on the operational behaviour of residential CHP facilities and the overall CO2 emissions," *Renewable and Sustainable Energy Reviews,* vol. 11, pp. 1227-1243, 2007.

[45] X. Q. Kong, R. Z. Wang, and X. H. Huang, "Energy optimization model for a CCHP system with available gas turbines," *Applied Thermal Engineering,* vol. 25, pp. 377-391, 2005.

[46] H. M. Khodr, J. F. Gomez, L. Barnique, J. H. Vivas, P. Paiva, J. M. Yusta*, et al.*, "A linear programming methodology for the optimization of electric power-generation schemes," *Power Systems, IEEE Transactions on,* vol. 17, pp. 864-869, 2002.

[47] R. Yokoyama, K. Ito, and Y. Matsumoto, "Optimal Sizing of a Gas Turbine Cogeneration Plant in Consideration of Its Operational Strategy," *Journal of Engineering for Gas Turbines and Power,* vol. 116, pp. 32-38, 1994.

[48] K. A. Pruitt, S. Leyffer, A. M. Newman, and R. J. Braun, "A mixed-integer nonlinear program for the optimal design and dispatch of distributed generation systems," *Distributed generation system design and dispatch,* 2013.

[49] J. S. Kim and T. F. Edgar, "Optimal scheduling of combined heat and power plants using mixed-integer nonlinear programming," *Energy,* vol. 77, pp. 675-690, 12/1/ 2014.

[50] M. Huber, F. Sanger, and T. Hamacher, "Coordinating smart homes in microgrids: A quantification of benefits," in *Innovative Smart Grid Technologies Europe (ISGT EUROPE), 2013 4th IEEE/PES*, 2013, pp. 1-5.

[51] G. Kayo and R. Ooka, "Building energy system optimizations with utilization of waste heat from cogenerations by means of genetic algorithm," *Energy and Buildings,* vol. 42, pp. 985-991, 7/ 2010.

[52] M. J. Risbeck, C. T. Maravelias, J. B. Rawlings, and R. D. Turney, "Cost optimization of combined building heating/cooling equipment via mixed-integer linear programming," in *American Control Conference (ACC), 2015*, 2015, pp. 1689-1694.

[53] S. K. Mukherjee, A. Recio, and C. Douligeris, "Optimal power flow by linear programming based optimization," in *Southeastcon '92, Proceedings., IEEE*, 1992, pp. 527-529 vol.2.

[54] L. Xiang, L. Tiejian, W. Jiahua, W. Guangqian, and W. W. G. Yeh, "Hydro Unit Commitment via Mixed Integer Linear Programming: A Case Study of the Three Gorges Project, China," *Power Systems, IEEE Transactions on,* vol. 29, pp. 1232-1241, 2014.

[55] W. Hua, H. Sasaki, J. Kubokawa, and R. Yokoyama, "An interior point nonlinear programming for optimal power flow problems with a novel data structure," *Power Systems, IEEE Transactions on,* vol. 13, pp. 870-877, 1998.

[56] Y. Lu, S. Wang, Y. Sun, and C. Yan, "Optimal scheduling of buildings with energy generation and thermal energy storage under dynamic electricity pricing using mixed-integer nonlinear programming," *Applied Energy,* vol. 147, pp. 49-58, 6/1/ 2015.

[57] M. C. McManus, "Environmental consequences of the use of batteries in low carbon systems: The impact of battery production," *Applied Energy,* vol. 93, pp. 288-295, 2012.

[58] P. Balcombe, D. Rigby, and A. Azapagic, "Investigating the importance of motivations and barriers related to microgeneration uptake in the UK," *Applied Energy,* vol. 130, pp. 403-418, 10/1/ 2014.

[59] P. Balcombe, D. Rigby, and A. Azapagic, "Environmental impacts of microgeneration: Integrating solar PV, Stirling engine CHP and battery storage," *Applied Energy,* vol. 139, pp. 245-259, 2/1/ 2015.

[60] R. Dufo-López, J. L. Bernal-Agustín, J. M. Yusta-Loyo, J. A. Domínguez-Navarro, I. J. Ramírez-Rosado, J. Lujano*, et al.*, "Multi-objective optimization minimizing cost and life cycle emissions of stand-alone PV–wind–diesel systems with batteries storage," *Applied Energy,* vol. 88, pp. 4033-4041, 2011.

[61] V. A. Boicea, "Energy Storage Technologies: The Past and the Present," *Proceedings of the IEEE,* vol. 102, pp. 1777-1794, 2014.

[62] S. K. Kollimalla, M. K. Mishra, and N. L. Narasamma, "Design and Analysis of Novel Control Strategy for Battery and Supercapacitor Storage System," *IEEE Transactions onSustainable Energy,* vol. 5, pp. 1137-1144, 2014.

[63] Z. Tianpei and S. Wei, "Optimization of Battery-Supercapacitor Hybrid Energy Storage Station in Wind/Solar Generation System," *IEEE Transactions on Sustainable Energy,* vol. 5, pp. 408-415, 2014.

[64] T. Ma, H. Yang, and L. Lu, "Development of hybrid battery–supercapacitor energy storage for remote area renewable energy systems," *Applied Energy,* vol. 153, pp. 56-62, 9/1/ 2015.

[65] D. P. Jenkins, J. Fletcher, and D. Kane, "Lifetime prediction and sizing of lead-acid batteries for microgeneration storage applications," *Renewable Power Generation, IET,* vol. 2, pp. 191-200, 2008.

[66] L. Benini, D. Bruni, A. Mach, E. Macii, and M. Poncino, "Discharge current steering for battery lifetime optimization," *IEEE Transactions on Computers,* vol. 52, pp. 985-995, 2003.

[67] Z. Bo, Z. Xuesong, C. Jian, W. Caisheng, and G. Li, "Operation Optimization of Standalone Microgrids Considering Lifetime Characteristics of Battery Energy Storage System," *IEEE Transactions on Sustainable Energy,* vol. 4, pp. 934-943, 2013.

[68] Panasonic, "Lead Acid Batteries Technical Handbook; Available at: http://pdf.datasheetarchive.com/indexerfiles/Datasheets-SL6/DSASL00110157.pdf," 2003.

[69] E. A. Hoxie, "Some discharge characteristics of lead acid batteries," *Transactions of the American Institute of Electrical Engineers, Part II: Applications and Industry,* vol. 73, pp. 17-22, 1954.

[70] I. Papic, "Simulation model for discharging a lead-acid battery energy storage system for load leveling," *IEEE Transactions on Energy Conversion,* vol. 21, pp. 608-615, 2006.

[71] T. Shuo, H. Munan, and O. Minggao, "An Experimental Study and Nonlinear Modeling of Discharge Behavior of Valve-Regulated Lead-Acid Batteries," *IEEE Transactions on Energy Conversion,* vol. 24, pp. 452-458, 2009.

[72] A. M. Gee, F. V. P. Robinson, and R. W. Dunn, "Analysis of Battery Lifetime Extension in a Small-Scale Wind-Energy System Using Supercapacitors," *IEEE Transactions onEnergy Conversion,* vol. 28, pp. 24-33, 2013.

[73] D. Linzen, S. Buller, E. Karden, and R. W. De Doncker, "Analysis and evaluation of charge-balancing circuits on performance, reliability, and lifetime of supercapacitor systems," *IEEE Transactions on Industry Applications,* vol. 41, pp. 1135-1141, 2005.

[74] C. Yonghua, "Assessments of Energy Capacity and Energy Losses of Supercapacitors in Fast Charging–Discharging Cycles," *IEEE Transactions on Energy Conversion,* vol. 25, pp. 253-261, 2010.

[75] Maxwell, "Maxwell Technologies BOOSTCAP Energy Stroage Modules Life Duration Estimation. Availlable at: http://www.datasheetarchive.com/dl/Datasheet-095/DSA00114147.pdf," 2007.

[76] P. Kreczanik, P. Venet, A. Hijazi, and G. Clerc, "Study of Supercapacitor Aging and Lifetime Estimation According to Voltage, Temperature, and RMS Current," *IEEE Transactions on Industrial Electronics,* vol. 61, pp. 4895-4902, 2014.

[77] M. Uno and K. Tanaka, "Accelerated Charge Discharge Cycling Test and Cycle Life Prediction Model for Supercapacitors in Alternative Battery Applications," *IEEE Transactions on Industrial Electronics,* vol. 59, pp. 4704-4712, 2012.

[78] Maxwell, "Mawell Technologies BOOSTCAP Ultracapactior Cell Sizing, Rev 3, Available at: http://www.datasheetarchive.com/dl/Datasheet-095/DSA00114140.pdf," 17/Feb/09.

[79] H. Lund, B. Moller, B. V. Mathiesen, and A. Dyrelund, "The role of district heating in future renewable energy systems," *Energy,* vol. 35, pp. 1381-1390, Mar 2010.
[80] Y. M. Atwa, E. F. El-Saadany, M. M. A. Salama, and R. Seethapathy, "Optimal Renewable Resources Mix for Distribution System Energy Loss Minimization," *Power Systems, IEEE Transactions on,* vol. 25, pp. 360-370, 2010.
[81] Z. Peng, S. Suryanarayanan, and M. G. Simoes, "An Energy Management System for Building Structures Using a Multi-Agent Decision-Making Control Methodology," *Industry Applications, IEEE Transactions on,* vol. 49, pp. 322-330, 2013.
[82] F. Kienzle, Ahc, x030C, P. in, and G. Andersson, "Valuing Investments in Multi-Energy Conversion, Storage, and Demand-Side Management Systems Under Uncertainty," *Sustainable Energy, IEEE Transactions on,* vol. 2, pp. 194-202, 2011.
[83] S. A. Pourmousavi, M. H. Nehrir, and R. K. Sharma, "Multi-Timescale Power Management for Islanded Microgrids Including Storage and Demand Response," *Smart Grid, IEEE Transactions on,* vol. 6, pp. 1185-1195, 2015.
[84] M. H. Moradi, M. Eskandari, and S. Mahdi Hosseinian, "Operational Strategy Optimization in an Optimal Sized Smart Microgrid," *Smart Grid, IEEE Transactions on,* vol. 6, pp. 1087-1095, 2015.
[85] F. Brahman, M. Honarmand, and S. Jadid, "Optimal electrical and thermal energy management of a residential energy hub, integrating demand response and energy storage system," *Energy and Buildings,* vol. 90, pp. 65-75, 3/1/ 2015.
[86] M. Rastegar, M. Fotuhi-Firuzabad, and M. Lehtonen, "Home load management in a residential energy hub," *Electric Power Systems Research,* vol. 119, pp. 322-328, 2/ 2015.
[87] M. Pehnt, Cames, M., Fischer, C., Praetorius, B., Schneider, L., Schumacher, K., Voß, J.-P. , "Micro Cogeneration :Towards Decentralized Energy Systems," 2006.
[88] M. Houwing, R. R. Negenborn, and B. De Schutter, "Demand Response With Micro-CHP Systems," *Proceedings of the IEEE,* vol. 99, pp. 200-213, 2011.
[89] W. Yue, A. Bermukhambetova, W. Jihong, L. Junfu, and G. Qirui, "Dynamic modelling and simulation study of a university campus CHP power plant," in *Automation and Computing (ICAC), 2014 20th International Conference on*, 2014, pp. 3-8.
[90] L. Hernandez, C. Baladron, J. M. Aguiar, B. Carro, A. J. Sanchez-Esguevillas, J. Lloret*, et al.*, "A Survey on Electric Power Demand Forecasting: Future Trends in Smart Grids, Microgrids and Smart Buildings," *Communications Surveys & Tutorials, IEEE,* vol. 16, pp. 1460-1495, 2014.
[91] N. Amjady, "Short-Term Bus Load Forecasting of Power Systems by a New Hybrid Method," *Power Systems, IEEE Transactions on,* vol. 22, pp. 333-341, 2007.
[92] N. Amjady, F. Keynia, and H. Zareipour, "Short-Term Load Forecast of Microgrids by a New Bilevel Prediction Strategy," *Smart Grid, IEEE Transactions on,* vol. 1, pp. 286-294, 2010.
[93] S. Sargunaraj, D. P. Sen Gupta, and S. Devi, "Short-term load forecasting for demand side management," *Generation, Transmission and Distribution, IEE Proceedings-,* vol. 144, pp. 68-74, 1997.
[94] Y. Dongmin, F. Robinson, Z. Wenhua, and S. Le Blond, "Using historical data processing method to optimize Energy Hub," in *Power Engineering Conference (UPEC), 2015 50th International Universities*, 2015, pp. 1-6.
[95] L. Benini, D. Bruni, A. Mach, E. Macii, and M. Poncino, "Discharge current steering for battery lifetime optimization," *Computers, IEEE Transactions on,* vol. 52, pp. 985-995, 2003.
[96] F. R. Dongmin yu, Wenhua Zha, Simon le Blond "Using Historical Data Processing Method to Optimize Energy Hub," *UPEC conference, 2015,* 2015.
[97] European-research-community. World Energy Technology Outlook -2050 , which availables at: https://ec.europa.eu/research/energy/pdf/weto-h2_en.pdf [Online].
[98] Battery-University. Battery Statistic, which availables at: http://batteryuniversity.com/learn/article/battery_statistics [Online].

Appendix

Appendix 1. Matlab code of the GA method to calculate daily energy costs

Constraint functions

```
function [c,ceq]=cons(x,k,eled,heatd)
nchpe=0.783*((11.67*log(x(3)*100/1000))-0.06459*x(3)*100/1000-18.76);
nchpg=1.610*((0.1256*x(3)*100/1000)+82.32*(1000/(x(3)*100))+28.73);
ceq(1)=x(1)+nchpe*x(3)/100-eled(k);
ceq(2)=x(2)*0.88+nchpg*x(3)/100-heatd(k);
c=[];
```

Objective functions

```
function f=object(x,k,elep,gasp)
pele=x(1);
pg=x(2);
pchp=x(3);
f=pele*elep(k)+(pg+pchp)*gasp(k);
```

The GA code

```
aa=zeros(1440,3);
bb=zeros(1440,1);
cc=zeros(1440,1);
for k=1:1440
[aa(k,:),bb(k,1),cc(k,1)]=ga(@(x)object(x,k,elep,gasp),3,[],[],[],[],[0,0,100],[inf,inf,1000],@(x)cons(x,k,eled,heatd));
End
```

Appendix 2. CHP output efficiencies in each minute of other seasons (Summer, autumn and winter) based on different sizing criteria.

Summer:

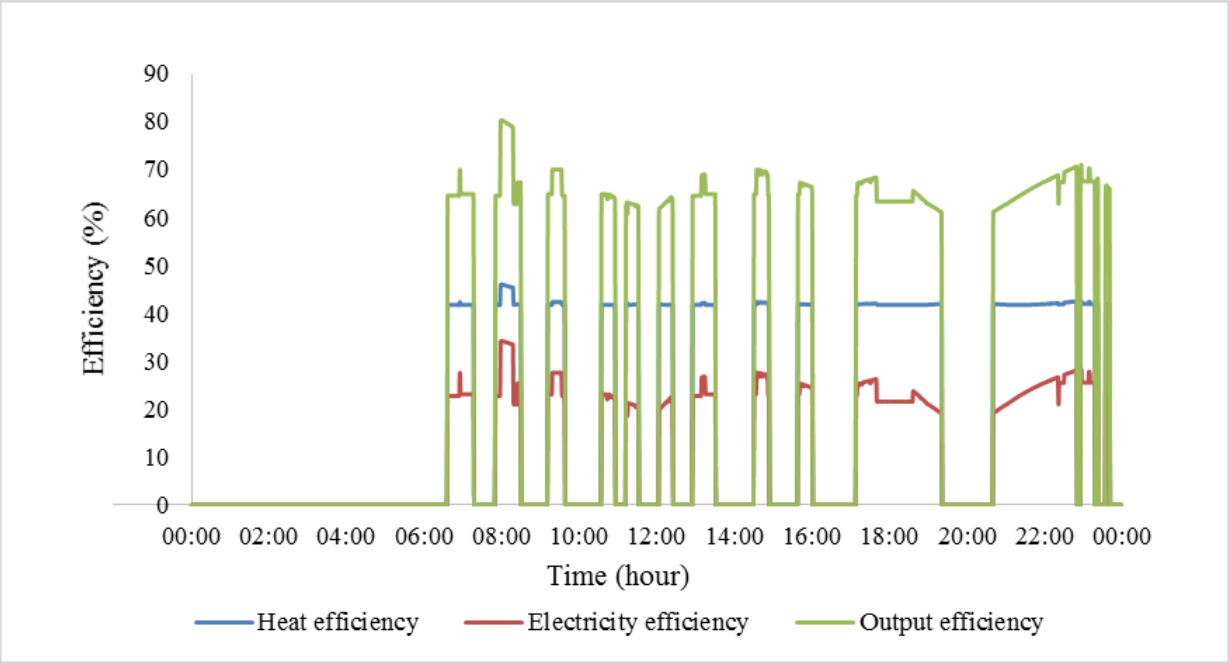

a) Summer , fuel cell CHP, heat dependant sizing CHP

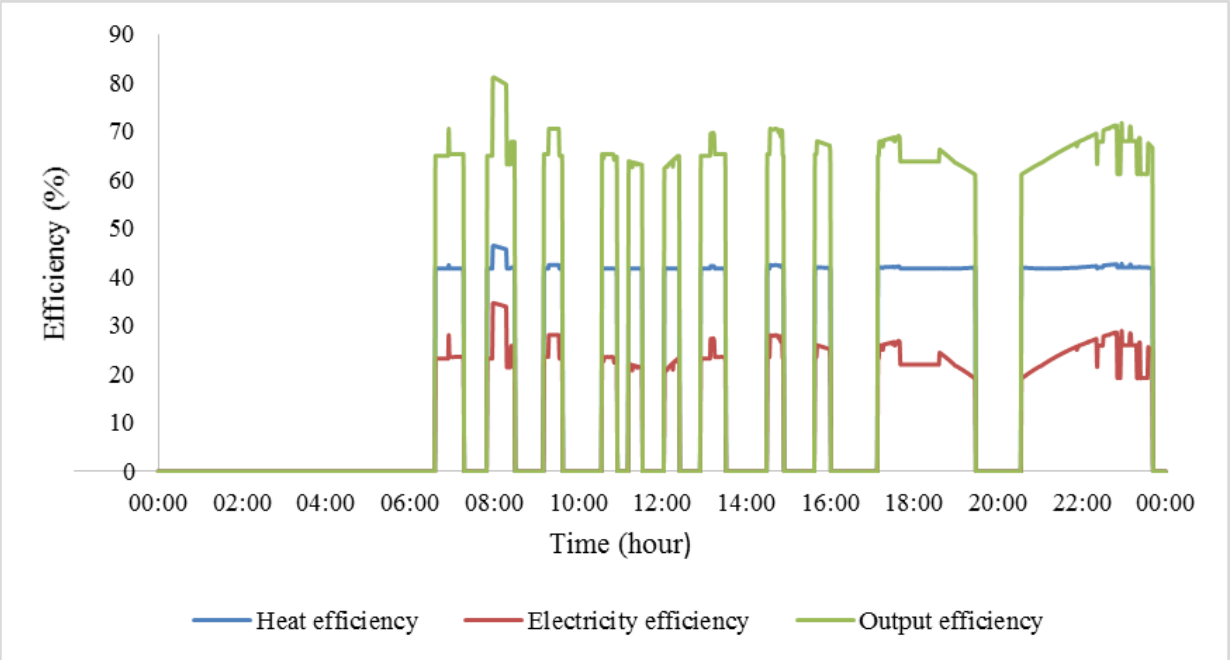

b) Summer , fuel cell CHP, electricity dependant sizing CHP

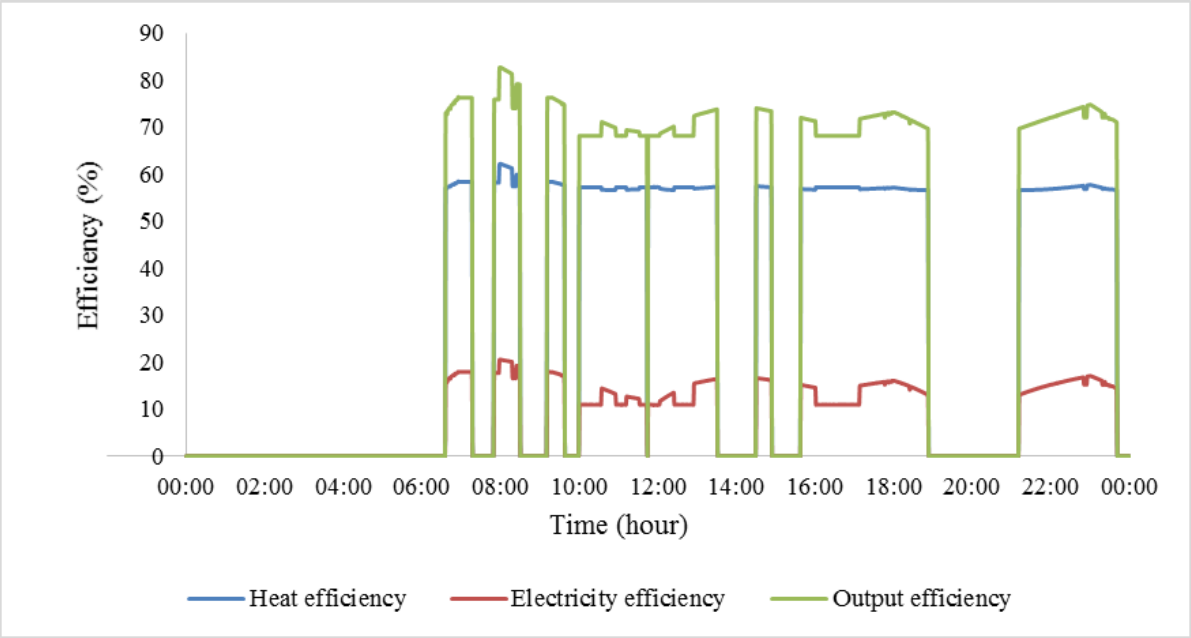

c) Summer , gas engine CHP, heat dependant sizing CHP

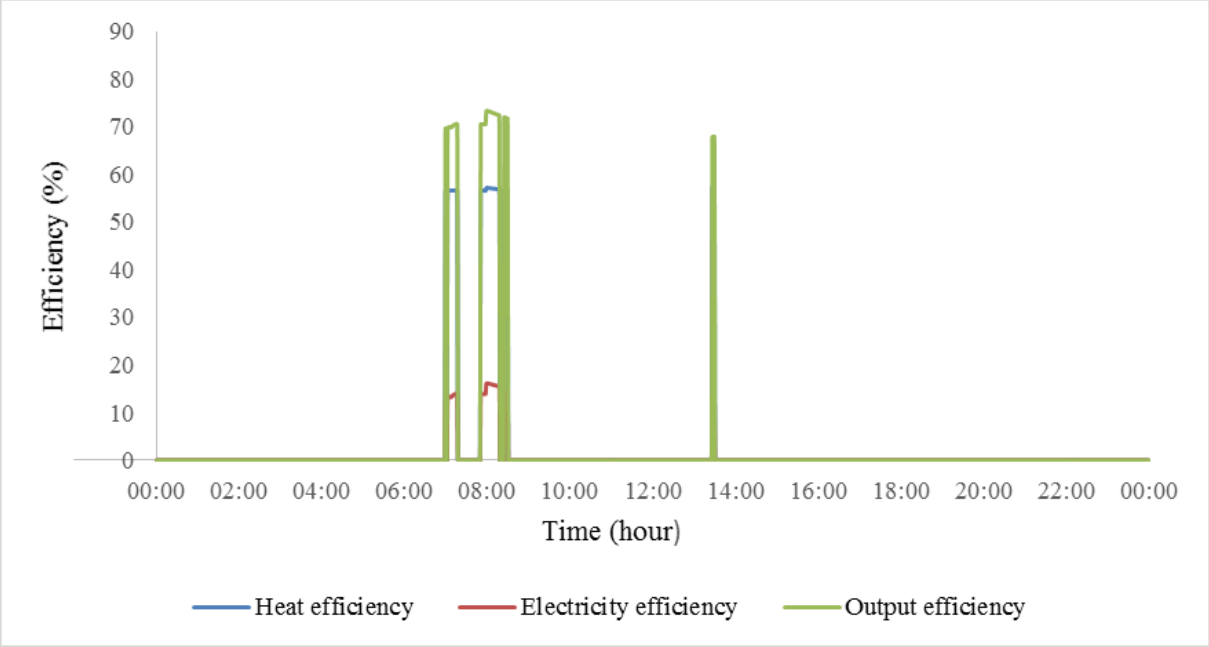

d) Summer , gas engine CHP, electricity dependant sizing CHP

Figure A2.1 CHP output efficiencies in each minute of a summer day based on different sizing criteria.

Autumn:

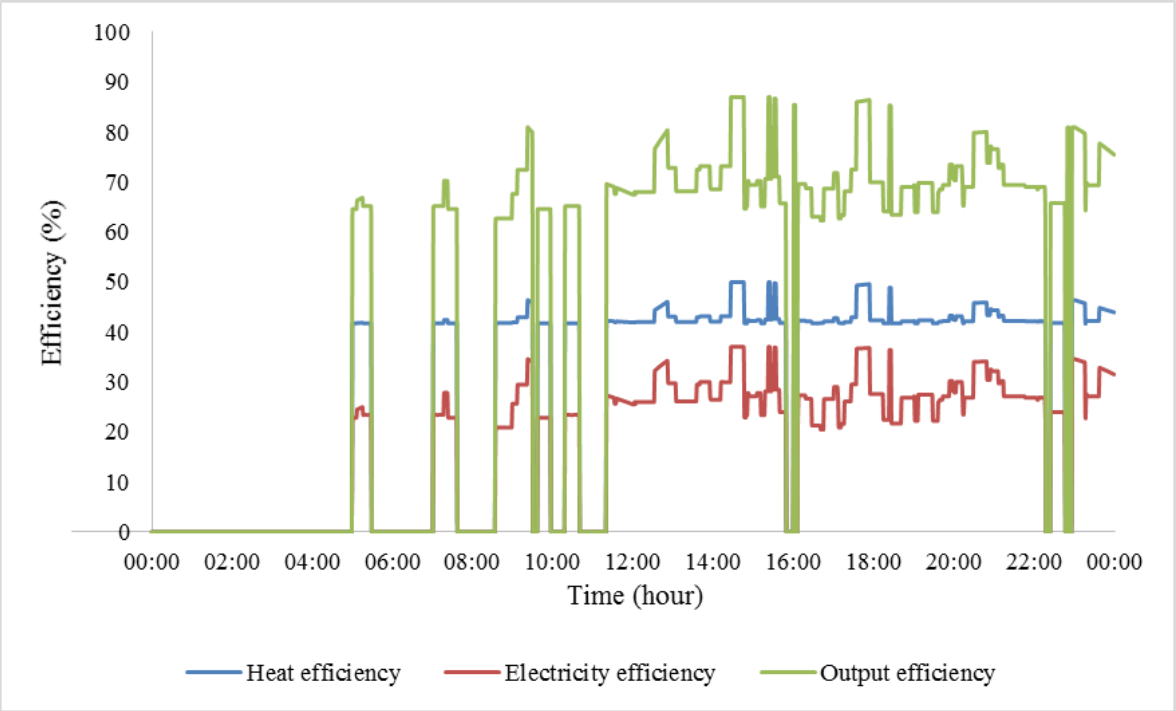

a) Autumn, fuel cell CHP, heat dependant sizing CHP

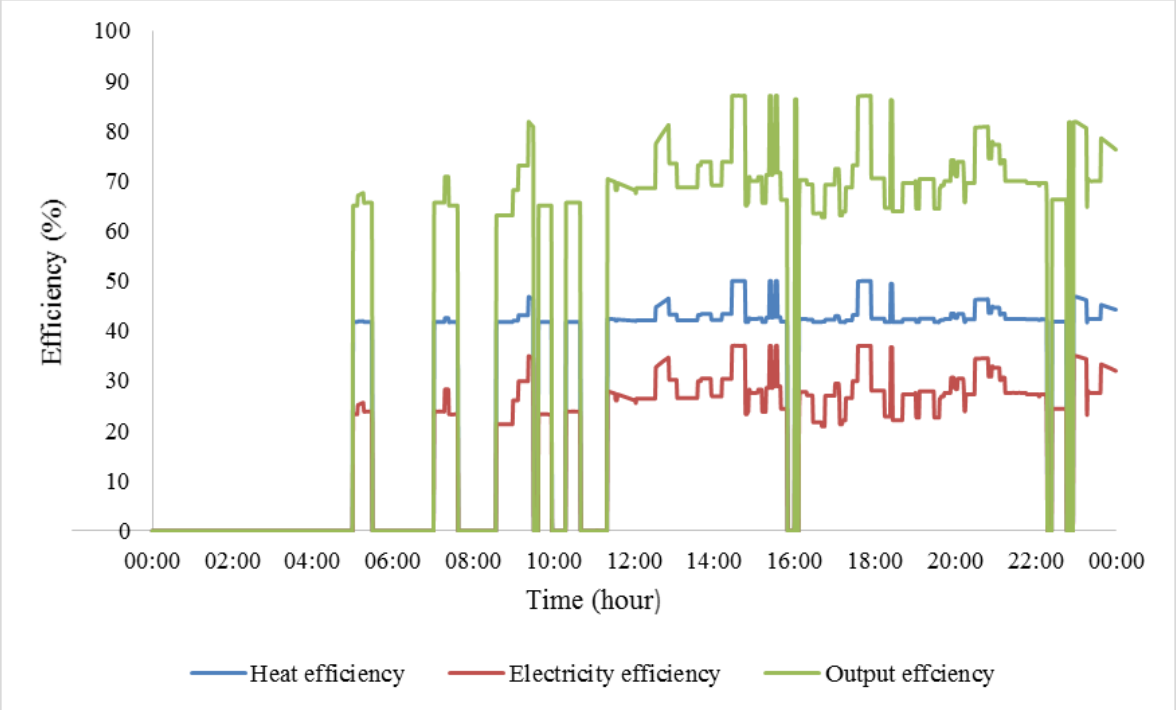

b) Autumn, fuel cell CHP, electricity dependant sizing CHP

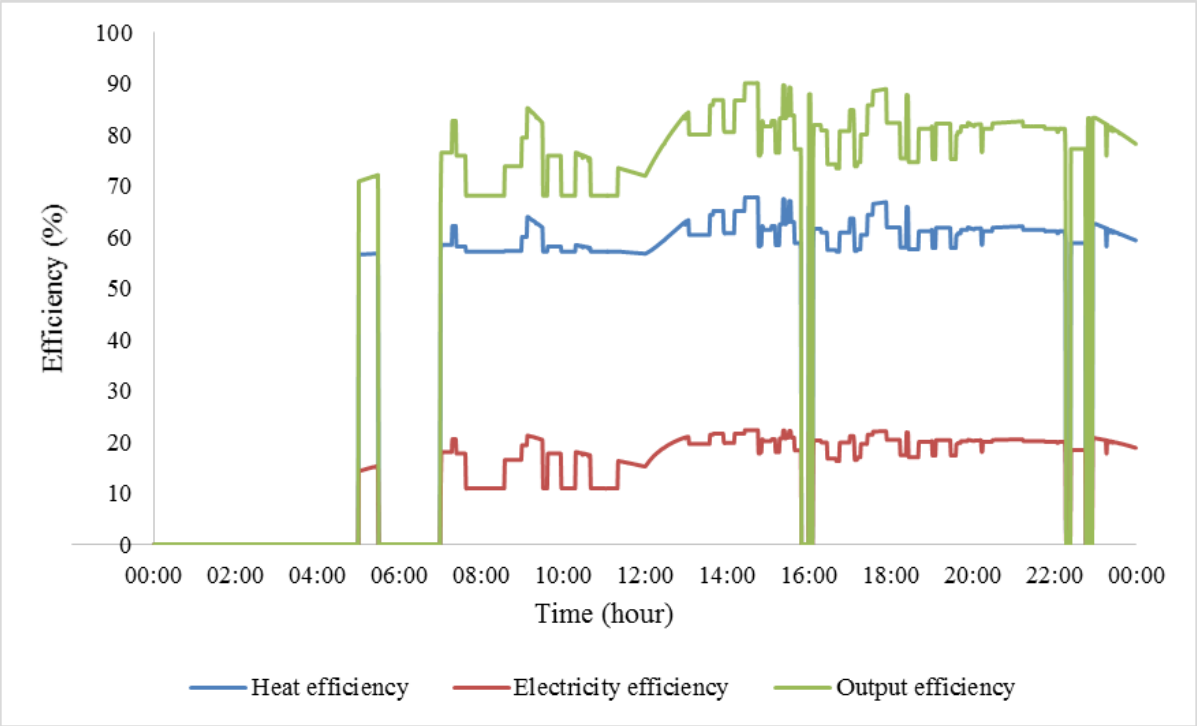

c) Autumn, gas engine CHP, heat dependant sizing CHP

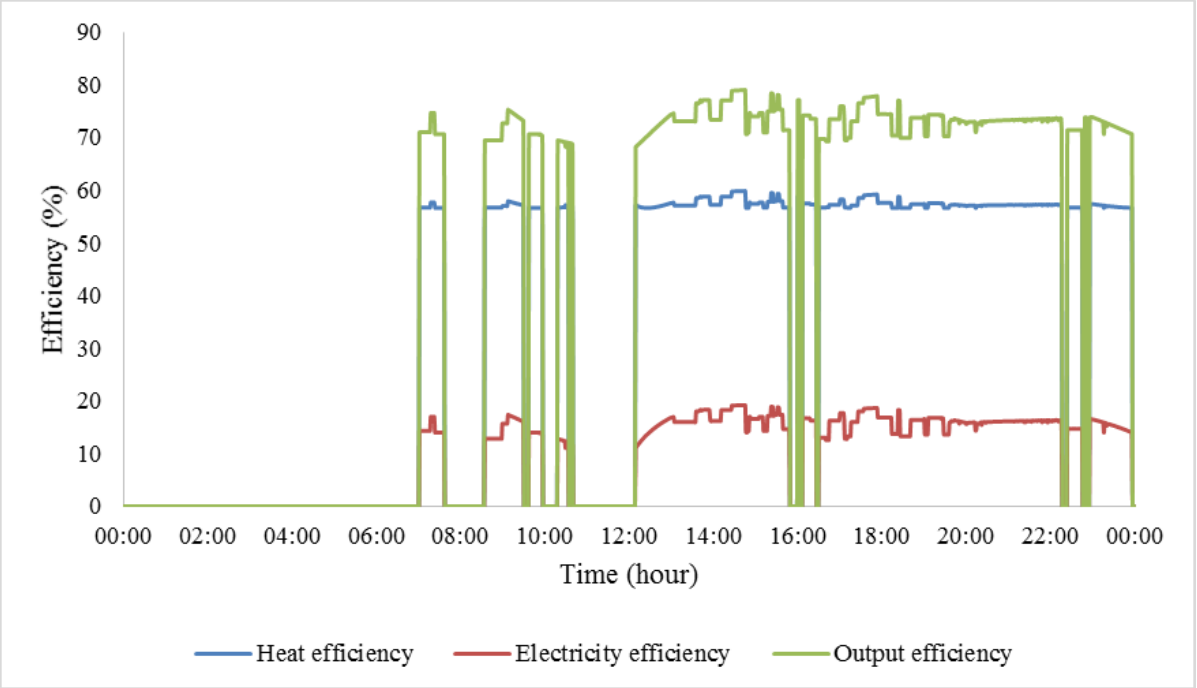

d) Autumn, gas engine CHP, electricity dependant sizing CHP

Figure A2.2 CHP output efficiencies in each minute of an autumn day based on different sizing criteria.

Winter

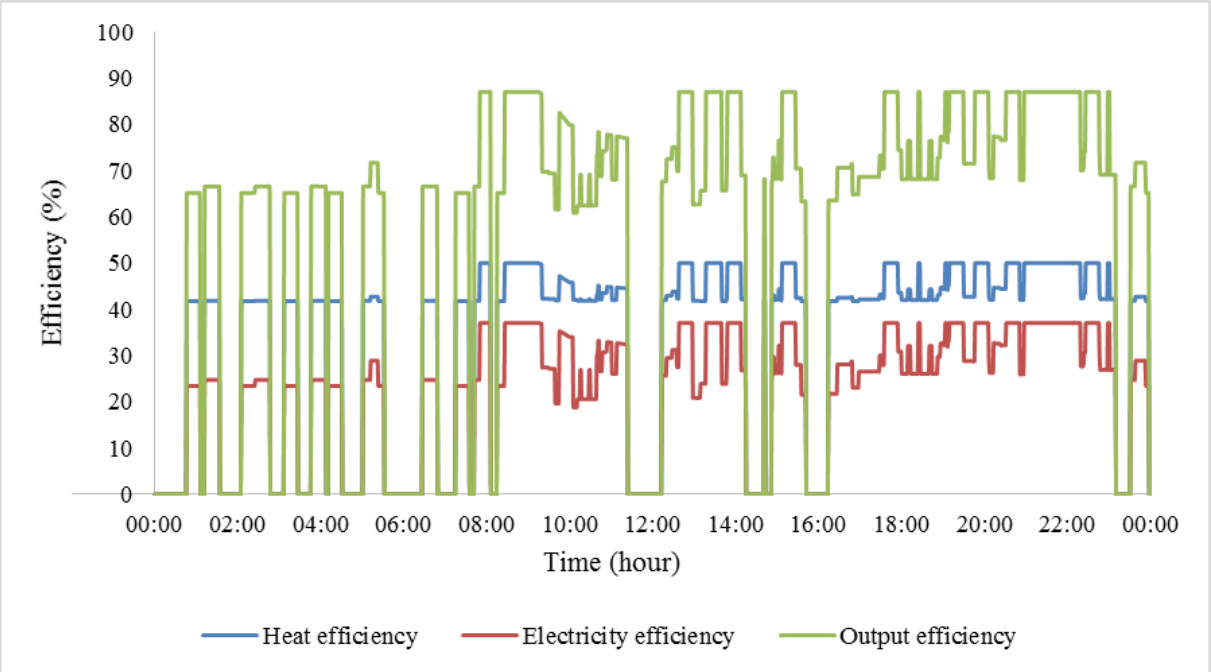

a) Winter, fuel cell CHP, heat dependant sizing CHP

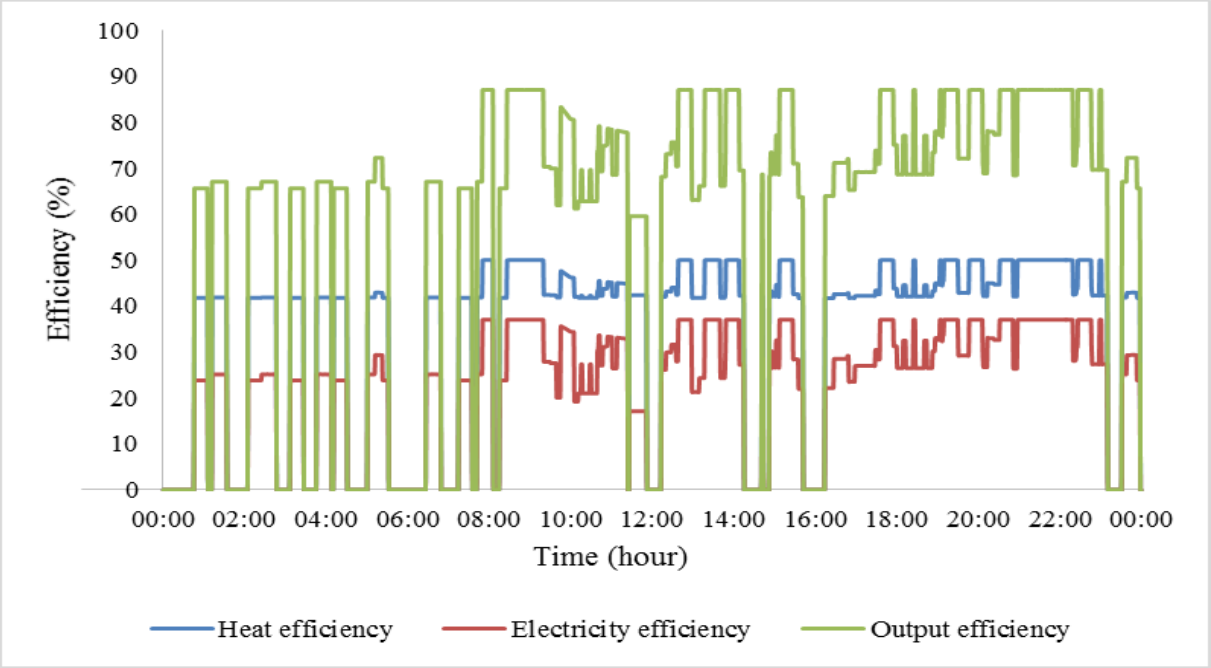

b) Winter, fuel cell CHP, electricity dependant sizing CHP

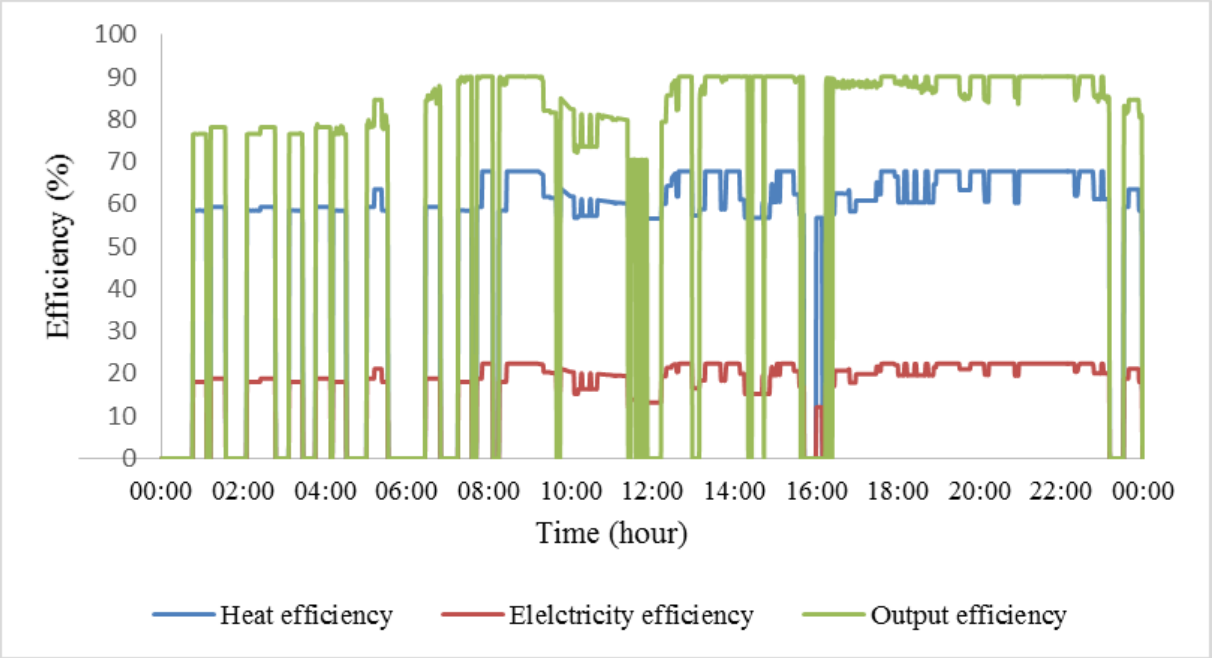

c) Winter, gas engine CHP, heat dependant sizing CHP

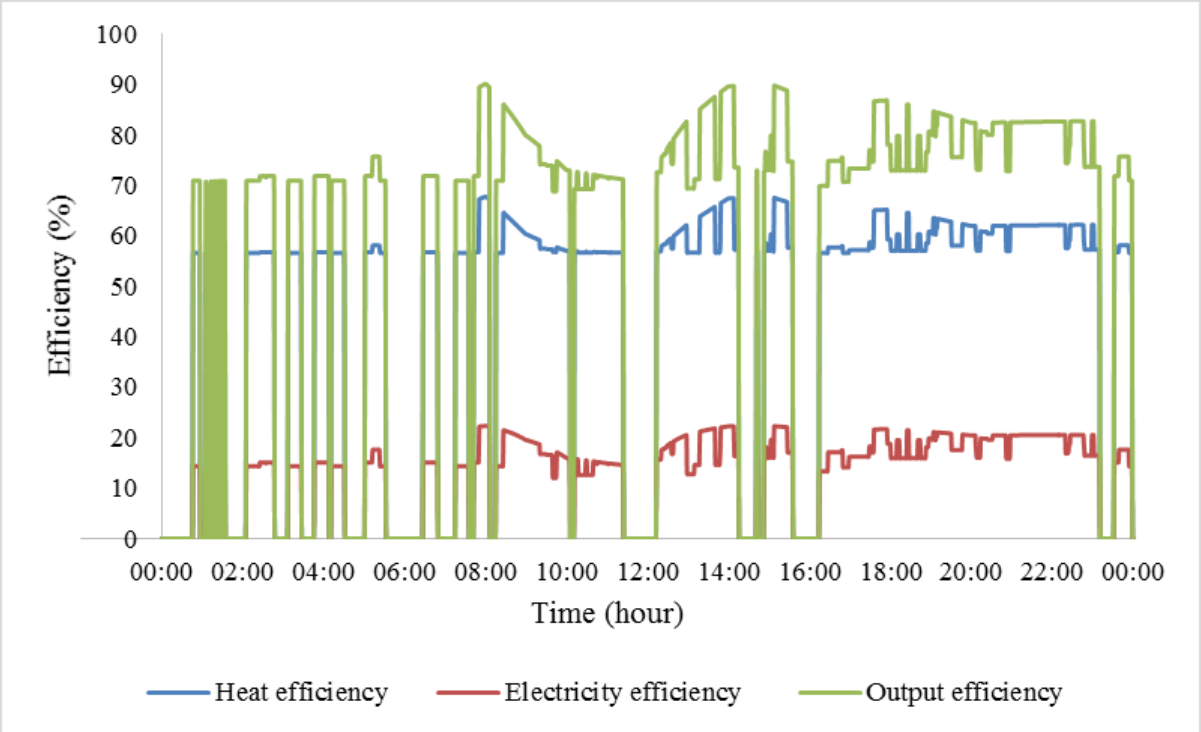

d) Winter, gas engine CHP, electricity dependant sizing CHP

Figure A2.3 CHP output efficiencies in each minute of a winter day based on different sizing criteria.